Performance Analysis and Enhancement of Proportional Navigation Guidance Systems

Ming-Yan Li

B.E., *Xi'an Jiaotong*

Thesis submitted for the degree of

Master of Engineering Science

in

Department of Electrical and Electronic Engineering

The University of Adelaide

Supervisor: **Dr Cheng-Chew Lim**

July 1999

Contents

Abstract

Proportional navigation has long been an active area of research in the guidance and control community. It is easy to implement and effective in most applications. However, proportional navigation leads to poor observability problems when using bearings-only measurements. Bearings-only measurement systems are common in guidance and target tracking, as they are low-cost and free from jam noise. Proportional navigation guidance systems with bearings-only measurements are not only practically important, but also theoretically interesting and nontrivial, due to their time-varying dynamics, highly nonlinear measurements, and complex engagement geometry when the target is maneuverable.

This thesis is concerned with observability enhancement and performance analysis of proportional navigation guidance systems. To tackle the low observability problem involved in proportional navigation systems with angle-only information, observability analysis is rigorously performed in order to grasp a better understanding of the essence of the problem. Necessary and sufficient conditions for system observability are firmly established, and are general enough to encompass most previous results. Extensions of these conditions are readily applicable to observability checks with practical guidance laws in closed loop. The observability analysis paves the way for improvement of system performance and development of new guidance laws.

Among existing guidance laws proposed to improve system observability as well as interception performance, additive proportional navigation is a class of guidance that preserves the simplicity in design and realization, while enhancing system observability by incorporating a measure of information content. Based on the thermal noise model, a new form of additive observable proportional navigation is presented in this thesis. Analysis undertaken

demonstrates that this new guidance law outperforms true proportional navigation, which is the most accepted guidance law, by offering a better possibility of observable systems and a larger region of interception. The effectiveness of this new control law is also confirmed by simulations. Bounds of system navigation constants to ensure interception are provided as guidelines for system design.

To account for the finite acceleration capability of real-world guidance systems due to physical limitations, effects of acceleration saturation constraint are investigated. In contrast to the ideal system with infinite acceleration capability, more stringent requirements on system initial launch conditions and different bounds of design parameters must be met to achieve interception, using more total control effort. The degradation of system performance due to saturation constraint is verified by extensive simulations.

Statement of Originality

I hereby declare that this work contains no material which has been accepted for the award of any other degree or diploma in any university or other tertiary institution and to the best of my knowledge and belief, contains no material previously published or written by another person, except where due reference has been made in the text.

I give consent to this copy of my thesis, when deposited in the University Library, being available for loan and photocopying.

Mingyan Li

23 July 1999

Acknowledgments

I wish to express my gratitude and appreciation to my supervisor, Dr C.C. Lim, for his guidance, encouragement, and assistance throughout the entire course of this research. He has been always there to answer my questions. His valuable suggestions and ideas, and his thorough and detailed review of my work are greatly appreciated. I would also like to take this opportunity to give my thanks to Mrs Soo Lim, whose cheerful nature and kind help have made my study in Adelaide an enjoyable and unforgettable one. Were not for Dr Lim and Mrs Lim, this thesis would not have been possible.

Many thanks must go to the staff and students of the Department of Electrical and Electronic Engineering at the University of Adelaide for providing pleasant and friendly atmosphere. In particular, I would like to thank my colleagues, Eric Chong, Kiet To, Carmine Pontecorvo, Zhishun She, and Jun Fang for their friendship and help.

My Chinese friends, Chunni Zhu, Ping Gao, Bingang He, Tian Qiu, Xinshu Zhang, Guizhi Su, and Bailing Wang have also been of a great encouragement and support to me.

I am deeply indebted to my mother and father for their unfailing love, constant support, and strong confidence in me throughout my life. I must express my special gratitude to my fiance, Gang Zhao, whose love has always been with me. They have a great share in this thesis.

This work was supported by an Overseas Postgraduate Research Scholarship Award and a University of Adelaide Scholarship, both of which I gratefully acknowledge.

Publications

1. **Mingyan Li** and C.C. Lim, "Observability-enhanced proportional navigation guidance with bearings-only measurements", *Journal of Australian Mathematical Society (Series B)*, Vol. 40, pp. 497-512, 1999

2. C.C. Lim and **Mingyan Li**, "Observability analysis of two closed loop guidance systems with bearings-only measurements", to appear in *Nonlinear Analysis*, 1999.

3. **Mingyan Li** and C.C.Lim, "Analysis of proportional navigation guidance systems with acceleration saturation constraints", *International Congress on Dynamics and Control Systems*, Ontario, Canada, invited paper, August 1999.

4. **Mingyan Li** and C.C. Lim, "Performance analysis of an observable proportional navigation guidance for missiles with bearings-only measurements", *The Third Biennial Engineering Mathematics and Applications Conference*, pp. 319-322, Adelaide, Australia, July 1998.

5. C.C.Lim and **Mingyan Li**, "Observability requirements for bearings-only guidance systems", *The Fourth International Conference on Optimization: Techniques and Application*, pp. 899-906, Perth, Australia, July 1998

6. **Mingyan Li** and C.C.Lim, "Saturation constraint problems in the performance of proportional navigation guidance systems", *IEEE Transactions on Aerospace and Electronic Systems*, submitted.

List of Figures

List of Tables

Chapter 1

Introduction

The background of navigation guidance and control systems is first introduced by explaining the block diagram of a guidance system. Some issues worthy of research are pointed out. The objectives of research on guidance systems with bearings-only measurements are highlighted after a literature survey.

1.1 Background

Since the 1940's, classical control theory has been used effectively in improving performance of guidance systems [1]. However, advancement in aircraft and anti-missile technologies has presented more stringent requirements for guidance systems. Consequently, research towards advanced theory and technology facing these challenges must be conducted.

One of the most challenging problems in modern guidance systems is that of a tactile missile in pursuit of a highly maneuverable target [2]. The problem involves estimation of uncertain dynamics of the target, guidance of the missile in a complex engagement geometry, and control of the nonlinear missile. All these three areas, i.e., estimation, guidance, and control, are nontrivial because the dynamics of guidance systems are inherently time-varying and nonlinear. The nontriviality of guidance systems has attracted considerable research attention [3].

Bearings-only measurement systems are very common in modern flight guidance. The system is low-cost because it relies solely on a simple passive seeker, which provides only bearing measurements. One added advantage of the system is that it is not subject to jamming interference imposed by an intelligent target during the engagement. Besides being practically significant, the system is theoretically interesting due to its time-varying dynamics and nonlinear measurements. Therefore, the guidance system with bearings-only measurements has attracted a great deal of interest in the literature [4]. This research focuses on bearings-only guidance systems, aiming to improve the effectiveness of advanced guidance.

A typical flight guidance system can be represented as given in Figure 1.1. The functions of each block are explained in the following paragraphs.

Seeker

The dynamics of the pursuer and the target are measured by on-board sensors in the seeker. The sensored data are sent to a filter for processing. When a low-cost passive seeker is used as in the case of bearings-only measurement systems, only angle information of the pursuer and the target is available from its sensors.

Filter and Estimator

A filter provides state estimates that must be consistent and reliable. In dealing with the

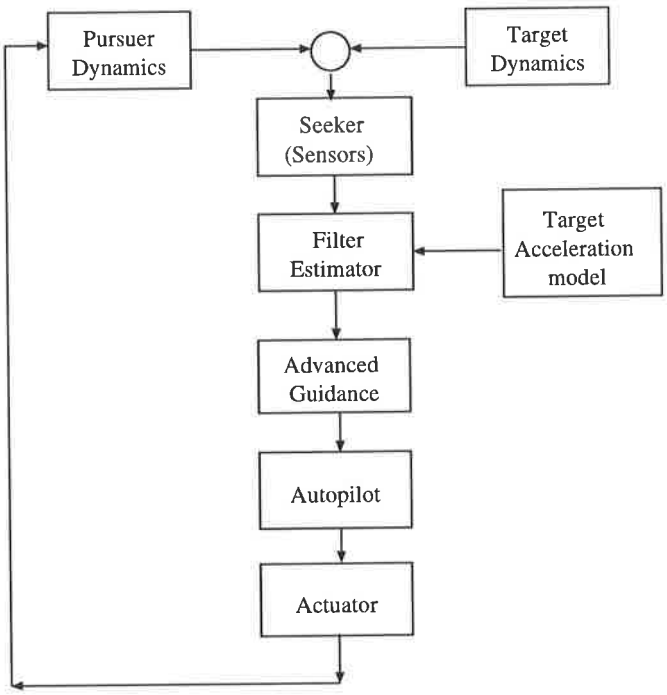

Figure 1.1: Block diagram of a guidance system

problem of a maneuverable target, a target acceleration model is required for the purpose of target maneuver detection and target tracking. With an assumed target acceleration model, the filter processes the sensor information obtained by the seeker to provide such state estimates as relative pursuer-target position, relative velocity, and relative acceleration.

Advanced Guidance

The role played by an advanced guidance law is to use the state estimates to generate commanded acceleration in an effort to guide the pursuer toward its target. In designing a guidance law, there are several requirements to consider. These include terminal interception accuracy, insensitivity toward parameter variation, and robustness against uncertainty in target maneuver. Because of the target's high agility, the ever changing target-pursuer geometry, and the actuator constraints, the guidance law design is a nonlinear, time-varying, and multi-objective problem. The presence of bearings-only measurements makes the design even more complicated. For the angle-only measurement case, the well-known guidance law, true proportional navigation (TPN) guidance law, shows poor interception performance due to the lack of system observability. Therefore, in addition to the general design re-

quirements, observability enhancement becomes one of the major concerns in the design of guidance for bearings-only measurement systems. When all the requirements are combined, the guidance law design for bearings-only guidance systems becomes a challenging task, and the main task of this thesis.

Autopilot

The commanded outputs from the guidance law are translated by an autopilot into fin commands that steer the pursuer towards the target. For the purpose of guidance law design in this study, the autopilot is regarded as an ideal autopilot that has unity gain with no dynamics. Such an autopilot has an immediate command response, and is able to drive the missile precisely according to the commands of a guidance law.

Actuator

An actuator changes the electronic signals from the autopilot into mechanical forces which physically drive the missile. In practice, an actuator is always subject to acceleration saturation constraint. The effects of acceleration saturation constraint are studied in this work.

Pursuer and Target Dynamics

The engagement geometry of a missile in pursuit of a target is illustrated in Figure 1.2.

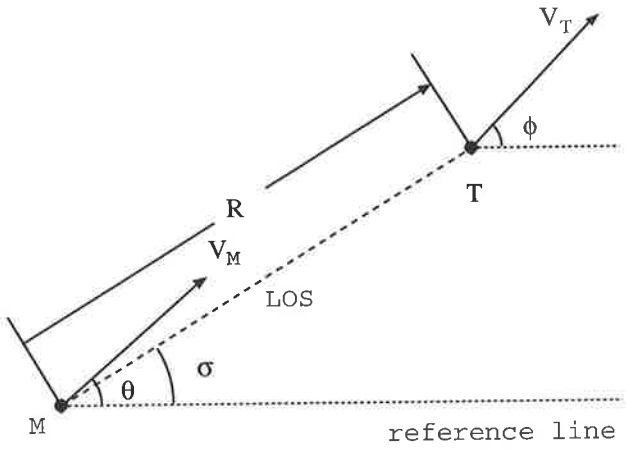

Figure 1.2: Two-dimensional geometry of pursuer-target engagement

A pursuer traveling at the velocity V_P with heading angle θ is aiming to intercept a target evading at the velocity V_T with heading angle ϕ. It is well-known that the speed of a tactical

missile is determined mainly by the propulsion system, and is not significantly changed by the operation and control systems [5]. This physical characteristic justifies the assumption that the pursuer's speed is a known time function, and is taken as constant for design purpose. Experience also suggests that the missile and the target can be treated as point mass for the purpose of steering [5]. In this thesis, we consider a two-dimensional, point mass missile-target engagement with constant speeds.

Two most frequently used terms in this thesis are introduced here.

Definition 1 *line-of-sight angle: The line-of-sight (LOS) is defined as the imaginary line connecting the pursuer and the target. The orientation of the line-of-sight with respect to the fixed reference line is known as line-of-sight angle.*

The line-of-sight (LOS) angle is shown as σ in Figure 1.2 .

Definition 2 *miss distance: The miss distance defined at time t, is the relative distance that would result if guidance were terminated at a particular time t.*

In this thesis, the closest approach of the missile and the target at the final point of pursuit is referred to as the *miss distance*.

With the background of guidance systems presented, we are now ready to identify some research problems in this area.

1.2 Motivation and Significance

Utilizing only bearing angle measurements for guidance and target tracking is common in homing missiles with passive sensors and in underwater passive target tracking. Their control and estimation problems are theoretically interesting and practically significant. These problems are nontrivial due to the time varying system dynamics, the nonlinear measurements, and the complex target-pursuit geometry when the target is maneuverable.

When considering the homing missile guidance with bearings-only measurements, proportional navigation guidance is the most popular [6, 7]. The law generates the command acceleration proportional to the line-of-sight angular rate in an effort to turn the missile in

the direction needed to reduce the line-of-sight angular rate to zero, and to form a collision course. To achieve effective target interception, good sensor measurements on the range rate and the line-of-sight angular rate are needed. This may not be possible because the sensor measurement available in this case gives bearing angle only. Even if an active sensor is available, the range and the range rate can be jammed by an intelligent target, and consequently, only angle information is reliable. State estimation errors can however become large especially towards the end of the missile-target interception. This is undesirable since accurate control action during this time is essential to accomplish the mission. Investigation in [8] shows that unsatisfactory terminal performance is due to the lack of observability in the range and the range rate. The problem of low observability has been approached in two research directions. One is to analyze observability characteristic of guidance systems for the purpose of a better understanding of the essence of the problem, the other is to design new guidance algorithms with the aim of enhancing observability and ensuring final interception.

1.2.1 Observability Analysis

The mathematical observability analysis of guidance systems and target tracking systems that use bearings-only measurements has received considerable attention. In general, establishing solution uniqueness requirements for such systems is difficult because the pertinent system models are nonlinear. By setting up the problem in a linear framework, necessary observability conditions for non-maneuvering targets in naval applications are reported in [9] for a two-dimensional model, and in [10] for a three-dimensional case. A necessary and sufficient condition for an Nth-order dynamic target model is established in [11], where a different problem formulation from [9, 10] is employed. Since the missile-target pursuit is nonlinear in measurement, two approaches have been proposed to tackle the observability analysis problem. Linearization is used in [12, 13] to derive sufficient conditions for the system to be unobservable and the conditions provide insights into the relationship between the system observability and the system state. The second approach is to recast the intrinsically nonlinear measurement in a linear framework via the construction of a pseudo-measurement

[14, 15]. Necessary and sufficient conditions for system observability for bearings-only target motion analysis are then derived based on this measurement model.

Although it is known that a guidance law has some effects on the system observability [16], few studies on the linkage between practical guidance laws and system observability have been reported. In most cases, only mathematical derivations on the observability criteria without guidance laws in the loop have been presented. One exception is in [15], where the effect of the true proportional navigation (TPN) law on system observability is analyzed, yet there is no work done on examining more advanced guidance laws on the basis of the obtained observability criteria.

An aim of this research is to investigate the observability characteristics and requirements of a two-dimensional bearings-only missile-target system under practical guidance laws. Prior to studying how guidance laws affect system observability, necessary and sufficient conditions for observability of guidance systems, incorporating a general target model, are rigorously established in Chapter 2. The criteria are sufficiently general, and readily applicable to observability analysis in a closed loop environment.

1.2.2 Observability-Enhanced Guidance Laws

There have been numerous studies dealing with observability-enhanced guidance control laws in homing missiles [8], [16]-[19]. Investigation [8] reveals that when the missile and the target are in a collision course, the information content of the bearings-only measurements may not be sufficient to excite the Kalman filter under the proportional navigation strategy of nullifying the line-of-sight angular rate. It follows that a more effective guidance system should aim not only to nullify the angular rate, but also to enhance the information content of the measurements in order to offer the filter sufficient information to generate consistent estimates. One approach to obtain observability-enhanced guidance [16, 18] is to formulate the guidance as an optimal quadratic control problem and to incorporate the Fisher information matrix [20] as an index to modulate the trajectory in an information-enhanced way. This control law is fairly effective but complex to implement.

A simple control scheme using a scalar variable which is computed from the trace of the

observability matrix, in conjunction with proportional navigation control, is first proposed in [19]. This scheme is motivated by meeting the two design aims of (i) retaining the simple design and implementation feature of conventional proportional navigation, and (ii) offering better observability in the homing phase of the mission. The guidance law is referred to as the additive observable proportional navigation (AOPN) control law. Simulation studies given in [21] show that the control enhances the observability of the system in both non-maneuvering and maneuvering target engagements, and helps in overcoming the Kalman filter divergence problem. Rudimentary guidelines are presented in [19] and [21] on how to select the navigation constant of the added term. It is clear that the AOPN guidance control is well-suited for low-cost homing missiles with bearings-only measurements, although refinement on the guidelines to ensure effective interception and further investigation into the effect of the new term on the interception must be carried out.

Another AOPN guidance law based on a different noise model is proposed in this thesis. The AOPN guidance law in [19] is referred to as AOPN-I, while the new law is termed AOPN-II. The new control law also aims to offer better observability as well as to preserve the simplicity in design and implementation. The investigation into AOPN-II and further exploration into AOPN-I are conducted in Chapter 3.

Although observability-enhancement of all the proposed guidance laws have been verified by simulations, confirmation by rigorous analytical means for general cases has not been conducted. The observability characteristics of the AOPN based guidance systems are studied by applying the derived observability criteria to these systems in Chapter 3.

1.2.3 Acceleration Saturation Constraints

In the preceding discussion, it is implicitly assumed that the pursuer has adequate acceleration capability in order to guide and hit the target. In fact, most studies on missile guidance systems are carried out under the assumption that the pursuer could always provide sufficient acceleration. In real-world applications, this assumption is impractical, as the pursuer's acceleration is subject to saturation constraints.

Nonideal operating conditions under acceleration saturation constraints are quite com-

mon. However, it has received very little treatment in the literature, except in [22], [23] and [6]. In [22] and [23], the influence of acceleration saturation on system interception is studied mainly via simulation for sinusoidal target models. It shows that the saturation tends to enlarge the miss distance. In [6], the effects of saturation constraints on total control effort, as well as on terminal performance, are investigated. The simulation in [6] reveals that saturation constraints can result in more fuel consumption. All the findings are significant, but there is no analytical justification to confirm the generality and accuracy of these findings. The effects of the saturation constraints on system performance will be studied on a firm analytical basis in Chapter 4.

1.3 Objectives and Research Methods

There are four main aims in this research.

Aim One *Explore the characteristics of classical proportional navigation guidance laws.*

Aim Two *Establish observability criteria with guidance laws in closed loop.*

Aim Three *Develop effective guidance laws suitable for missiles with angle-only measurements.*

Aim Four *Investigate the effects of acceleration constraints on system performance.*

To fulfill these research aims, research methods used in the study are briefly described here. In view of the mathematical analysis as a basis of studying the general case, all the identified problems are first theoretically analyzed. Results drawn from the mathematical analysis will be verified by simulations, which are conducted by two approaches. One is the deterministic approach, in which the system is not subject to disturbance and all measurements are assumed noise-free. In the deterministic approach, no state estimator is used, so that the estimation errors need not be considered when studying the effect of guidance control. The second is the stochastic approach. The system and the measurements are subject to noise and uncertainty, and a state estimator is needed. Since the process is stochastic, Monte Carlo simulation is used to obtain results, which are statistically analyzed.

1.4 Thesis Outline

There are five chapters in this thesis. In Chapter 2, true proportional navigation (TPN), being one of most widely used guidance laws, is thoroughly studied. The target-pursuit motion equations under the TPN guidance law are solved, the conditions to ensure interception are derived, and total control effort is calculated. Observability conditions for systems with bearings-only measurements are firmly established, and are applied to observability analysis for both non-maneuvering and maneuvering target cases. The analysis reveals one major limitation of TPN based systems.

In Chapter 3, a new proportional navigation guidance law is proposed to enhance system observability by augmenting TPN with an additive information-enhanced term. This guidance method is termed additive observable proportional navigation (AOPN). In investigating this guidance law, closed-form solutions to the pursuit problem are obtained. Constraints on system initial value and navigation constants for interception, and the optimal value of the navigation constant of the additive term are derived, thus providing guidelines for the design of the guidance systems. Analysis and simulation are carried out to confirm the observability-enhancement behavior of the AOPN guidance laws. Comparative studies of three guidance laws are conducted to provide a better understanding of their strength and limitations.

In Chapter 4, the problem of acceleration saturation constraint is addressed. Four different operating modes are discussed under the TPN and the AOPN guidance laws, and interception conditions for these operating modes are considered. Total control efforts consumed in different modes are compared to stress the unfavorable effects of saturation constraints on system performance.

In Chapter 5, all the major conclusions made in the thesis are summarized, and future work is suggested.

1.5 Major Contributions

Contributions made in this research are now listed.

- Establishing necessary and sufficient observability conditions for guidance systems engaging a maneuvering target when using bearings-only measurements;
- Applying the derived observability criteria to guidance systems under practical control laws to gain insights into the linkage between systems observability and guidance laws;
- Developing a new form of additive observable proportional navigation (AOPN) as a guidance law to enhance system observability as well as to maintain simplicity in implementation and effectiveness in interception;
- Deriving complete closed-form solutions to target-pursuit equations and interception requirements on system initial launch conditions under two AOPN guidance laws;
- Providing guidelines on choosing design coefficients of two AOPN laws in terms of the bounds and the optimal value of navigation constants;
- Investigating rigorously the effects of acceleration saturation constraints on system performance.

Chapter 2

True Proportional Navigation

As a major class of traditional guidance, true proportional navigation (TPN) has been very popular both in theoretical research and in practical applications. In analyzing the performance of TPN based guidance systems, the closed-form solution to pursuer-target motion equations is derived, and constraints on system parameters and initial conditions to ensure effective interception are determined. Investigation shows that target maneuver causes deterioration in the system capturability. Based on the derived necessary and sufficient conditions, observability characteristics of bearings-only pursuer-target motion under TPN are investigated. Analysis reveals that the TPN based system suffers from the problem of poor observability when using bearings-only measurements.

Proportional navigation is most widely used in short range guidance. It probably had its origins among the mariners who realized that a collision was ensured if two constant velocity vessels maintained a constant relative bearing while closing in range [24]. The first application of proportional navigation in modern air-to-air and surface-to-air missile systems can be dated back to the 1940s [25]. Since then, proportional navigation has been most commonly used as an empirical guidance law, due to its simplicity, effectiveness, and ease of implementation. It also has attracted a considerable amount of interest in the literature.

Proportional navigation schemes can be categorized into two major classes [26] as the interceptor/pursuer velocity referenced class, and the line-of-sight referenced class. Pure proportional navigation [27] belongs to the former, while true proportional navigation belongs to the latter. This research is focused on true proportional navigation, because it is mathematically more tractable than pure proportional navigation. Rigorous analysis on true proportional navigation provides insights into various important aspects of proportional navigation systems.

The structure of this chapter is as follows. The definition of true proportional navigation is first introduced, followed by establishment of the system equations describing a target-pursuit motion. Based on the closed-form solutions to the system motion equations, several important properties of the guidance systems are studied, including capturability and total control effort. Finally, the observability of the TPN based systems with bearings-only measurements is analyzed by applying the derived observability criteria for general guidance systems to a specific TPN system.

2.1 What Is True Proportional Navigation?

True proportional navigation (TPN) issues the commanded acceleration which is perpendicular to the instantaneous pursuer-target line-of-sight (LOS) and is proportional to the line-of-sight angular rate and closing velocity. The TPN guidance law can be mathematically stated as

$$A_P = N_1 V_c \dot{\sigma} \tag{2.1}$$

where A_p is the commanded pursuer's acceleration; N_1 is a positive navigation constant which is a design gain; (the subscript "1" here is to make it distinguishable from other navigation constants in the following chapters;) $\dot{\sigma}$ is the line-of-sight (LOS) angular rate; V_c is the closing velocity, which is defined as the negative rate of change of the distance from the pursuer to the target, i.e.,

$$V_c = -\dot{R}. \tag{2.2}$$

A pursuer employing TPN aims not at the target but at the expected interception point leading the target. From the expression of TPN given in (2.1), it implies that this true proportional navigation drives the LOS angle from the pursuer to target to a constant value, so that the pursuer and the target are on a "collision course", and an interception can be accomplished without further guidance. This fact underpins the rationale of TPN. That is, if the LOS angle is constant, with faster speed of the pursuer over the target, the pursuer will eventually intercept the target. Note that $\dot{\sigma} = 0$ is only one sufficient condition for being on a collision course. The intuitively simple, operating principle of TPN is one reason which contributes to its durability as a favorable guidance scheme.

In addition, the ease of design and implementation of TPN adds greatly to its popularity. N_1 is a navigation constant, and the range of $3 - 6$ for N_1 normally gives satisfactory performance, even when the target follows a curved trajectory. When implementing TPN, measurements of the LOS angular rate and the closing velocity are provided by a seeker, or are estimated by a filter. Compared with many other sophisticated guidance laws, TPN only requires low levels of information input, and thus simplifies onboard sensor requirements.

However, the mathematical description of a TPN based guidance system for the simplest two dimensional engagement involving only a non-maneuvering target can be highly nonlinear. The inherent nonlinearity of the guidance system on one hand, renders system analysis difficult and complex; on the other hand, has opened an exciting research area and thus has received considerable attention. In the following sections, several aspects of TPN based guidance systems are discussed in detail, including closed-form solution, capturability, total control effort, and observability.

2.2 System Equation

Consider the geometry of a guidance engagement shown in Figure 2.1, where a pursuer P

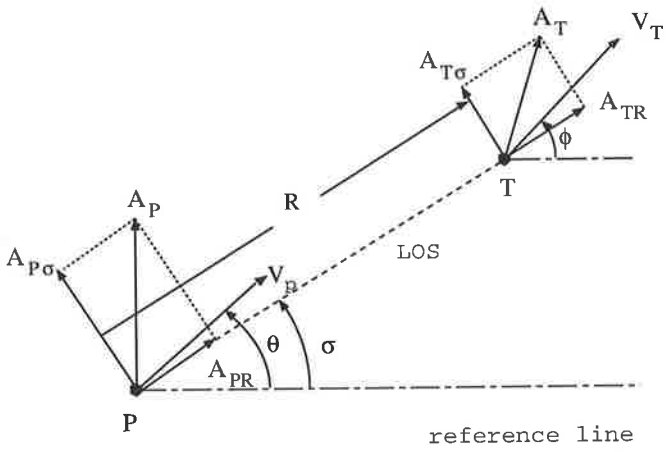

Figure 2.1: Two-dimensional guidance engagement with pursuer heading angle θ and target heading angle ϕ in polar coordinate

and a target T are points on a plane, moving with constant velocities V_P and V_T, respectively. When developing system equations, the gravitational effects have been simply neglected in hope of gaining more understanding. The relative motion between the pursuer and the target can be described in terms of the range R and LOS angular rate $\dot{\sigma}$ as [6, 12]

$$\ddot{R} - R\dot{\sigma}^2 = A_{TR} - A_{PR} \tag{2.3}$$

$$R\ddot{\sigma} + 2\dot{R}\dot{\sigma} = A_{T\sigma} - A_{P\sigma} \tag{2.4}$$

where R is the relative range with initial value R_0; $\dot{\sigma}$ is the line-of-sight (LOS) angular rate with initial value $\dot{\sigma}_0$; A_{TR} (respectively, $A_{T\sigma}$) is the target acceleration component along LOS (respectively, normal to LOS); A_{PR} (respectively, $A_{P\sigma}$) is the pursuer acceleration component along LOS (respectively, normal to LOS).

When using the TPN guidance law, which is applied normal to the pursuer-target line-of-sight (LOS) with the magnitude proportional to the LOS angular rate $\dot{\sigma}$, the pursuer acceleration A_P is given, according to (2.1), as

$$A_{PR} = 0; \qquad A_{P\sigma} = -N_1\dot{R}\dot{\sigma} \tag{2.5}$$

where N_1 is a positive navigation constant.

In developing the system governing equations, a maneuvering target is modeled. There are numerous target maneuver models proposed in the literature for three purposes: (i) designing better guidance laws, as in augmented proportional navigation [28]; (ii) forming effective filters in conjunction with those assumed models, as in [29]; (iii) obtaining the performance of guidance laws against maneuvering targets, as in [30]. For the purpose of performance analysis, we adopt the target model proposed in [31], as it is mathematically tractable as well as practically reasonable.

The acceleration of a maneuvering target is assumed to be proportional to the range rate $\dot{R}$ and normal to LOS. The target maneuver acceleration takes the form as in [31],

$$A_{TR} = 0; \qquad A_{T\sigma} = -c\dot{\sigma}_0\dot{R} \tag{2.6}$$

where c is a non-negative constant of the target maneuver acceleration, and represents the maneuverability of the target. That is, the larger the c, the more maneuverable the target. When $c = 0$, the target model reduces to a non-maneuvering target case, i.e., the target is not accelerating. With $\dot{\sigma}_0$ being the system initial LOS angular rate, the target model (2.6) is therefore scenario-related. Comparing (2.5) and (2.6), we observe that the target still maintains maneuverability when the pursuer is on a conducive condition for interception (i.e. when $\dot{\sigma} = 0$). The evasion from the pursuer in the final phase is exactly what an intelligent target is expected to do.

From (2.3) to (2.6), the governing equations of the target-pursuit motion under the TPN guidance law are obtained as

$$\ddot{R} - R\dot{\sigma}^2 = 0 \tag{2.7}$$

$$R\ddot{\sigma} + 2\dot{R}\dot{\sigma} = N_1\dot{R}\dot{\sigma} - c\dot{\sigma}_0\dot{R} \tag{2.8}$$

After establishing the system equations describing the target-pursuit motion, we are ready to derive the solution to these nonlinear differential equations.

2.3 Closed-Form Solution

A closed-form solution plays an important role in analysis of system performance, and provides insights into many important design parameters. Despite its importance, an analytical solution is not easy to derive, due to the high nonlinearity of the pursuer-target motion equations under TPN guidance laws. Since the first solution was reported for a non-maneuvering target in [32], many attempts have been made to solve nonlinear differential equations for maneuvering targets [33]-[37].

For the motion equations of TPN base systems established in (2.7) and (2.8), Yuan and Chern derived the closed-form solution which yields comprehensible interpretation [31]. The approach and solution are summarized here with a modification which is explained in the remarks.

Theorem 2.1 *A closed-form solution to the differential equations (2.7) and (2.8), which represent an interceptor in pursuit of a maneuvering target under the TPN guidance law, consists of two parts.*

(i) The LOS angular rate $\dot{\sigma}$ is

$$\dot{\sigma} = \dot{\sigma}_0 \left(\frac{R}{R_0}\right)^{N_1-2} + \frac{c\dot{\sigma}_0}{N_1-2}\left[1-\left(\frac{R}{R_0}\right)^{N_1-2}\right]; \tag{2.9}$$

(ii) The relative velocity $\dot{R}$ is

$$\begin{aligned}\dot{R}^2 = {} & R_0^2\dot{\sigma}_0^2\left[n^2\left(\frac{R}{R_0}\right)^2 + \frac{(1-n)^2}{N_1-1}\left(\frac{R}{R_0}\right)^{2N_1-2} + \frac{4n(1-n)}{N_1}\left(\frac{R}{R_0}\right)^{N_1}\right] \\ & + \dot{R_0}^2 - R_0^2\dot{\sigma}_0^2\left[n^2 + \frac{(1-n)^2}{N_1-1} + \frac{4n(1-n)}{N_1}\right],\end{aligned} \tag{2.10}$$

where

$$n = \frac{c}{N_1-2} \tag{2.11}$$

which is directly proportional to the target maneuver constant c.

Proof. Multiplying (2.8) by $\frac{R}{R}$ and using the unit mass angular momentum of the pursuer (defined by $R^2\sigma$) and initial conditions, the LOS angular rate $\dot{\sigma}$ can be obtained as (2.9).

Note the LOS angular rate $\dot{\sigma}$ given in (2.9) is also derived by imposing $N_1 > 3$ which is a necessary condition for interception.

Substituting $\dot{\sigma}$ in (2.9) into (2.7), and using $\ddot{R}dR = d\left(\frac{\dot{R}^2}{2}\right)$, the solution of the range rate can be written as (2.10). ∎

Remarks.

- The constraint $N_1 > 3$ will be shown to be necessary for effective interception in Theorem 2.2, hence the solution obtained for case $N_1 = 2$ in [31] is discarded.

- The solution given in (2.9) and (2.10) reduces to that for a non-maneuvering target when $c = 0$. For a non-maneuvering target, the solution also consists of two parts.

  (i) The LOS angular rate $\dot{\sigma}$ is

  $$\dot{\sigma} = \dot{\sigma}_0 \left(\frac{R}{R_0}\right)^{N_1-2} \tag{2.12}$$

  (ii) The relative velocity $\dot{R}$ is

  $$\dot{R}^2 = \frac{R_0^2\dot{\sigma}_0^2}{N_1-1}\left(\frac{R}{R_0}\right)^{2N_1-2} + \dot{R}_0^2 - \frac{R_0^2\dot{\sigma}_0^2}{N_1-1} \tag{2.13}$$

- For a non-maneuvering target, i.e., when $c = 0$, the LOS angular rate $\dot{\sigma}$ approaches zero provided the range R approaches zero at the end of the engagement. That is, the TPN law attempts to nullify the LOS angular rate. It follows that the pursuer and the target are on a collision course at the end of pursuit and the interception is assured. This confirms that TPN is very effective against a non-maneuvering target.

- The final LOS angular rate $\dot{\sigma}_f$ is given from (2.9) as

  $$\dot{\sigma}_f = \frac{c\dot{\sigma}_0}{N_1-2} \tag{2.14}$$

  when $R \to 0$. The expression (2.14) indicates the final LOS angular rate is proportional to the target maneuver constant c.

- The expression of the range rate $\dot{R}$, given in (2.10) for a maneuvering target case, or in (2.13) for a non-maneuvering target case, consists of two parts. The first part is linked to the pursuit motion and the rest is determined by the system initial conditions and the navigation constant N_1.

- To illustrate how the target maneuver affects the closing speed, (2.10) is plotted in Figure 2.2. It is observed that the closing speed is the fastest for a non-maneuvering target case, as shown in the solid line. Figure 2.2 demonstrates that the target maneuver causes the slowing down of the closing speed, and thus implies a longer time to intercept a target.

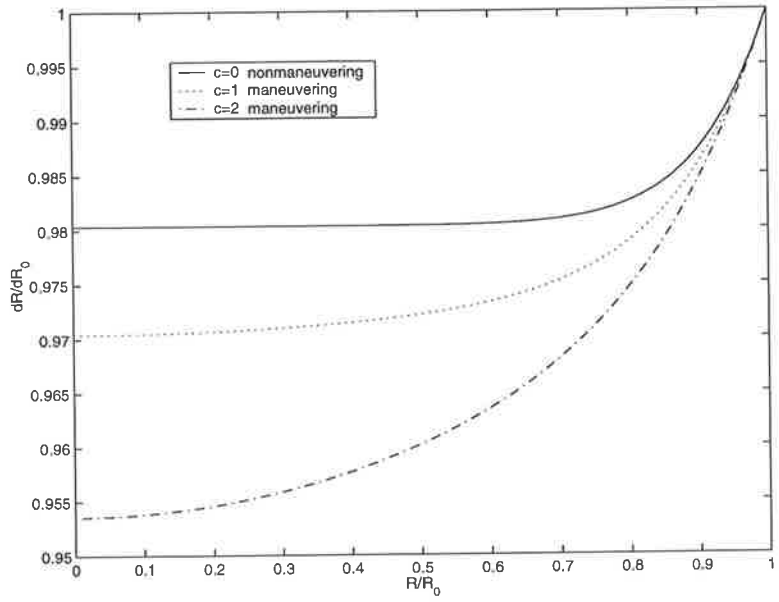

Figure 2.2: $\frac{\dot{R}}{\dot{R}_0}$ versus $\frac{R}{R_0}$ for three different target maneuvers under TPN

- The final closing speed, denoted as $\dot{R}_f$, is obtained by substituting $R = 0$ into (2.10) as

$$\frac{\dot{R}_f}{\dot{R}_0} = \sqrt{1 - \frac{R_0^2 \dot{\sigma}_0^2}{\dot{R}_0^2} \left[\frac{1}{N_1 - 1} + \frac{c^2 + 2c}{N_1(N_1 - 1)} \right]} \tag{2.15}$$

2.4 Capture Area

The ability of a pursuer to capture a target, which is referred to as capturability, is determined not only by guidance laws and target dynamics, but also by the initial launch conditions of pursuer-target engagements. To understand how initial conditions affect capturability, we introduce the term *capture area*.

When a pursuer employing TPN is to intercept a target, the capture is restricted to those systems whose initial conditions fall within a determined area, known as *capture area* [38]. If the region formed by the system initial conditions is laying outside the *capture area*, an interception is not achievable.

For the pursuer-target dynamics modeled by (2.7) and (2.8), the capture area and the constraint on the navigation constant N_1 to ensure effective interception are given in Theorem 2.2.

Theorem 2.2 *To effectively intercept a maneuvering target modeled by (2.6) when the true proportional navigation guidance is used, the following conditions must be satisfied*

$$N_1 > 3 \tag{2.16}$$

$$C^2 > \frac{1}{N_1 - 1} + \frac{c^2 + 2c}{N_1(N_1 - 1)} \tag{2.17}$$

where

$$C = \frac{\dot{R}_0}{R_0 \dot{\sigma}_0}. \tag{2.18}$$

Proof. To guarantee effective capture, the pursuer should intercept the target with a finite acceleration and within a finite time [33]. From (2.9), N_1 should be larger than two to prevent $\dot{\sigma}$ from becoming infinity when R approaches zero at the final course of pursuit. Otherwise, an infinite control force $N_1 \dot{R} \dot{\sigma}$ is required in the final engagement.

Differentiating (2.9) leads to

$$\ddot{\sigma} = \dot{\sigma}_0 (N_1 - 2 - c) \left(\frac{R}{R_0}\right)^{N_1 - 3} \left(\frac{\dot{R}}{R_0}\right) \tag{2.19}$$

From (2.19), it follows that $N_1 > 3$ can prevent the LOS angular acceleration $\ddot{\sigma}$ from approaching infinity as $R \to 0$. Therefore, $N_1 > 3$ should hold to avoid an infinite torque on the seeker, and hence to obtain good measurements.

From the final closing speed $\dot{R}_f$ given in (2.15), we observe that condition (2.17) must be satisfied in order to obtain a real $\dot{R}_f$. ∎

Remarks.

- The inequality (2.17) determines the ranges of $\dot{\sigma}_0$, R_0, and $\dot{R}_0$. If these initial conditions with a given N_1 cannot satisfy the inequality, an interception (or capture) will not be achieved. Thus the inequality defines the *capture area* for TPN based systems.
- Conditions (2.16) and (2.17) are necessary conditions for effective interception.
- Condition (2.16) provides a guideline for choosing N_1 in the system design.
- In real applications, the navigation constant N_1 is chosen between 3 and 6. The constraint $N_1 > 3$ obtained in Theorem 2.2 substantiates the empirical rule. As to the upper limit $N_1 < 6$, it prevents the pursuer from being too sensitive in response.
- For the case engaging a non-maneuvering target, i.e., when $c = 0$, the capture area becomes

$$C^2 > \frac{1}{N_1 - 1} \tag{2.20}$$

Note the smaller the lower bound of C^2 means the less stringent the constraints on system initial conditions for effective interception, and thus the larger the capture area. Comparing (2.17) and (2.20) reveals that under the TPN guidance law, the capture area decreases with an increase in target maneuverability. The guidance system has the largest capture area when pursuing a non-maneuvering target, as shown in the solid line in Figure 2.3, which is constructed from (2.16) and (2.17). The effect of the target maneuver in causing the capture area to shrink is illustrated in Figure 2.3.

2.5 Total Control Effort

Total control effort, which is determined by cumulative velocity increment, represents the total fuel requirement on an interceptor in the entire pursuit. Therefore, total control effort is an important factor when evaluating system performance.

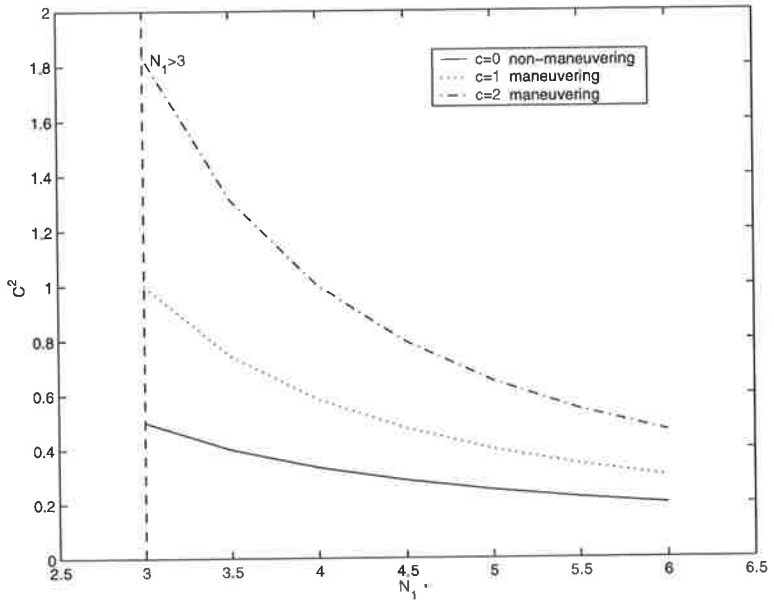

Figure 2.3: Capture area when pursuing non-maneuvering and maneuvering targets under TPN

The cumulative velocity increment necessary for interception is defined for any pursuer trajectory as [39]

$$\Delta V = \int_0^{t_f} |A_P| dt \tag{2.21}$$

where t_f is the final time when interception occurs, and A_P is the pursuer acceleration.

Theorem 2.3 *Given a TPN based interceptor engaging a maneuvering target, as described in (2.7) and (2.8), the cumulative velocity increment which defined the total control effort during the entire engagement is given as [40]*

$$\Delta V = \frac{R_0 N_1 (1+c)}{N_1 - 1} |\dot{\sigma}_0| \tag{2.22}$$

Proof. To make the best use of the obtained solutions in terms of the range, the cumulative velocity increment ΔV in (2.21) can be rewritten as

$$\Delta V = \int_{R_0}^{0} \left| \frac{A_P}{\dot{R}} \right| dR \tag{2.23}$$

Substituting the definition of TPN in (2.1) into (2.23) and normalizing the resultant integral, we obtain ΔV as

$$\Delta V = R_0 \int_0^1 |N_1 \dot{\sigma}| d\left(\frac{R}{R_0}\right) \tag{2.24}$$

Without loss of generality, it is assumed here that the interceptor can provide the acceleration called for. That is, the system has sufficient acceleration capability to avoid saturation. The saturation problem will be investigated in detail in Chapter 4. Substituting the expression of $\dot{\sigma}$ given in (2.9) into (2.24), the ΔV required on a TPN based interceptor in pursuit of a maneuvering target is obtained as (2.22). ∎

Remarks.

- From (2.22), it follows that the total control effort required to intercept a target is proportional to the target maneuverability represented by the constant c. The more maneuverable the target, the more control effort needed. This is understandable as more control effort is consumed to counteract the target maneuver. The total control effort reaches its minimum as $\Delta V = \frac{R_0 N_1}{N_1 - 1} |\dot{\sigma}_0|$ when $c = 0$, which represents engaging a non-maneuvering target.

- The term $\frac{N_1}{N_1 - 1}$ in (2.22) can be equivalently rewritten as $\left(1 + \frac{1}{N_1 - 1}\right)$. It suggests that the larger navigation constant N_1, the less total control effort needed. This is not obvious. It can be explained as a larger navigation constant enabling the pursuer to reduce initial error more rapidly, resulting in using less propellant.

2.6 Observability Analysis

Systems with bearings-only measurements, provided by passive low-cost seekers, are very common in modern guidance and target tracking. Unfortunately, when TPN is utilized for such guidance systems with limited information via angle measurements, its closed loop may show unsatisfactory performance near the end of the interception [8, 19]. The problem is caused by the lack of observability in the range and the range rate when the pursuer and the target are in a collision course. As a result, the estimates may diverge, and the implementation of the TPN guidance law during the critical end game can be problematic.

To better understand the problem of the poor observability associated with bearings-only pursuer-target systems under the TPN guidance scheme, the observability characteristics and requirements are investigated in this section. Firstly, necessary and sufficient observability criteria for general target-pursuit systems are rigorously established. To illustrate the approach used to derive necessary and sufficient observability conditions for the bearings-only measurement models, a non-maneuvering target model is first considered due to its simpler geometry. We present the observability grammian for the model and investigate the linear dependency test of the grammian. Building on the results of the non-maneuvering target, a maneuvering target characterized by a first-order lag target acceleration model with a first-order dynamic acceleration input is considered. Then, a set of observability requirements suitable for practical applications involving commonly used proportional navigation guidance is derived. We show that the observability conditions obtained are general ones, which cover results of previous work. Finally, we study the observability of the bearings-only measurement guidance systems incorporating TPN in closed loop with the aid of the established observability criteria.

2.6.1 Non-maneuvering Target Engagement

In studying system observability, it is convenient to use Cartesian coordinate because the system model recast in the Cartesian coordinate yields a set of linear state equations. The two-dimensional pursuer-target engagement geometry in the Cartesian coordinate is redrawn as Figure 2.4. Consider the geometry of the pursuer-target system with bearings-only measurements in the two-dimensional Cartesian coordinate shown in Fig 2.4. For an interceptor with a constant forward velocity V_P pursuing a target with a constant forward velocity V_T, the dynamical equations can be expressed in terms of the relative range vector $R(t) = [R_x(t), R_y(t)]^T$ and the relative velocity vector $V(t) = [V_x(t), V_y(t)]^T$ as

$$\begin{array}{rclcrcl} \dot{R}(t) & = & V(t); & & R(t_0) & = & R_0 = [R_{x0}, R_{y0}]^T \\ \dot{V}(t) & = & -A_P(t); & & V(t_0) & = & V_0 = [V_{x0}, V_{y0}]^T \end{array} \tag{2.25}$$

where $A_P(t) = [A_{Px}(t), A_{Py}(t)]^T$ is the control command acceleration.

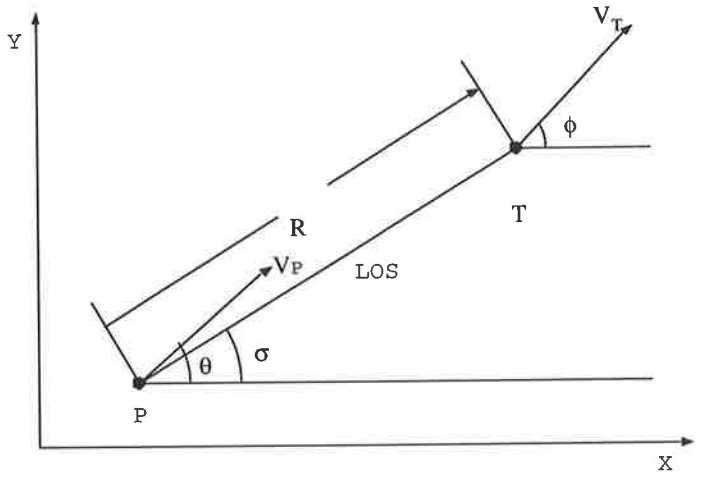

Figure 2.4: Two-dimensional guidance engagement with pursuer heading angle θ and target heading angle ϕ in Cartesian coordinate

With the system state vector $X(t) = [R_x(t), R_y(t), V_x(t), V_y(t)]^T$, the system motion (2.25) written in the state equation form is

$$\dot{X}(t) = FX(t) + GA_P(t) \tag{2.26}$$

where

$$F = \begin{bmatrix} 0 & I_2 \\ 0 & 0 \end{bmatrix} \quad \text{and} \quad G = \begin{bmatrix} 0 \\ -I_2 \end{bmatrix}$$

with I_2 being a 2×2 identity matrix.

The solution to the state equation (2.26) is

$$X(t) = \Phi(t, t_0)X(t_0) + \int_{t_0}^{t} \Phi(t, s)GA_P(s)ds \tag{2.27}$$

where Φ is the state transition matrix, taking the form

$$\Phi(t, t_0) = \begin{bmatrix} I_2 & \Delta t I_2 \\ 0 & I_2 \end{bmatrix} \quad \text{with } \Delta t = t - t_0 \tag{2.28}$$

For a two-dimensional bearings-only spatial guidance system, only the line-of-sight (LOS) angle $\sigma(t)$ can be measured, and it is expressed as

$$\sigma(t) = \tan^{-1} \frac{R_y(t)}{R_x(t)} \tag{2.29}$$

The presence of nonlinear measurement poses considerable difficulties in analyzing the system observability. The usual approach to handle such a nonlinear problem is via linearization, which is used in [12] and [13]. Insights into the relationship between the state variables and the system observability after linearization are provided in these papers. However, only sufficient conditions for unobservability of the system are derived. In order to benefit from the equivalent linear form of real measurement (2.29) without involving linearization, we write the measurement equation as

$$\begin{aligned} Y(t) &= [\tan\sigma(t) \quad -1 \;\; 0 \;\; 0]X(t) \\ &= M(t)X(t) \;=\; 0 \end{aligned} \tag{2.30}$$

which is called the pseudo-measurement equation. Now the issue of interest is whether or not the system described by (2.26) with the measurement (2.30) is observable, that is, whether a *unique* state trajectory at t_0 is constructible from the observation of $\sigma(t)$ over a finite time $(t_0, t]$.

Theorem 2.4 *A necessary and sufficient observability condition for the pursuer guidance system engaged in a non-maneuvering target described by (2.26) and (2.30) is*

$$\begin{bmatrix} R_x(t) \\ R_y(t) \end{bmatrix} \neq f(t) \begin{bmatrix} a_{11} + a_{12}\Delta t \\ a_{21} + a_{22}\Delta t \end{bmatrix} \tag{2.31}$$

or its equivalence

$$\begin{bmatrix} \int_{t_0}^{t}(t-s)A_{Px}(s)ds \\ \int_{t_0}^{t}(t-s)A_{Py}(s)ds \end{bmatrix} \neq \begin{bmatrix} R_{x0} - a_{11}f(t) + (V_{x0} - a_{12}f(t))\,\Delta t \\ R_{y0} - a_{21}f(t) + (V_{y0} - a_{22}f(t))\,\Delta t \end{bmatrix} \tag{2.32}$$

where $f(t)$ is an arbitrary scalar function, not excluding zero, and a_{ij}s are arbitrary constants but not all zeros.

Proof. According to the observability theorem [41], the system model described by (2.26) and (2.30) at time t_0 is observable over the interval $(t_0, t]$, if and only if, the grammian matrix

$$D(t, t_0) = \int_{t_0}^{t} \Phi^T(\tau, t_0) M^T(\tau) M(\tau) \Phi(\tau, t_0) d\tau \tag{2.33}$$

is positive definite for some $t > t_0$. Note that the positive definiteness of $D(t, t_0)$, the non-singularity of $D(t, t_0)$, and the linear independence of the columns of $M(t)\Phi(t, t_0)$ are equivalent to one another. In our study, linear independence of the columns of $M(t)\Phi(t, t_0)$ is examined to derive a necessary and sufficient condition for system observability.

The system is observable at time t_0 over the interval $(t_0, t]$ if and only if the columns of $M(t)\Phi(t, t_0)$ are linearly independent [41]. It follows that the observability condition for the system described by (2.26) and (2.30) is that, for any 4×1 nonzero constant vector α,

$$M(t)\Phi(t, t_0)\alpha \neq 0 \text{ for some } t > t_0 \tag{2.34}$$

The column vector $\alpha = [a_{11}, a_{21}, a_{12}, a_{22}]^T$, where a_{ij}s are arbitrary constants, not all zero. Substituting the transition matrix (2.28) into (2.34), and using the expression of the pseudo-measurement in (2.30), we obtain the condition for the system observability

$$(a_{11} + a_{12}\Delta t)\tan\sigma(t) - (a_{21} + a_{22}\Delta t) \neq 0 \tag{2.35}$$

Replacing $\sigma(t)$ in (2.35) with (2.29) yields the observability criterion in relation to the relative position $[R_x, R_y]^T$ given in (2.31).

In addition, because of (2.27) and (2.28), we can obtain

$$\begin{bmatrix} R_x(t) \\ R_y(t) \end{bmatrix} = \begin{bmatrix} R_{x0} + V_{x0}\Delta t \\ R_{y0} + V_{y0}\Delta t \end{bmatrix} - \begin{bmatrix} \int_{t_0}^{t}(t-s)A_{Px}ds \\ \int_{t_0}^{t}(t-s)A_{Py}ds \end{bmatrix} \tag{2.36}$$

Substituting (2.36) into (2.31), a necessary and sufficient condition for the system to be observable involving the pursuer command acceleration is given in (2.32). ∎

To demonstrate that the observability condition (2.32) is a general one, we apply it to some particular cases which appear in [9, 11].

- Let $\alpha = [R_{x0}, R_{y0}, V_{x0}, V_{y0}]$ and $f(t) = 1$ in (2.32), we have

$$\int_{t_0}^{t}(t-s)A_P(s)ds \neq 0 \tag{2.37}$$

  as a necessary condition for the system to be observable. This condition implies that in the absence of a pursuer acceleration, the motion of pursuer-target represented by $[R_x, R_y]^T$ remains unobservable.

- Replacing α with $[R_{x0}, R_{y0}, V_{x0}, V_{y0}]$ in (2.32) and then using (2.29) and (2.36), the condition can be rearranged as

$$\int_{t_0}^{t} (t-s)[A_{Px}(s)\tan\sigma(s) - A_{Py}(s)]ds \neq 0 \tag{2.38}$$

  This condition is in essence the criterion of Nardone and Aidala [9]. It is only a necessary observability condition, as Fogel and Gavish pointed out [11], since the arbitrary constants a_{ij}s are substituted with the values of the system state variables at the duration when observability is of interest. Note that t_0 is the time when observability is examined. The expression in (2.38) also reveals that there exists a constraint such that $A_{Px}(t)/A_{Py}(t) \neq \tan\sigma(t)$. This constraint means that the command acceleration of the pursuer cannot always be lateral to the line-of-sight (LOS) throughout the whole engagement if observability is to be maintained.

- Although only a two-dimensional case is treated here, the approach to derive the observability condition is applicable to a three-dimensional pursuer-target engagement. This can be done by introducing Z-axis components to the system model (2.26) and the pseudo-measurement (2.30).

Necessary observability conditions (2.37) and (2.38) can be converted into sufficient unobservability conditions for the system. These sufficient conditions are particularly useful in identifying those control laws which may have the undesirable effect of introducing unobservability to the system. The use of the sufficient conditions is discussed further in section 2.6.3.

2.6.2 Maneuvering Target Engagement

The criteria obtained for the non-maneuvering target engagement have served to illustrate some essential observability concepts in bearings-only guidance systems. To be practically useful, we need additional criteria to handle observability with maneuverable targets. We now extend the results in the previous section to maneuvering target models.

The system motion of the maneuvering target engagement can be described by (2.26). The system state vector consists of not only the relative range and the relative velocity, but

also the maneuvering target acceleration $[A_{Tx}, A_{Ty}]^T$, i.e.,

$$X(t) = [R_y, R_y, V_x, V_y, A_{Tx}, A_{Ty}]^T.$$

The maneuvering target acceleration can take different forms, such as constant acceleration [13, 15], first-order lag target model with zero input [16, 42], and first-order lag target model with constant acceleration input [15]. A first-order lag target model with a first-order dynamic input is used in the derivation.

The maneuvering target acceleration model is

$$\dot{A}_T + \lambda A_T = U_T \tag{2.39}$$

where $U_T = [U_{Tx}, U_{Ty}]^T$ represents the target acceleration input vector, and λ is a constant. The associated target acceleration input U_T is modeled as

$$\dot{U}_T + \beta U_T = \mu \tag{2.40}$$

where β is a constant, and μ is a constant variable. This first-order dynamic input models the inertia due to the actuator and the pilot response.

The target acceleration model (2.39) with input model (2.40) is a more general one since it encompasses the constant target acceleration model as well as the first-order lag target acceleration model with constant input. The observability criteria are derived for this target model.

With (2.39) and (2.40), the system state model is

$$\dot{X}(t) = FX(t) + GA_P(t) \tag{2.41}$$

where $X = [R_x, R_y, V_x, V_y, A_{Tx}, A_{Ty}, U_{Tx}, U_{Ty}, \mu_x, \mu_y]^T$,

$$F = \begin{bmatrix} 0 & I_2 & 0 & 0 & 0 \\ 0 & 0 & I_2 & 0 & 0 \\ 0 & 0 & -\lambda I_2 & I_2 & 0 \\ 0 & 0 & 0 & -\beta I_2 & I_2 \\ 0 & 0 & 0 & 0 & 0 \end{bmatrix} \quad \text{and} \quad G = \begin{bmatrix} 0 \\ -I_2 \\ 0 \\ 0 \\ 0 \end{bmatrix}$$

The pseudo-measurement takes the form, which is similar to (2.30), as

$$Y(t) = [\tan\sigma(t) \quad -1 \quad \mathbf{0}_{1\times 8}]X(t) = M(t)X(t) \tag{2.42}$$

where $\mathbf{0}_{1\times 8}$ denotes a 1×8 zero vector here.

The observability criteria for the maneuvering target engagement is as follows.

Theorem 2.5 *A necessary and sufficient observability condition for the pursuer guidance system described by (2.41) and (2.42), engaging a maneuvering target characterized by (2.39) with a first-order dynamic target acceleration input (2.40), is*

$$\begin{bmatrix} R_x(t) \\ R_y(t) \end{bmatrix} \neq f(t) \begin{bmatrix} a_{11} + a_{12}\Delta t + a_{13}\Phi_{13}(\Delta t) + a_{14}\Phi_{14}(\Delta t) + a_{15}\Phi_{15}(\Delta t) \\ a_{21} + a_{22}\Delta t + a_{23}\Phi_{13}(\Delta t) + a_{24}\Phi_{14}(\Delta t) + a_{25}\Phi_{15}(\Delta t) \end{bmatrix} \tag{2.43}$$

or its equivalence

$$\begin{aligned} \begin{bmatrix} \int_{t_0}^{t}(t-s)A_{Px}(s)ds \\ \int_{t_0}^{t}(t-s)A_{Py}(s)ds \end{bmatrix} \neq \begin{bmatrix} R_{x0} - a_{11}f(t) + (V_{x0} - a_{12}f(t))\,\Delta t \\ R_{y0} - a_{21}f(t) + (V_{y0} - a_{22}f(t))\,\Delta t \end{bmatrix} \\ + (A_{Tx0} - a_{13}f(t))\,\Phi_{13}(\Delta t) + (U_{Tx0} - a_{14}f(t))\,\Phi_{14}(\Delta t) \\ + (A_{Ty0} - a_{23}f(t))\,\Phi_{13}(\Delta t) + (U_{Ty0} - a_{24}f(t))\,\Phi_{14}(\Delta t) \\ \begin{bmatrix} + (\mu_x - a_{15}f(t))\,\Phi_{15}(\Delta t) \\ + (\mu_y - a_{25}f(t))\,\Phi_{15}(\Delta t) \end{bmatrix} \end{aligned} \tag{2.44}$$

where $f(t)$ is an arbitrary scalar function, not excluding zero, a_{ij}s are arbitrary constants but not all zeros, and

$$\Phi_{13}(\Delta t) = \frac{1}{\lambda^2}(e^{-\lambda\Delta t} + \lambda\Delta t - 1) \tag{2.45}$$

$$\Phi_{14}(\Delta t) = \frac{1}{\beta - \lambda}\left[\frac{1}{\lambda^2}(e^{-\lambda\Delta t} + \lambda\Delta t - 1) - \frac{1}{\beta^2}(e^{-\beta\Delta t} + \beta\Delta t - 1)\right] \tag{2.46}$$

$$\begin{aligned} \Phi_{15}(\Delta t) = \frac{1}{\beta - \lambda}\left\{\left[\frac{\Delta t^2}{2\lambda} - \frac{(e^{-\lambda\Delta t} + \lambda\Delta t - 1)}{\lambda^3}\right]\right. \\ \left. - \left[\frac{\Delta t^2}{2\beta} - \frac{(e^{-\beta\Delta t} + \beta\Delta t - 1)}{\beta^3}\right]\right\} \end{aligned} \tag{2.47}$$

Proof. Similar to the non-maneuvering target engagement, a necessary and sufficient observability condition for the system given by (2.41) and (2.42) can be established by studying the linear independence of the columns of the measurement matrix times the transition matrix.

With the pseudo-measurement (2.42), the measurement matrix $M(t)$ is given as

$$M(t) = [\tan\sigma(t) \quad -1 \quad \mathbf{0}_{1\times 8}].$$

The transition matrix is obtained as

$$\Phi(t,t_0) =$$

$$\begin{bmatrix} I_2 & \Delta t I_2 & \Phi_{13}(\Delta t)I_2 & \Phi_{14}(\Delta t)I_2 & \Phi_{15}(\Delta t)I_2 \\ 0 & I_2 & \frac{1}{\lambda}\left(1-e^{-\lambda\Delta t}\right)I_2 & \Phi_{24}(\Delta t)I_2 & \Phi_{25}(\Delta t)I_2 \\ 0 & 0 & e^{-\lambda\Delta t}I_2 & \frac{1}{\beta-\lambda}\left(e^{-\lambda\Delta t}-e^{-\beta\Delta t}\right)I_2 & \Phi_{35}(\Delta t)I_2 \\ 0 & 0 & 0 & e^{-\beta\Delta t}I_2 & \frac{1}{\beta}\left(1-e^{-\beta\Delta t}\right)I_2 \\ 0 & 0 & 0 & 0 & I_2 \end{bmatrix} \tag{2.48}$$

where Φ_{13}, Φ_{14}, and Φ_{15} are given in (2.45), (2.46), and (2.47), respectively, and

$$\Phi_{24}(\Delta t) = \frac{1}{\beta-\lambda}\left(\frac{1-e^{-\lambda\Delta t}}{\lambda} - \frac{1-e^{-\beta\Delta t}}{\beta}\right) \tag{2.49}$$

$$\Phi_{25}(\Delta t) = \Phi_{14}(\Delta t) \tag{2.50}$$

$$\Phi_{35}(\Delta t) = \Phi_{24}(\Delta t)$$

The system described by (2.41) with the measurement (2.42) is observable, if and only if,

$$M(t)\Phi(t,t_0)\alpha \neq 0 \text{ for some } t > t_0 \tag{2.51}$$

where α is any 10×1 nonzero constant vector, written as

$$\alpha = [a_{11}, a_{21}, a_{12}, a_{22}, a_{13}, a_{23}, a_{14}, a_{24}, a_{15}, a_{25}]^T \tag{2.52}$$

Substituting (2.42) and (2.48) into (2.51) leads to the observability condition (2.43), which is expressed with respect to $[R_x, R_y]^T$.

From (2.27) and (2.48), part of the solution to (2.41) is

$$\begin{bmatrix} R_x(t) \\ R_y(t) \end{bmatrix} = \begin{bmatrix} R_{x0} + V_{x0}\Delta t + A_{Tx0}\Phi_{13}(\Delta t) + U_{Tx0}\Phi_{14}(\Delta t) + \mu_x\Phi_{15}(\Delta t) \\ R_{y0} + V_{y0}\Delta t + A_{Ty0}\Phi_{13}(\Delta t) + U_{Ty0}\Phi_{14}(\Delta t) + \mu_y\Phi_{15}(\Delta t) \end{bmatrix} - \begin{bmatrix} \int_{t_0}^{t}(t-s)A_{Px}ds \\ \int_{t_0}^{t}(t-s)A_{Py}ds \end{bmatrix} \tag{2.53}$$

Combining (2.43) and (2.53), the observability criterion in terms of pursuer command acceleration is given in (2.44). ∎

To illustrate the generality of (2.44) as an observability requirement, we will show how the different choices of the components of α in (2.52), and the different values of β and μ, give different observability conditions in which results of some previous work are covered.

- If α defined in (2.52) equals

  $$[R_{x0}, R_{y0}, V_{x0}, V_{y0}, A_{Tx0}, A_{Ty0}, U_{Tx0}, U_{Ty0}, \mu_x, \mu_y]^T$$

  and $f(t) = 1$, then (2.44) becomes

  $$\int_{t_0}^{t}(t-s)A_P(s)ds \neq 0 \tag{2.54}$$

  This necessary observability condition requires that the pursuer acceleration cannot be absent. This condition is the same as the condition for the non-maneuvering target case shown in (2.37). It thus follows that the pursuer acceleration must present for the system to be observable in both a non-maneuvering engagement and a maneuvering engagement.

- If the components of α are such that

  $$\alpha = [R_{x0}, R_{y0}, V_{x0}, V_{y0}, A_{Tx0}, A_{Ty0}, U_{Tx0}, U_{Ty0}, \mu_x, \mu_y]^T$$

  then a necessary condition for system to be observable is

  $$\int_{t_0}^{t}(t-s)\left\{[A_{Px}(s) - A_{Tx}(s)]\tan\sigma(s) - [A_{Py}(s) - A_{Ty}(s)]\right\}ds \neq 0 \tag{2.55}$$

  which is one of the main results in [13]. This condition indicates that the target maneuvering acceleration cannot be the mirror image of the pursuer acceleration for an

observable engagement. It also implies that the command acceleration of the pursuer A_P and the target acceleration A_T cannot be both along the line-of-sight (LOS) throughout the whole pursuit if the system is to be observable.

- If some components of α are fixed, *viz*,

$$[a_{13}, a_{23}, a_{14}, a_{24}, a_{15}, a_{25}]^T = [A_{Tx0}, A_{Ty0}, U_{Tx0}, U_{Ty0}, \mu_x, \mu_y]^T$$

then the observability condition is

$$\begin{bmatrix} \int_{t_0}^{t}(t-s)[A_{Px}(s) - A_{Tx}(s)]ds \\ \int_{t_0}^{t}(t-s)[A_{Py}(s) - A_{Ty}(s)]ds \end{bmatrix} \neq \begin{bmatrix} R_{x0} - a_{11}f(t) + (V_{x0} - a_{12}f(t))\,\Delta t \\ R_{y0} - a_{21}f(t) + (V_{y0} - a_{22}f(t))\,\Delta t \end{bmatrix} \tag{2.56}$$

Note that (2.32) and (2.56) are very similar, except that the former is a necessary and sufficient condition for a non-maneuvering target case, while the latter is only a necessary observability condition for a maneuvering target case.

Although the derivation of (2.56) is based on a target model with first-order dynamic input, the result can indeed be extended to any target acceleration model. The pursuer-target engagement for any target acceleration model can be represented as:

$$\begin{aligned} \dot{R}(t) &= V(t) \\ \dot{V}(t) &= A_T(t) - A_P(t) \end{aligned} \tag{2.57}$$

Following the same approach as in section 2.6.1, the condition same as (2.56) can be derived for the range and the velocity to be observable.

- When $\beta = \mu = 0$, the target becomes a first-order lag target acceleration model with constant acceleration input. This is the model studied by Song [15]. As μ is zero, it is excluded from the state vector, i.e., the state vector X becomes

$$[R_x, R_y, V_x, V_y, A_{Tx}, A_{Ty}, U_{Tx}, U_{Ty}]^T.$$

Meanwhile, F, G in (2.41), and the transition matrix (2.48) reduce to an 8×8 matrix, an 8×2 matrix, and an 8×8 matrix, respectively. Correspondingly, $\Phi_{15}(\Delta t)$ in

transition matrix (2.48) vanishes. The observability condition can still be represented by (2.43) and (2.44), but Φ_{14} and Φ_{15} take simpler forms, as

$$\Phi_{14}(\Delta t) = \frac{\Delta t^2}{2\lambda} - \frac{1}{\lambda^3}(e^{-\lambda\Delta t} + \lambda\Delta t - 1) \tag{2.58}$$

and

$$\Phi_{15}(\Delta t) = 0. \tag{2.59}$$

This result matches the observability criteria developed in [15].

- It is informative to compare the observability characteristics of the first-order lag target acceleration model with constant input, against the same target acceleration model with first-order input. For the former, the related equations are (2.43), (2.44), (2.45), (2.58), and (2.59), while for the latter, the equations are (2.43), (2.44), (2.45), (2.46), and (2.47). We observe that the more complicated the target acceleration input is, the more variables need to be estimated. Consequently, in order for the system to be observable, more stringent conditions need to be satisfied. In other words, it is more difficult to find observable trajectories, and harder to select a control law to guarantee the observability, when the acceleration input of the maneuverer is more sophisticated.

2.6.3 Observability with TPN

Observability during the final stage of pursuit is a major part of this study. Sufficient unobservability conditions will be utilized in the performance analysis of the control laws, as sufficient conditions allow us to check observability with a greater degree of certainty.

Sufficiency of unobservability is equivalent to necessity of observability. The equivalence comes from the fact that all the necessary observability conditions in (2.37), (2.38), (2.54), (2.55) and (2.56) can be changed into sufficient conditions for the system to be unobservable if each unequal sign is replaced by an equal sign.

For a non-maneuvering target case, sufficient unobservability conditions at t_0 over the duration $(t_0, t]$ can be obtained from (2.37) and (2.38), respectively, as

$$\int_{t_0}^{t} (t-s) A_P(s) ds = 0 \tag{2.60}$$

and

$$\int_{t_0}^{t} (t-s)[A_{Px}(s)\tan\sigma(s) - A_{Py}(s)] ds = 0 \tag{2.61}$$

Note that sufficient condition (2.60) is less stringent than (2.61), since (2.60) covers less unobservable cases than those in (2.61). However, (2.60) is easier to utilize in observability analysis due to its simple expression.

For a maneuvering target case, sufficient unobservability conditions at t_0 over the duration $(t_0, t]$ derived from (2.54), (2.55), and (2.56), respectively, are

$$\int_{t_0}^{t}(t-s)A_P(s)ds = 0 \tag{2.62}$$

$$\int_{t_0}^{t}(t-s)\left\{[A_{Px}(s)-A_{Tx}(s)]\tan\sigma(s)-[A_{Py}(s)-A_{Ty}(s)]\right\}ds = 0 \tag{2.63}$$

and

$$\begin{bmatrix} \int_{t_0}^{t}(t-s)[A_{Px}(s)-A_{Tx}(s)]ds \\ \int_{t_0}^{t}(t-s)[A_{Py}(s)-A_{Ty}(s)]ds \end{bmatrix} = \begin{bmatrix} R_{x0}-a_{11}f(t)+(V_{x0}-a_{12}f(t))\,\Delta t \\ R_{y0}-a_{21}f(t)+(V_{y0}-a_{22}f(t))\,\Delta t \end{bmatrix} \tag{2.64}$$

From (2.62) to (2.64), the stringency of these three sufficient conditions increases. In other words, the constraint (2.64) covers the most unobservability engagements among them.

In the following discussion, both the command acceleration A_P and the target acceleration A_T are assumed to be perpendicular to LOS. For notational convenience, we define the *range observability index* $I_A(t_0, t)$ as

$$I_A(t_0,t) = \int_{t_0}^{t}(t-s)\left[A_P(s)-A_T(s)\right]ds. \tag{2.65}$$

This index plays an important role in observability check.

Non-maneuvering Target with TPN

When the pursuer guidance system engages in a non-maneuvering target, we have $A_T = 0$. The range observability index $I_A(t_0, t)$ reduces to $\int_{t_0}^{t}(t-s)A_P(s)ds$, which agrees with the left-hand side of (2.60).

When t approaches the final interception time t_f, from the solutions given in section 2.3, the LOS angular rate $\dot{\sigma}$ approaches zero, and range rate $\dot{R}$ approaches a constant.

Under TPN, the range observability index is

$$\begin{aligned} I_A(t_0, t_f) &= \int_{t_0}^{t_f} (t_f - s) A_P(s) ds \\ &= \int_{t_0}^{t_f} (t_f - s)(N_1 \dot{\sigma} \dot{R}) ds \\ &\approx \int_{t_0}^{t_f} (t_f - s)(N_1 \cdot 0 \cdot \dot{R}) = 0 \end{aligned} \tag{2.66}$$

As the LOS angular rate $\dot{\sigma}$ is nullified by the TPN control scheme, the integral vanishes for any value of the navigation constant N_1. Based on the sufficient unobservability condition in (2.60), we find that if the TPN guidance law is used in a non-maneuvering target engagement, the system is most likely to become unobservable near the final course. A direct consequence is that the Kalman filter of the TPN based guidance system will suffer from the divergence problem in the final phase of the engagement, when it estimates the system state variables. When no reliable estimates are available to be fed back to the guidance laws, it is highly likely that the pursuer will be misled from the target, and will fail in accomplishing the interception mission.

Maneuvering Target with TPN

For the maneuvering target case, the target acceleration is assumed to take the form

$$A_T = c\dot{\sigma}_0 \dot{R} \tag{2.67}$$

where c is the target maneuver constant. The target model is obtained by the application of composition $A_T = \sqrt{A_{TR}^2 + A_{T\sigma}^2}$ to (2.6). From (2.67), we see that $\dot{A}_T \approx c\dot{\sigma}_0(A_T - A_P)$. Therefore, the target model (2.67) represents approximately a first-order lag target model and matches well with the target model (2.39) used in section 2.6.2.

When t approaches t_f, the LOS angular rate approaches $c\dot{\sigma}_0/(N_1 - 2)$. This constant is very small since $\dot{\sigma}_0$ is usually small in practice. The final closing speed $\dot{R}_f$ also approaches a constant.

Since none of the conditions (2.62)–(2.64) is obviously satisfied for maneuvering engagements with TPN, condition (2.64), being the most stringent, is chosen to check observability.

With TPN, we have the range observability index

$$\begin{aligned} I_A(t_0, t_f) &= \int_{t_0}^{t_f} (t_f - s)[A_P(s) - A_T(s)]ds \\ &= \int_{t_0}^{t_f} (t_f - s)(N_1 \dot{\sigma} \dot{R} - c\dot{\sigma}_0 \dot{R})ds \\ &\approx \frac{c\dot{\sigma}_0 \dot{R}_f}{N_1 - 2}(t_f - t_0)^2 \end{aligned} \tag{2.68}$$

The left-hand side of the sufficient unobservability condition (2.64) becomes

$$\begin{bmatrix} \frac{c\dot{\sigma}_0 \dot{R}_f}{N_1 - 2} \cdot (t_f - t_0)^2 \cdot \sin\sigma(t) \\ \frac{c\dot{\sigma}_0 \dot{R}_f}{N_1 - 2} \cdot (t_f - t_0)^2 \cdot \cos\sigma(t) \end{bmatrix} \approx \begin{bmatrix} C_{Tx}(\Delta t)^2 \\ C_{Ty}(\Delta t)^2 \end{bmatrix} \tag{2.69}$$

where $\Delta t = t_f - t_0$ is the duration of observation, since the the system observability is examined at t_0; C_{Tx} and C_{Ty} are constants, as $\sigma(t)$ is approximately a constant since $\dot{\sigma}(t)$ is very small. According to the condition (2.64), the system is unobservable only if

$$\begin{bmatrix} C_{Tx}(\Delta t)^2 \\ C_{Ty}(\Delta t)^2 \end{bmatrix} = \begin{bmatrix} R_{x0} - a_{11}f(t) + (V_{x0} - a_{12}f(t))\,\Delta t \\ R_{y0} - a_{21}f(t) + (V_{y0} - a_{22}f(t))\,\Delta t \end{bmatrix} \tag{2.70}$$

Comparing (2.66) with (2.68), the range observability index indicates that for the TPN guidance systems with angle-only measurements engaging a maneuvering target, the range R is more likely to be observable than those engaging a non-maneuvering target. It can be interpreted as the maneuvering target may follow a curved trajectory which provides more information about itself than a straight-line trajectory of a non-maneuvering target does.

2.7 Concluding Remarks

In this chapter, the characteristics of true proportional navigation have been explored, and the observability criteria with guidance laws in closed loop have been established.

In analyzing the interception performance of TPN based systems, the exact and closed-form solution to the TPN guidance problem has been derived for a maneuvering target engagement in (2.9) and (2.10) with a non-maneuvering target engagement as a special case. Based on Theorem 2.2 that gives constraints on the system initial conditions and the navigation constant to ensure interception, predications of the occurrence of target interception can

be made. Capture area has been obtained in (2.17), which provides guidelines for launching favorable initial conditions. Total control effort of a TPN based system has been derived, as given in (2.22). Analysis indicates that a target maneuver can degrade system interception performance by slowing down the closing speed, reducing the capture area, and causing more propellant to be consumed.

To study the observability of TPN based systems with bearing-only measurements, necessary and sufficient observability conditions are first established for bearings-only guidance systems engaged in non-maneuvering targets and maneuvering targets. The constraints (2.32) and (2.44) have been shown to be general ones, which cover main results of some previous work. Using the observability criteria (2.60) and (2.64) with the range observability index (2.65), the observability of TPN based systems has been analyzed. Analysis reveals that TPN fails to offer observability when pursuing a non-maneuvering target towards the end of an engagement.

Chapter 3

Observability-Enhanced Proportional Navigation

A new observability-enhanced control law, as one of additive observable proportional navigation (AOPN) guidance laws suitable for bearings-only guidance systems, is proposed. It builds on the well established true proportional navigation (TPN) with an information enhanced term added to improve observability. Analytical studies on AOPN guidance systems are presented. A comparative study on three guidance laws is conducted to compare their observability, capturability, and sensitivity to uncertainty in initial conditions. The AOPN guidance laws are found to have favorable features in terms of offering the potential of observability enhancement and covering a larger capture area.

In short range homing missiles with angle-only measurements, true proportional navigation (TPN) is commonly used. However, the Kalman filter within the TPN guidance system has shown a deficiency in providing consistent estimation of those variables required to implement proportional guidance laws towards the end of an engagement. The degradation of the filter performance is due mainly to the fact that when the pursuer and the target are in a homing collision course in which LOS rates are nullified by proportional navigation controller, the target position and the relative velocity are unobservable from bearings-only measurements. It follows that an effective guidance law should seek to achieve not only terminal accuracy, but also information content enhancement of essential measurements, in order to excite the filter with sufficient information to generate consistent estimates.

In selecting an information measure for enhancing filter performance, a suitable candidate is the Fisher information matrix which is a commonly used measure of accuracy in determining unknown parameters from a sequence of measurements [20]. The matrix can be related to the pursuer-target interception problem through a local observability matrix when the measurement is subject to Gaussian white noise [8]. As it is easier to handle scalar quality in mathematical derivation and practical implementation, the trace or the determinant of the information matrix is used instead. Indeed, Speyer *et al* [8] and Hull *et al* [16] use the trace of the matrix as the performance index to derive numerous LQ based guidance control laws. The LQ based guidance control is effective but fairly complex to implement.

Motivated by keeping the simplicity of the true proportional navigation law, and offering better observability at the same time, a new control scheme is proposed by Hassoun and Lim [19]. It builds on the concept of TPN with an information-enhanced term added. This term is chosen to be proportional to the trace of the Fisher information matrix. The guidance laws following this control scheme are termed additive observable proportional navigation (AOPN). Simulation [19] shows that this guidance law helps in overcoming the problem of divergent estimation of the Kalman filter associated with TPN based systems, and thus is well-suited for low-cost bearing-only measurement systems. Although some preliminary work on properties of this guidance law has been carried out in [19] and [21], rigorous analysis of observability and capturability is yet to be provided.

Based on different noise models of measurements, different additive observable proportional navigation laws can be derived. A new AOPN guidance law, which is easy to realize, is proposed and analyzed in this chapter.

There are four objectives in this chapter. Firstly, complete closed-form solutions of the pursuer-target engagement under AOPN are derived. Secondly, necessary conditions for forming a collision course are established, thus providing guidelines for choosing navigation constants. We show that in terms of the best capture ability and the fastest final closing speed, AOPN guidance laws have an optimal value for their navigation constant related to the additive information term. Thirdly, the ability of AOPN laws to enhance system observability is analyzed and confirmed. Finally, system robustness performance is investigated by means of sensitivity function. The results reveal that the new AOPN law is practical because it is easy to realize, and the pertinent system is robust when subject to uncertain initial conditions. To gain further insights, we carry out comparative studies of the performance of AOPN, against that of TPN. Simulation studies are conducted to confirm the analytical findings.

3.1 System Model and Control Laws

The motion equations describing target-pursuit dynamics, which are given in (2.3) and (2.4) in section 2.2 are, for completeness, rewritten here.

$$\ddot{R} - R\dot{\sigma}^2 = A_{TR} - A_{PR} \tag{3.1}$$

$$R\ddot{\sigma} + 2\dot{R}\dot{\sigma} = A_{T\sigma} - A_{P\sigma} \tag{3.2}$$

where R is the relative range with initial value R_0; $\dot{\sigma}$ is the line-of-sight (LOS) angular rate with initial value $\dot{\sigma}_0$; A_{TR} (respectively, $A_{T\sigma}$) is the target acceleration component along LOS (respectively, normal to LOS); A_{PR} (respectively, $A_{P\sigma}$) is the pursuer acceleration component along LOS (respectively, normal to LOS).

True proportional navigation, among the guidance laws, is the most popular in short range

homing missiles [6, 7]. The control law is written as

$$A_{PR} = 0; \qquad A_{P\sigma} = -N_1 \dot{R}\dot{\sigma} \tag{3.3}$$

where N_1 is the navigation constant. TPN, however, is not always satisfactory for homing missiles with bearings-only measurements. This is because of the poor observability of the relative range and of the range rate caused by the TPN law attempting to nullify the LOS angle rate at the final pursuit [8].

To enhance the observability of the system, Hassoun and Lim [19] propose to augment TPN with an information enhanced term. The principle of the proposed guidance law is to maintain not only a constant line-of-sight angle to ensure interception, but also system observability via an additional term proportional to the range rate and the trace of Fisher information matrix [20]. The guidance law takes the form

$$A_{PR} = 0; \qquad A_{P\sigma} = -N_1 \dot{R}\dot{\sigma} - k\dot{R}\dot{\mu} \tag{3.4}$$

where k is a constant, and $\dot{\mu}$ is the trace of the rate of the Fisher information matrix. This guidance is referred to as additive observable proportional navigation (AOPN). The information related variable $\dot{\mu}$ is expressed as [8]

$$\dot{\mu} = \mathrm{tr}W \int_{t_0}^{t_f} \Phi^T H^T V^{-1} H \Phi dt = \int_{t_0}^{t_f} \mathrm{tr} H^T W H \Phi^T V^{-1} \Phi dt \tag{3.5}$$

where Φ represents the system transition matrix, H is the linearization result of the measurement equation, V is a weighting matrix taken to be the power spectral density of the measurement noise, and W is a weighting matrix. Under certain fairly general assumptions [16], $\dot{\mu}$ can be simplified as the reciprocal of the power spectral density of the measurement noise, i.e., $\dot{\mu} = V^{-1}$. For the seeker that provides bearings-only measurements, the thermal noise is modeled as a random process with a constant spectral density, while the glint noise is modeled as a random noise whose spectral density is inversely proportional to R^2.

Based on the noise models, a class of guidance laws, which offer enhanced observability and are applied in the direction of LOS, can be derived. When the glint noise is taken into account, the additive observable proportional navigation (AOPN) law becomes

$$A_{PR} = 0; \qquad A_{P\sigma} = -N_1 \dot{R}\dot{\sigma} - N_2 \dot{R} R^2 \tag{3.6}$$

where N_1 and N_2 are navigation constants. The guidance law in (3.6) is discussed in [21], and we should refer the law as AOPN-I.

When the thermal noise is taken into consideration, the additive observable proportional navigation is obtained as

$$A_{PR} = 0; \qquad A_{P\sigma} = -N_1 \dot{R}\dot{\sigma} - N_3 \dot{R} \tag{3.7}$$

where N_3 is the navigation constant related to the additive observable term. This guidance law is called AOPN-II.

Although some rudimentary study on AOPN-I is performed in [21], insights into the effects of the the new term on system interception performance and observability are needed. In this chapter, we will focus on analyzing newly proposed AOPN-II, further investigating AOPN-I, and comparing their performance with TPN, which has been studied in Chapter 2.

In analyzing the performance of the guidance system under AOPN-I and AOPN-II, closed-form solutions are first derived because the solutions constitute a tool in the analysis of system performance. Based on the solutions, the constraints required for effective interception are established. Then, observability analysis is carried out to verify that the AOPN guidance laws have provided enhanced system observability. The robustness of the AOPN and TPN guidance laws are evaluated.

3.2 Closed-Form Solution

To make our analysis practically useful, we incorporate a maneuvering target into a pursuer-target engagement. The target acceleration is chosen to take the form, as [31],

$$A_{TR} = 0; \qquad A_{T\sigma} = -c\dot{\sigma}_0 \dot{R} \tag{3.8}$$

where c is a non-negative constant. When $c = 0$, it corresponds to a non-maneuvering target engagement. When $c > 0$, the maneuvering target has the effect of reducing the effectiveness of guidance laws. The expression $A_{TR} = 0$ implies that A_T is normal to the line-of-sight (LOS).

3.2.1 AOPN-I Guidance Law

When the AOPN-I guidance law is employed, the governing equations of the pursuer-target motion are obtained by substituting the expression of AOPN-I in (3.6) and the maneuvering target acceleration model in (3.8) into (3.1) and (3.2), as

$$\ddot{R} - R\dot{\sigma}^2 = 0 \tag{3.9}$$

$$R\ddot{\sigma} + 2\dot{R}\dot{\sigma} = N_1\dot{R}\dot{\sigma} + N_2\dot{R}R^2 - c\dot{\sigma}_0\dot{R} \tag{3.10}$$

While a closed-form solution to (3.9) and (3.10) is given in [19], it does not include the solution for the $N_1 = 4$ case. A complete solution with an expression for the special case $N_1 = 4$ is now derived.

Theorem 3.1 *A closed-form solution to the target-pursuit motion equations in (3.9) and (3.10), which represent a maneuvering target engagement using the additive observable proportional navigation law AOPN-I, consists of two parts.*

(i) The LOS angular rate,

when $N_1 \neq 4$ *and* $N_1 > 3$, *is*

$$\dot{\sigma} = \dot{\sigma}_0\left(\frac{R}{R_0}\right)^{N_1-2} + \frac{N_2}{4-N_1}R^2\left[1-\left(\frac{R}{R_0}\right)^{N_1-4}\right] + \frac{c\dot{\sigma}_0}{N_1-2}\left[1-\left(\frac{R}{R_0}\right)^{N_1-2}\right]; \tag{3.11}$$

when $N_1 = 4$, *is*

$$\dot{\sigma} = \dot{\sigma}_0\left(\frac{R}{R_0}\right)^2 + N_2R^2\ln\left(\frac{R}{R_0}\right) + \frac{c\dot{\sigma}_0}{N_1-2}\left[1-\left(\frac{R}{R_0}\right)^2\right]. \tag{3.12}$$

(ii) The relative velocity $\dot{R}$,

when $N_1 \neq 4$ *and* $N_1 > 3$, *is*

$$\dot{R}^2 = R_0^2\dot{\sigma}_0^2\left[\frac{m^2}{3}\left(\frac{R}{R_0}\right)^6 + mn\left(\frac{R}{R_0}\right)^4 + n^2\left(\frac{R}{R_0}\right)^2 + \frac{(1-n-m)^2}{N_1-1}\left(\frac{R}{R_0}\right)^{2N_1-2} + \frac{4m(1-n-m)}{N_1+2}\left(\frac{R}{R_0}\right)^{N_1+2} + \frac{4n(1-n-m)}{N_1}\left(\frac{R}{R_0}\right)^{N_1}\right] + \dot{R_0}^2 - R_0^2\dot{\sigma}_0^2\left[\frac{m^2}{3} + mn + n^2 + \frac{(1-n-m)^2}{N_1-1}\right.$$

$$+\frac{4m(1-n-m)}{N_1+2}+\frac{4n(1-n-m)}{N_1}\Bigg]; \tag{3.13}$$

when $N_1 = 4$, *is*

$$\begin{aligned}\dot{R}^2 &= R_0^2\dot{\sigma}_0^2\left\{\left(\frac{N_2R_0^2}{\dot{\sigma}_0}\right)^2\left[\frac{1}{3}(\frac{R}{R_0})^6\ln^2(\frac{R}{R_0})-\frac{1}{9}(\frac{R}{R_0})^6\ln(\frac{R}{R_0})+\frac{1}{54}(\frac{R}{R_0})^6\right]\right.\\
&+\frac{2N_2R_0^2(1-n)}{\dot{\sigma}_0}\left[\frac{1}{3}(\frac{R}{R_0})^6\ln(\frac{R}{R_0})-\frac{1}{18}(\frac{R}{R_0})^6\right]\\
&+\frac{N_2R_0^2n}{\dot{\sigma}_0}\left[(\frac{R}{R_0})^4\ln(\frac{R}{R_0})-\frac{1}{4}(\frac{R}{R_0})^4\right]\\
&\left.+\frac{(1-n)^2}{3}(\frac{R}{R_0})^6+n(1-n)(\frac{R}{R_0})^4+n^2(\frac{R}{R_0})^2\right\}+\dot{R}_0^2\\
&-R_0^2\dot{\sigma}_0^2\left[\frac{1}{54}\left(\frac{N_2R_0^2}{\dot{\sigma}_0}\right)^2-\frac{5n+4}{36}\left(\frac{N_2R_0^2}{\dot{\sigma}_0}\right)+\frac{(1-n)^2}{3}+n\right],\end{aligned} \tag{3.14}$$

where

$$m=\frac{N_2R_0^2}{(4-N_1)\dot{\sigma}_0} \tag{3.15}$$

and

$$n=\frac{c}{N_1-2}. \tag{3.16}$$

Proof. The same method as that used in the solution derivation under TPN in Chapter 2 is used here. Multiplying $\frac{R}{\dot{R}}$ on both sides of (3.10), and rearranging the equations with respect to the unit mass angular momentum of the pursuer (defined by $R^2\sigma$), yields the LOS angular rate $\dot{\sigma}$ as (3.11) and (3.12). Note that $\dot{\sigma}$ is obtained by imposing the constraint $N_1 > 3$, which will be shown to be necessary for effective interception in Theorem 3.3.

Substituting $\dot{\sigma}$ in (3.11) and (3.12) into (3.9), and noting that $\ddot{R}dR = d\left(\frac{\dot{R}^2}{2}\right)$, the solution in terms of the range rate can be expressed as in (3.13) and (3.14). ∎

Remarks.

- The solution given in (3.11)–(3.14) is fairly general and is directly applicable to a non-maneuvering target case as follows.

  (i) The LOS angular rate $\dot{\sigma}$ is,

  when $N_1 \neq 4$ and $N_1 > 3$,

$$\dot{\sigma} = \dot{\sigma}_0(\frac{R}{R_0})^{N_1-2} + \frac{N_2}{(4-N_1)}R^2\left[1-(\frac{R}{R_0})^{N_1-4}\right]; \tag{3.17}$$

when $N_1 = 4$,

$$\dot{\sigma} = \dot{\sigma}_0(\frac{R}{R_0})^2 + N_2R^2\ln(\frac{R}{R_0}). \tag{3.18}$$

(ii) The relative velocity $\dot{R}$ is,

when $N_1 \neq 4$ and $N_1 > 3$,

$$\begin{aligned}\dot{R}^2 &= R_0^2\dot{\sigma}_0^2\left[\frac{m^2}{3}(\frac{R}{R_0})^6 + \frac{4m(1-m)}{N_1+2}(\frac{R}{R_0})^{N_1+2} + \frac{(1-m)^2}{N_1-1}(\frac{R}{R_0})^{2N_1-2}\right] \\ &+ \dot{R}_0^2 - R_0^2\dot{\sigma}_0^2\left[\frac{m^2}{3} + \frac{4m(1-m)}{N_1+2} + \frac{(1-m)^2}{N_1-1}\right];\end{aligned} \tag{3.19}$$

when $N_1 = 4$,

$$\begin{aligned}\dot{R}^2 &= \frac{R_0^2\dot{\sigma}^2}{3}(\frac{R}{R_0})^6\left\{1+\left(\frac{N_2R_0^2}{\dot{\sigma}_0}\right)^2\left[\ln^2(\frac{R}{R_0}) - \frac{1}{3}\ln(\frac{R}{R_0}) + \frac{1}{18}\right]\right. \\ &\left.+\frac{2N_2R_0^2}{\dot{\sigma}_0}\left[\ln(\frac{R}{R_0}) - \frac{1}{6}\right]\right\} + \dot{R}_0^2 \\ &- \frac{R_0^2\dot{\sigma}_0^2}{3}\left[1 - \frac{N_2R_0^2}{3\dot{\sigma}_0} + \frac{1}{18}\left(\frac{N_2R_0^2}{\dot{\sigma}_0}\right)^2\right],\end{aligned} \tag{3.20}$$

where m is defined in (3.15).

- The system performance at the terminal stage is of particular research interest, especially when studying observability. To facilitate the observability analysis in section 3.5, the system behaviors at the final engagement are summarized here.

  For non-maneuvering target engagements, as $\lim_{R\to 0} R^2\ln(\frac{R}{R_0}) = 0$, it can be concluded from (3.17) and (3.18) that the final LOS angular rate $\dot{\sigma}_f$ approaches zero; and the final range rate $\dot{R}_f$ approaches a constant, which can be obtained by substituting $R = 0$ into (3.19) and (3.20), as

  when $N_1 \neq 4$ and $N_1 > 3$,

$$\frac{\dot{R}_f}{\dot{R}_0} = \sqrt{1 - \frac{1}{C^2}\left[\frac{m^2}{3} + \frac{4m(1-m)}{N_1+2} + \frac{(1-m)^2}{N_1-1}\right]}; \tag{3.21}$$

  when $N_1 = 4$,

$$\frac{\dot{R}_f}{\dot{R}_0} = \sqrt{1 - \frac{1}{C^2}\left[\frac{1}{18}\left(\frac{N_2 R_0^2}{\dot{\sigma}_0}\right)^2 - \frac{N_2 R_0^2}{3\dot{\sigma}_0} + 1\right]}, \tag{3.22}$$

where

$$C = \frac{\dot{R}_0}{R_0 \dot{\sigma}_0}, \tag{3.23}$$

which is determined by system initial conditions.

For maneuvering target engagements, according to (3.11) and (3.12), the LOS angular rate $\dot{\sigma}$ will approach $c\dot{\sigma}_0/(N_1 - 2)$ rather than zero, as in a non-maneuvering target case at the end of a pursuit. The final closing speed $\dot{R}_f$ can be obtained from (3.13) and (3.14) to give

when $N_1 \neq 4$ and $N_1 > 3$,

$$\frac{\dot{R}_f}{\dot{R}_0} = \left\{1 - \frac{1}{C^2}\left[\frac{m^2}{3} + mn + n^2 + \frac{(1-n-m)^2}{N_1 - 1} + \frac{4m(1-n-m)}{N_1 + 2} + \frac{4n(1-n-m)}{N_1}\right]\right\}^{\frac{1}{2}}; \tag{3.24}$$

when $N_1 = 4$,

$$\frac{\dot{R}_f}{\dot{R}_0} = \left\{1 - \frac{1}{C^2}\left[\frac{1}{54}\left(\frac{N_2 R_0^2}{\dot{\sigma}_0}\right)^2 - \frac{5n+4}{36}\left(\frac{N_2 R_0^2}{\dot{\sigma}_0}\right) + \frac{(1-n)^2}{3} + n\right]\right\}^{\frac{1}{2}} \tag{3.25}$$

where m and n are defined in (3.15) and (3.16), respectively.

- The final LOS angular rate, given as $c\dot{\sigma}_0/(N_1 - 2)$, is proportional to the target maneuver constant c. This means that the angular rate will increase with the increase of the target maneuver constant.

- The solutions (3.11)–(3.20) for AOPN-I are readily applicable to TPN, by having $N_2 = 0$.

3.2.2 AOPN-II Guidance Law

The differential equations describing the pursuer-target dynamics under the AOPN-II guidance law is written, from (3.1), (3.2), (3.7) and (3.8), as

$$\ddot{R} - R\dot{\sigma}^2 = 0 \tag{3.26}$$

$$R\ddot{\sigma} + 2\dot{R}\dot{\sigma} = N_1\dot{R}\dot{\sigma} + N_3\dot{R} - c\dot{\sigma}_0\dot{R} \tag{3.27}$$

It is shown in Theorem 3.4 that N_1 should be larger than 3 for effective capture under AOPN-II. When $N_1 > 3$, a solution to (3.26) and (3.27) is obtained in Theorem 3.2.

Theorem 3.2 *A closed-form solution to the target-pursuit motion equations under AOPN-II consists of two parts.*

(i) The LOS angular rate $\dot{\sigma}$ is

$$\begin{aligned}\dot{\sigma} &= \dot{\sigma}_0\left\{\left(\frac{R}{R_0}\right)^{N_1-2} - \frac{N_3}{\dot{\sigma}_0(N_1-2)}\left[1-\left(\frac{R}{R_0}\right)^{N_1-2}\right]\right. \\ &+ \left.\frac{c}{(N_1-2)}\left[1-\left(\frac{R}{R_0}\right)^{N_1-2}\right]\right\};\end{aligned} \tag{3.28}$$

(ii) The relative velocity $\dot{R}$ is

$$\begin{aligned}\dot{R}^2 &= {R_0}^2{\dot{\sigma}_0}^2\left\{\frac{1}{N_1-1}\left[1+\frac{N_3}{(N_1-2)\dot{\sigma}_0}-\frac{c}{N_1-2}\right]^2\left(\frac{R}{R_0}\right)^{2N_1-2}\right. \\ &+ \frac{4c\dot{\sigma}_0 - N_3}{\dot{\sigma}_0 N_1(N_1-2)}\left[1+\frac{N_3}{(N_1-2)\dot{\sigma}_0}-\frac{c}{N_1-2}\right]\left(\frac{R}{R_0}\right)^{N_1} \\ &+ \left.\frac{(c\dot{\sigma}_0 - N_3)^2}{{\dot{\sigma}_0}^2(N_1-2)^2}\left(\frac{R}{R_0}\right)^2\right\} \\ &+ \dot{R}_0^2 - \frac{{R_0}^2{\dot{\sigma}_0}^2}{N_1-1}\left\{1+\frac{1}{N_1}\left[\left(1+c-\frac{N_3}{\dot{\sigma}_0}\right)^2-1\right]\right\}.\end{aligned} \tag{3.29}$$

Proof. Because of the similarity between AOPN-I and AOPN-II, the proof is identical to that of Theorem 3.1, and thus is omitted. ∎

Remarks.

- Given the solution to the target-pursuit problem under AOPN-II in (3.28) and (3.29), a solution for a non-maneuvering target engagement, as a special case of maneuvering engagements when $c = 0$, is readily obtained as follows.

  (i) The LOS angular rate $\dot{\sigma}$ is

$$\dot{\sigma} = \dot{\sigma}_0 \left(\frac{R}{R_0}\right)^{N_1-2} - \frac{N_3}{(N_1-2)}\left[1 - \left(\frac{R}{R_0}\right)^{N_1-2}\right]; \tag{3.30}$$

  (ii) The relative velocity $\dot{R}$ is

$$\begin{aligned}\dot{R}^2 &= {R_0}^2{\dot{\sigma}_0}^2\left\{\frac{1}{N_1-1}\left[1+\frac{N_3}{(N_1-2)\dot{\sigma}_0}\right]^2\left(\frac{R}{R_0}\right)^{2N_1-2}\right. \\ &- \left.\frac{N_3}{\dot{\sigma}_0 N_1(N_1-2)}\left[1+\frac{N_3}{(N_1-2)\dot{\sigma}_0}\right]\left(\frac{R}{R_0}\right)^{N_1} + \frac{N_3^2}{{\dot{\sigma}_0}^2(N_1-2)^2}\left(\frac{R}{R_0}\right)^2\right\} \\ &+ \dot{R}_0^2 - \frac{{R_0}^2{\dot{\sigma}_0}^2}{N_1-1}\left\{1+\frac{1}{N_1}\left[\left(1-\frac{N_3}{\dot{\sigma}_0}\right)^2-1\right]\right\}.\end{aligned} \tag{3.31}$$

- It can be seen from (3.28) that the final LOS angular rate $\dot{\sigma}_f$ is $\frac{c\dot{\sigma}_0 - N_3}{(N_1-2)}$ when the range R is zero at the final point of pursuit. For the non-maneuvering target case (i.e., $c = 0$), the final LOS angular rate is $\frac{-N_3}{(N_1-2)}$, rather than zero when using TPN or AOPN-I.

- At the final stage of pursuit when the range approaches zero, the final closing speed $\dot{R}_f$ is obtained from (3.29) to give

$${\dot{R}_f}^2 = {\dot{R}_0}^2 - \frac{{R_0}^2{\dot{\sigma}_0}^2}{N_1-1}\left\{1+\frac{1}{N_1}\left[\left(1+c-\frac{N_3}{\dot{\sigma}_0}\right)^2-1\right]\right\} \tag{3.32}$$

- The expressions for $\dot{\sigma}$ in (3.28) consist of three parts. The first is caused by TPN, the second is due to the additive term to enhance observability, and the last part is due to the target maneuver.

- The solutions (3.28)–(3.29) for AOPN-II reduce to those of TPN with $N_3 = 0$.

3.3 Capture Area

Capture area is defined in section 2.4 as the region formed by the constraints which should be imposed on the initial conditions of a system to guarantee the interception. Now we derive these constraints for effective capture when using AOPN guidance.

3.3.1 AOPN-I Guidance Law

Theorem 3.3 *For effective interception of a maneuvering target, the following constraints must be satisfied when using the additive observable proportional navigation guidance law AOPN-I given by (3.6):*

$$N_1 > 3 \tag{3.33}$$

$$C^2 > \frac{1}{N_1+2} + \frac{(c^2-4c)N_1+3c^2}{4N_1^2(N_1+2)} \tag{3.34}$$

$$N_2 < \frac{\dot{\sigma}_0}{2R_0^2 N_1}[3(cN_1+2N_1+c)+e] \tag{3.35}$$

where

$$e = \sqrt{3(N_1-1)\left[4C^2N_1^3+(8C^2-4)N_1^2+(4c-c^2)N_1-3c^2\right]}, \tag{3.36}$$

and C is defined in (3.23).

Proof. According to [33], a finite pursuer acceleration is a necessary condition for effective capture. This requires that $\dot{\sigma}$ should be finite during the entire engagement. We first consider the cases when $N_1 \neq 4$. From (3.11), N_1 should be larger than 2 to achieve a finite $\dot{\sigma}$ when R approaches zero at the final course of pursuit.

We also know that a finite LOS angular acceleration $\ddot{\sigma}$ is necessary to obtain a finite torque on the seeker in order to ensure good measurements. Differentiating (3.11), $\ddot{\sigma}$ can be expressed as

$$\ddot{\sigma} = \dot{\sigma}_0(N_1-2-c)\left(\frac{R}{R_0}\right)^{N_1-3}\left(\frac{\dot{R}}{R_0}\right) + \frac{N_2\dot{R}}{4-N_1}\left[2R-(N_1-2)\frac{R^{N_1-3}}{R_0^{N_1-4}}\right] \tag{3.37}$$

Equation (3.37) shows that only when $N_1 > 3$ can we obtain a finite $\ddot{\sigma}$ to ensure interception.

To obtain a real final closing speed $\dot{R}_f$ in (3.24), the following constraint must be satisfied

$$C^2 > \frac{m^2}{3} + mn + n^2 + \frac{(1-n-m)^2}{N_1 - 1} + \frac{4m(1-n-m)}{N_1 + 2} + \frac{4n(1-n-m)}{N_1} \tag{3.38}$$

Inequality (3.38) defines the ranges of $\dot{\sigma}_0$, R_0, and $\dot{R}_0$. If these initial conditions with given N_1 and N_2 fall outside the ranges, the pursuer cannot hit the target. Therefore, the inequality defines the *capture area* for AOPN-I based systems. Rewriting (3.38) with m in (3.15) and n in (3.16), we obtain

$$0 > \left[\left(\frac{{R_0}^2}{\dot{\sigma}_0}\right)^2 N_1\right] N_2^2 - \left\{\frac{3{R_0}^2}{\dot{\sigma}_0}\left[(c+2)N_1 + c\right]\right\} N_2 + 3(N_1+2)\left[N_1 + (c+2)c - N_1(N_1-1)C^2\right] \tag{3.39}$$

Solving the inequality, the upper bound of N_2 in (3.35) is obtained. If and only if e, given by (3.36), is real, then the bound of N_2 is real. Thus, we have the constraint

$$(N_1 - 1)\left\{4N_1^2(N_1+2)C^2 - \left[4N_1^2 + (c^2 - 4c)N_1 + 3c^2\right]\right\} > 0 \tag{3.40}$$

Note that $N_1 > 1$ because of (3.33), therefore, (3.40) leads to the bound of C^2 in (3.34).

Repeating the same derivation for the special case $N_1 = 4$, we can prove that conditions (3.33)–(3.35) are general to cover the $N_1 = 4$ case. ∎

Remarks.

- The constraints (3.33), (3.34), and (3.35) are necessary conditions for effective capture.
- Inequalities (3.33) and (3.35) provide guidelines for choosing N_1 and N_2, and hence help in guidance law design.
- Because of the mathematical simplicity of the non-maneuvering target engagement, the more specific requirement with both the lower and upper bounds of the navigation constant N_2 can be obtained. The conditions for effective interception of a non-maneuvering target are now stated.

Corollary 1 *For an AOPN-I based pursuer to intercept a non-maneuvering target, the constraints that must be satisfied to ensure interception are*

$$N_1 > 3 \tag{3.41}$$

$$C^2 > \frac{1}{N_1 + 2} \tag{3.42}$$

$$\text{for} \quad C^2 > \frac{1}{N_1 - 1},$$

$$\frac{\dot{\sigma}_0}{R_0^2}(3 + e) > N_2 \geq 0$$

$$\text{for} \quad \frac{1}{N_1 - 1} \geq C^2 > \frac{1}{N_1 + 2}$$

$$\frac{\dot{\sigma}_0}{R_0^2}(3 + e) > N_2 > \frac{\dot{\sigma}_0}{R_0^2}(3 - e) \tag{3.43}$$

where e is defined in (3.36).

- Comparing (3.35) with (3.43), the upper bound of N_2 for a maneuvering target is larger than that for a non-maneuvering target. This is because greater pursuer maneuverability is required when the target is maneuvering.

- Comparing (3.34) with (3.42), the lower bound for C^2 involved in a maneuvering target engagement given by (3.34) can be separated into two parts. The first is equal to that of a non-maneuvering target as in (3.42), and the second is caused by the target maneuver.

- When $N_1 > 3$ and $0 < c < 2$, the lower bound of C^2 for maneuvering target cases (3.34) is less than that for non-maneuvering targets (3.42). This means that for a pursuer to intercept a maneuvering target under AOPN-I, a larger capture area than that of a non-maneuvering target is more likely. This is a major advantage of AOPN-I over TPN. Under TPN, the capture area decreases with an increase in target maneuverability [31]; while under AOPN-I the capture area in the presence of a target maneuver will be larger than that of a non-maneuvering case, provided $N_1 > 3$ and $0 < c < 2$.

3.3.2 AOPN-II Guidance Law

Theorem 3.4 *To effectively intercept a maneuvering target under the AOPN-II guidance law (3.7), the system must satisfy the following requirements on navigation constants and launch conditions*

$$N_1 > 3 \tag{3.44}$$

$$(1+c-d) < \frac{N_3}{\dot{\sigma}_0} < (1+c+d) \tag{3.45}$$

$$C^2 > 1/N_1 \tag{3.46}$$

where C is defined in (3.23), and

$$d = \sqrt{(N_1-1)(N_1C^2-1)} \tag{3.47}$$

Proof. The proof follows the same strategy as in Theorem 3.3. It is included here for ease of reference in Chapter 4 (Theorem 4.6).

To ensure a finite acceleration, from (3.28), N_1 should be larger than 2 to prevent $\dot{\sigma}$ from becoming infinity when R approaches zero at the final course of pursuit.

The LOS angular acceleration is obtained by differentiating (3.28) as

$$\ddot{\sigma} = \dot{\sigma}_0 \left(N_1 - 2 - c + \frac{N_3}{\dot{\sigma}_0}\right) \left(\frac{R}{R_0}\right)^{N_1-3} \left(\frac{\dot{R}}{R_0}\right) \tag{3.48}$$

According to (3.48), $N_1 > 3$ should hold to prevent the LOS angular acceleration $\ddot{\sigma}$ from approaching infinity as $R \to 0$, so as to obtain a finite torque on the seeker to ensure good measurements.

With C defined by (3.23), the final closing speed $\dot{R}_f$ given in (3.32) can be rewritten as

$$\dot{R}_f = \dot{R}_0 \sqrt{1 - \frac{1}{C^2(N_1-1)} \left\{1 + \frac{1}{N_1}\left[\left(1+c-\frac{N_3}{\dot{\sigma}_0}\right)^2 - 1\right]\right\}} \tag{3.49}$$

Therefore, the following condition should be satisfied to obtain a real final closing speed,

$$C^2 > \frac{1}{N_1-1} + \frac{1}{(N_1-1)N_1}\left[\left(1+c-\frac{N_3}{\dot{\sigma}_0}\right)^2 - 1\right]. \tag{3.50}$$

Inequality (3.50) defines the *capture area* for AOPN-II based systems with two constants N_1 and N_3 given.

Solving (3.50) with respect to N_3 leads to the lower and upper bounds on N_3, as given in (3.45). The constraint in (3.46) is necessary in order to obtain from (3.47) a real d, which is part of the bounds of N_3. ■

Remarks.

- Constraints (3.44) and (3.45) provide guidelines for choosing N_1 and N_3.
- According to (3.35) the upper bound of N_2 of AOPN-I in (3.6) is proportional to $1/{R_0}^2$, and thus the typical value of N_2 is very small when the initial range R_0 is large. The small acceptable value of N_2 poses some difficulty in the realization of the AOPN-I guidance law. When AOPN-II is used, it can be seen from (3.45) that the range of the effective value of N_3 is much larger than that of N_2. This should facilitate the practical implementation of the AOPN-II control law.

3.4 Optimal AOPN

Compared to true proportional navigation (TPN), additive observable proportional navigation (AOPN) offers the choice of an additional navigation constant when designing the control laws. This additional constant provides one more degree of freedom, and thus offering the possibility of performance improvement over TPN by properly selecting the constant. We can now derive the optimal value of this second navigation constant.

Theorem 3.5 *N_2 of the AOPN-I guidance law has an optimal value, denoted as N_{2opt}, in terms of the largest capture area and the fastest final closing speed:*

$$N_{2opt} = \frac{3\dot{\sigma}_0}{2R_0^2}\left(c + 2 + \frac{c}{N_1}\right) \tag{3.51}$$

Proof. Rearranging the inequality (3.38) and replacing m with (3.15) and n with (3.16), we have

$$C^2 > \frac{\left[\left(\frac{R_0^2}{\dot{\sigma}_0}\right)^2 N_1\right] N_2^2 - \left\{\frac{3R_0^2}{\dot{\sigma}_0}[(c+2)N_1 + c]\right\} N_2 + 3(N_1+2)(N_1+2c+c^2)}{3N_1(N_1+2)(N_1-1)} \tag{3.52}$$

When $N_2 = N_{2opt}$, the lower bound of C^2 is found to be minimum, i.e.,

$$\frac{1}{N_1+2} + \frac{(c^2-4c)N_1+3c^2}{4N_1^2(N_1+2)}.$$

This means that the system has the largest capture area for a given N_1 and a given target maneuver acceleration c. At the same time, the absolute final closing speed $\dot{R}_f$ in (3.24) reaches its maximum given by

$$|\dot{R}_f|_{max} = |\dot{R}_0| \sqrt{1 - \frac{1}{C^2}\left[\frac{1}{N_1+2} + \frac{(c^2-4c)N_1+3c^2}{4N_1^2(N_1+2)}\right]} \tag{3.53}$$

Following the same approach, it is shown that N_{2opt} given in (3.51) remains an optimal value of N_2 for the $N_1 = 4$ case in terms of the fastest speed and the largest capture area. ∎

Theorem 3.6 *The optimal AOPN-II guidance law in terms of the best capture ability and the fastest final closing speed is obtained when N_3 is at its optimal value, i.e.,*

$$N_{3opt} = \dot{\sigma}_0(1+c) \tag{3.54}$$

Proof. See the proof of Theorem 3.5. ∎

Remarks.

- When $N_3 = N_{3opt}$, the lower bound of C^2 is found to be minimum, i.e., $\frac{1}{N_1}$. This means that the system with N_{3opt} has the largest capture area for a given N_1.
- When N_{3opt} is used, the absolute final closing speed $\dot{R}_f$ in (3.32) becomes

$$|\dot{R}_f|_{max} = |\dot{R}_0| \sqrt{1 - \frac{1}{C^2 N_1}} \tag{3.55}$$

  which is the maximum.

- Comparing the largest capture area attainable by AOPN-I given in (3.34) with that by AOPN-II in (3.46), it is found that the largest capture area under AOPN-I is determined by both navigation constant N_1 and target maneuver constant c; while the largest capture area offered by AOPN-II is only dependent on N_1.

- From (3.23), we notice that C represents the ratio of relative initial speed along LOS to the initial speed normal to LOS. The smaller the lower bound of C^2, the less string requirement on system launch conditions; that is, the larger the capture area the system can achieve.

  According to (2.17), The capture area attainable by TPN is

  $$C^2 > \frac{1}{N_1 - 1} + \frac{c^2 + 2c}{N_1(N_1 - 1)} \tag{3.56}$$

  Comparing (3.34), (3.46), and (3.56), among these three guidance laws, AOPN-I can achieve the largest capture area, followed by AOPN-II, and the capture area attainable by TPN is the smallest. The superior performance characteristic of the two AOPN guidance laws over the TPN law is therefore clear.

- When the TPN guidance law is used, from (2.15), the final closing speed is given as

  $$| \dot{R}_f |_{max} = | \dot{R}_0 | \sqrt{1 - \frac{1}{C^2}\left[\frac{1}{N_1 - 1} + \frac{c^2 + 2c}{N_1(N_1 - 1)}\right]} \tag{3.57}$$

  Using AOPN-I with the optimal value of N_2, the fastest closing speed is given (3.53) Comparison of (3.53), (3.55), and (3.57) reveals that AOPN-I is able to achieve the fastest final closing speed, while TPN offers the slowest. In terms of capture area and closing speed, AOPN-I exhibits some advantages over AOPN-II.

3.5 Observability Analysis

Both AOPN-I and AOPN-II are proposed with the motivation to enhance system observability by adopting an information-augmented term. The question on whether AOPN guidance laws have the ability to offer the potential of observability enhancement must be answered. Aiming to answer this question, we investigate the observability of AOPN based systems, and this is done by checking the *range observability index*. This index is introduced in section 2.6.3, and is defined as

$$I_A(t_0, t) = \int_{t_0}^{t} (t - s)\,[A_P(s) - A_T(s)]\,ds, \tag{3.58}$$

where t_0 is the time when observability is of interest. The range observability index is useful and important in observability checks. For a non-maneuvering target case, it reduces to

$$I_A(t_0, t) = \int_{t_0}^{t} (t - s) A_P(s) ds. \tag{3.59}$$

The observability criteria, which are established in Chapter 2 and will be utilized in the performance analysis in this section, are summarized here. Sufficient conditions for the pursuer-target guidance system to be unobservable at t_0 are given as follows.

- For a non-maneuvering target engagement, one sufficient condition for an unobservable system with the observation over $(t_0, t]$ is

$$\int_{t_0}^{t} (t - s) A_P(s) ds = 0 \tag{3.60}$$

  Note that the left-hand side of (3.60) matches the range observability index with $A_T = 0$ in (3.59), i.e., the target is not accelerating (or, non-maneuvering). The condition in (3.60) is easy to apply.

- For a maneuvering target engagement, one sufficient unobservable condition is

$$\begin{bmatrix} \int_{t_0}^{t} (t - s)[A_{Px}(s) - A_{Tx}(s)] ds \\ \int_{t_0}^{t} (t - s)[A_{Py}(s) - A_{Ty}(s)] ds \end{bmatrix} = \begin{bmatrix} R_{x0} - a_{11} f(t) + \left(\dot{R}_{x0} - a_{12} f(t)\right) \Delta t \\ R_{y0} - a_{21} f(t) + \left(\dot{R}_{y0} - a_{22} f(t)\right) \Delta t \end{bmatrix} \tag{3.61}$$

  where subscript x (respectively, y) denotes the decomposition component along x-axis (respectively, y-axis); $f(t)$ is an arbitrary scalar function, including zero; a_{ij}s are arbitrary constants, but not all zeros; and $\Delta t = t - t_0$ is the duration of observation. This condition, being the most stringent among the sufficient unobservable conditions derived in section 2.6, is chosen to be used, because no sufficient conditions are apparently satisfied for maneuvering target engagements.

After presenting the observability criteria, we are now ready to analyze the system observability under AOPN laws toward the end game, which is essential for terminal interception.

3.5.1 Non-maneuvering Target with AOPN

For a non-maneuvering target engagement, we know from section 2.6.3 that under TPN, the range observability index is approximately zero. Based on the sufficient unobservability condition in (3.60), this indicates that if the TPN guidance law is used in a non-maneuvering target engagement, the system is most likely to become unobservable near the final pursuit.

Under AOPN-I, the range observability index becomes

$$\begin{aligned} I_A(t_0, t_f) &= \int_{t_0}^{t_f} (t_f - s)(N_1 \dot{\sigma} \dot{R} + N_2 \dot{R} R^2) ds \\ &\approx \int_{t_0}^{t_f} (t_f - s)[N_1 \cdot 0 \cdot \dot{R}_f + N_2 \cdot \dot{R}_f \cdot \dot{R}_f^2 (t_f - s)^2] ds \\ &= \frac{N_2 \dot{R}_f^3}{4} (t_f - t_0)^4 \end{aligned} \tag{3.62}$$

where $\dot{R}_f$ is given in (3.24) and (3.25), but with their n set to zero for a non-maneuvering target.

Under AOPN-II, we have

$$\begin{aligned} I_A(t_0, t_f) &= \int_{t_0}^{t_f} (t_f - s)(N_1 \dot{\sigma} \dot{R} + N_3 \dot{R}) ds \\ &\approx \int_{t_0}^{t_f} (t_f - s) \left[N_1 \cdot \frac{-N_3}{N_1 - 2} \cdot \dot{R}_f + N_3 \cdot \dot{R}_f \right] ds \\ &= \frac{N_3 \dot{R}_f}{N_1 - 2} (t_f - t_0)^2 \end{aligned} \tag{3.63}$$

where $\dot{R}_f$ is given in (3.32) with $c = 0$ for a non-maneuvering case.

We can see from (3.62) and (3.63) that for both AOPN guidance laws, due to the additive term to enhance the information content, i.e., $N_2 \dot{R} R^2$ for AOPN-I, or $N_3 \dot{R}$ for AOPN-II, the range observability index will not be zero towards the end of the engagement until interception does occur, i.e., when $t_0 = t_f$. Note that t_0 here is the time at which observability is of interest. According to the condition given in (3.60), we observe that both AOPN laws enhance observablitiy in the non-maneuvering target engagement by providing the system state with a better opportunity to be observable.

3.5.2 Maneuvering Target with AOPN

For a maneuvering target engagement, the range observability index under TPN is shown in section 2.6.3 to be

$$I_A(t_0, t_f) \approx \frac{c\dot{\sigma}_0 \dot{R}_f}{N_1 - 2}(t_f - t_0)^2 \tag{3.64}$$

With AOPN-I, the range observability index $I_A(t_0, t_f)$ is

$$I_A(t_0, t_f) \approx \frac{c\dot{\sigma}_0 \dot{R}_f}{N_1 - 2}(t_f - t_0)^2 + \frac{1}{4}\dot{R}_f^3 N_2 (t_f - t_0)^4 \tag{3.65}$$

For AOPN-II, we have the range observability index as

$$I_A(t_0, t_f) \approx \left(\frac{c\dot{\sigma}_0}{N_1 - 2} - \frac{N_3}{N_1 - 2}\right)\dot{R}_f (t_f - t_0)^2 \tag{3.66}$$

Since the LOS angular rate is very small near the end game, σ is taken as a constant for analytical simplicity. On the basis of (3.61), the condition for an unobservable system under TPN, AOPN-I, or AOPN-II is

$$\begin{bmatrix} I_A(t_0, t_f) \cdot \sin\sigma(t) \\ I_A(t_0, t_f) \cdot \cos\sigma(t) \end{bmatrix} = \begin{bmatrix} R_{x0} - a_{11} f(t) + \left(\dot{R}_{x0} - a_{12} f(t)\right)\Delta t \\ R_{y0} - a_{21} f(t) + \left(\dot{R}_{y0} - a_{22} f(t)\right)\Delta t \end{bmatrix} \tag{3.67}$$

Observing from (3.67) with the three range observability indices (3.64), (3.65) and (3.66), it is clear that via the second navigation constant, i.e., N_2 in AOPN-I, or N_3 in AOPN-II, both AOPN guidance laws provide one additional degree of freedom to achieve observability than TPN. In other words, for some cases in which TPN renders the system unobservable, the guidance system under AOPN-I or AOPN-II still offer possibilities to be observable by choosing the appropriate second navigation constant. In terms of enhancing system observability in both non-maneuvering and maneuvering target engagements, the AOPN based systems perform better than their TPN based counterparts.

3.6 Sensitivity and Robustness Analysis

Guidance systems, as in all real-world applications, are subject to uncertainty in initial state conditions, system parameters, and measurements. It is of practical and theoretical interest to examine the robust performance of the TPN, AOPN-I, and AOPN-II guidance laws.

Firstly, we investigate how the availability of the variables influences the realization of the control laws. We find that the realizations of AOPN-II and TPN do not require the range information R, therefore, it is simpler to implement AOPN-II and TPN than to implement AOPN-I, especially when the range measurement is not readily available. It is clear that TPN and AOPN-II are more robust than AOPN-I because they have much less dependency on the information of the range than AOPN-I does, thus enhancing reliability.

Secondly, we are concerned about how uncertainty in the initial conditions affects the final interception. To study the system's robustness in terms of initial conditions, we consider the relative sensitivity function of the final relative speed $\dot{R}_f$ to the initial relative speed $\dot{R}_0$. To avoid unnecessary complexity, we calculate the relative sensitivity function of $\dot{R}_f^2$ to $\dot{R}_0^2$ rather than $\dot{R}_f$ to $\dot{R}_0$.

Based on the expression of the final closing speed for TPN in (2.15), for AOPN-I in (3.24) and (3.25), and for AOPN-II in (3.32), the relative sensitivity functions of $\dot{R}_f^2$ to $\dot{R}_0^2$ have the same expression as

$$S_{\dot{R}_0^2}^{\dot{R}_f^2} = \frac{\partial \dot{R}_f^2}{\partial \dot{R}_0^2} \cdot \frac{\dot{R}_0^2}{\dot{R}_f^2} = \frac{\dot{R}_0^2}{\dot{R}_f^2} \tag{3.68}$$

Under different control strategies, however, there are different $\dot{R}_f$. It has been shown in the remarks of Theorem 3.6 that:

$$| \dot{R}_f^{TPN} | < | \dot{R}_f^{AOPN-II} |_{max} < | \dot{R}_f^{AOPN-I} |_{max} \tag{3.69}$$

where the superscripts denote the control law used.

Combining (3.68) and (3.69), we see that the relative sensitivity of $\dot{R}_f$ to $\dot{R}_0$, when using TPN, AOPN-II with N_{3opt}, and AOPN-I with N_{2opt}, decreases in that order. In other word, the optimal AOPN-I based system is most robust with respect to variation of initial conditions, followed by the optimal AOPN-II based system, and then the TPN-based system. This result closely matches the result on the capture area shown in the remarks of Theorem 3.6.

It follows that the larger the capture area, the better the system's robustness performance. This can be interpreted as the less stringent conditions imposed on the initial system values to ensure interception, the less sensitive the interception with respect to initial conditions.

Finally, we examine the system performance in the presence of variations in system pa-

rameters. For AOPN-I, the sensitivity function of $\dot{\sigma}$ given in (3.17) with respect to N_2 is

$$\frac{\partial \dot{\sigma}}{\partial N_2} = -\frac{R^2}{N_1 - 4}\left[1 - \left(\frac{R}{R_0}\right)^{N_1-4}\right] \tag{3.70}$$

With AOPN-II, the sensitivity function of $\dot{\sigma}$ given by (3.28) to N_3 becomes

$$\frac{\partial \dot{\sigma}}{\partial N_3} = -\frac{1}{N_1 - 2}\left[1 - \left(\frac{R}{R_0}\right)^{N_1-2}\right] \tag{3.71}$$

As the sensitivity function of $\dot{\sigma}$ to N_2 under the AOPN-I control law is proportional to R^2, it follows that the LOS angular rate $\dot{\sigma}$ is less sensitive to the second navigation constant under AOPN-II than under AOPN-I. This is a desirable feature of AOPN-II over AOPN-I.

3.7 Simulation

In order to evaluate the performance of the additive observable proportional navigation laws AOPN-I and AOPN-II, and to confirm the results derived in this chapter, simulation studies with different scenarios are conducted.

All the simulations use the following data,

velocity of the pursuer,	$V_M = 600m/s$;
velocity of the target,	$V_T = 300m/s$;
initial heading angle of the pursuer,	$\theta_0 = 0°$;
initial heading angle of the target,	$\phi_0 = 30°$;
initial LOS angle,	$\sigma_0 = 0°$;
initial relative range,	$R_0 = 1000m$.

The initial conditions $\dot{R}_0$ and $\dot{\sigma}_0$ are computed by

$$\begin{aligned} \dot{\sigma}_0 &= \frac{V_T sin(\phi_0 - \sigma_0) - V_M sin(\theta_0 - \sigma_0)}{R_0} \\ \dot{R}_0 &= V_T cos(\phi_0 - \sigma_0) - V_M cos(\theta_0 - \sigma_0). \end{aligned}$$

Figure 3.1, Figure 3.2, Figure 3.3 show the trajectories of the maneuvering target modeled by (3.8) and the pursuer using the TPN law, the AOPN-I law with N_{2opt}, and the AOPN-II

law with N_{3opt}, respectively. Compared with that under TPN, the pursuer guided by AOPN-I in Figure 3.2 or AOPN-II in Figure 3.3 swings its way during the pursuit course so as to obtain more information about the relative range and the range rate. In this way, the aim to enhance the observability of the system can be fulfilled.

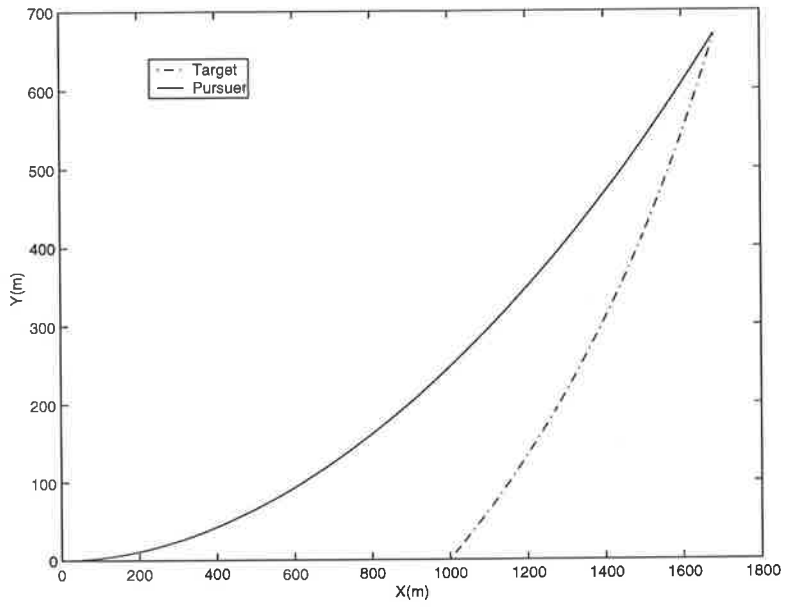

Figure 3.1: Pursuer and target trajectories using TPN for $N_1 = 4$ and $c = 1$; target initial acceleration $A_{T0} = 5.1g$.

Figure 3.4 is derived from (3.11). We can see from Figure 3.4 that the LOS angular rate $\dot{\sigma}$ under AOPN-I approaches zero for a non-maneuvering target (i.e., $c = 0$) towards the end of pursuit, i.e., when $\frac{R}{R_0} \to 0$. For the maneuvering target, the final angular rate increases with increase in target maneuverability, as discussed in Theorem 3.1.

Using (3.29), which is the expression for the range rate $\dot{R}$ under AOPN-II, we obtain Figure 3.5. This figure confirms that the final range rate, which occurred at $\frac{R}{R_0} = 0$, is the largest with optimal N_3 as discussed in Theorem 3.6.

The regions defined by the constraints (3.33), (3.34), and (3.35) are plotted in Figure 3.6. It demonstrates that when using AOPN-I as the guidance law, the system has the largest capture area when $N_2 = N_{2opt}$. Note that the smaller the lower bound of C^2, the larger the capture area, *cf.* (3.34).

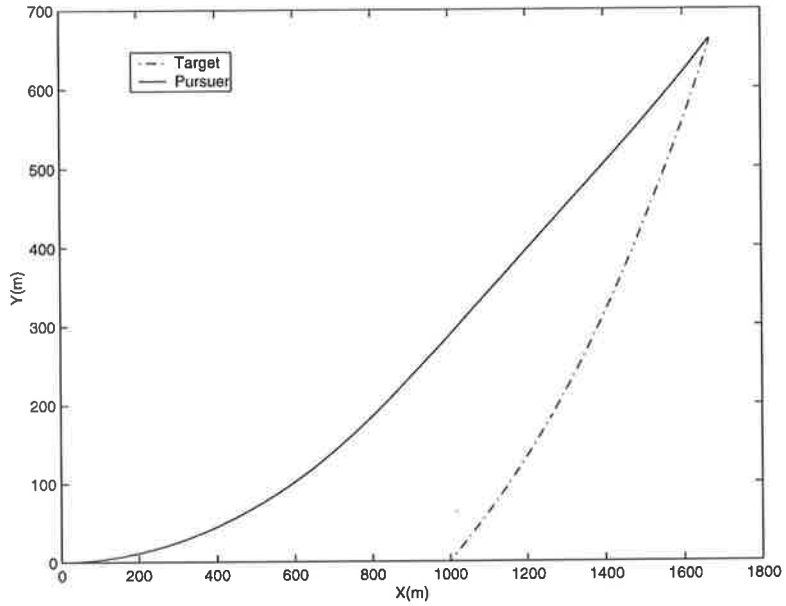

Figure 3.2: Pursuer and target trajectories using AOPN-I for $N_1 = 4$, $N_2 = N_{2opt}$ and $c = 1$; target initial acceleration $A_{T0} = 5.1g$.

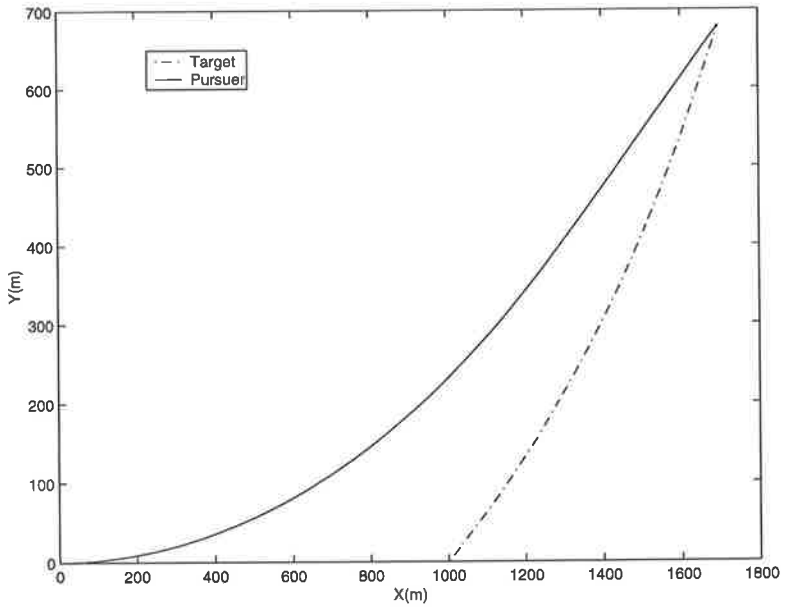

Figure 3.3: Pursuer and target trajectories using AOPN-II for $N_1 = 4$, $N_3 = N_{3opt}$ and $c = 1$; target initial acceleration $A_{T0} = 5.1g$.

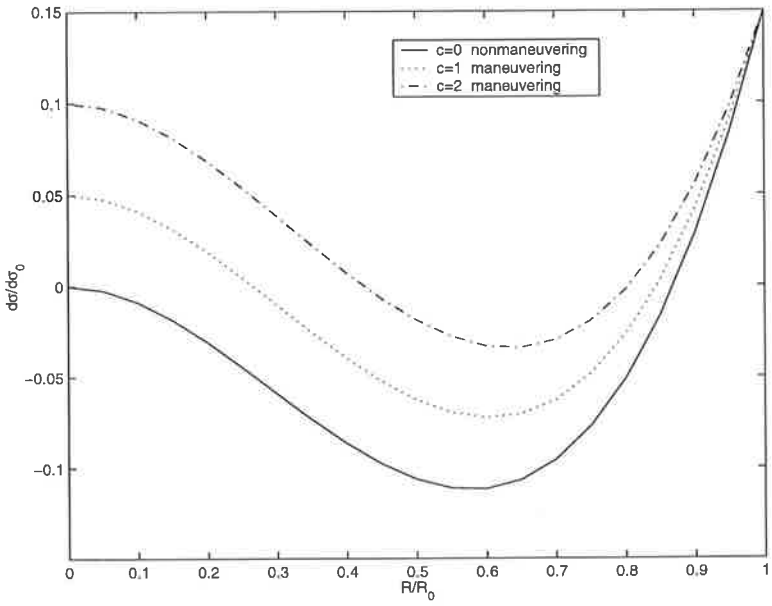

Figure 3.4: $\frac{\dot{\sigma}}{\dot{\sigma}_0}$ versus $\frac{R}{R_0}$ under AOPN-I with $N_1 = 5$, $N_2 = 1 \times 10^{-6}$ and three different c values.

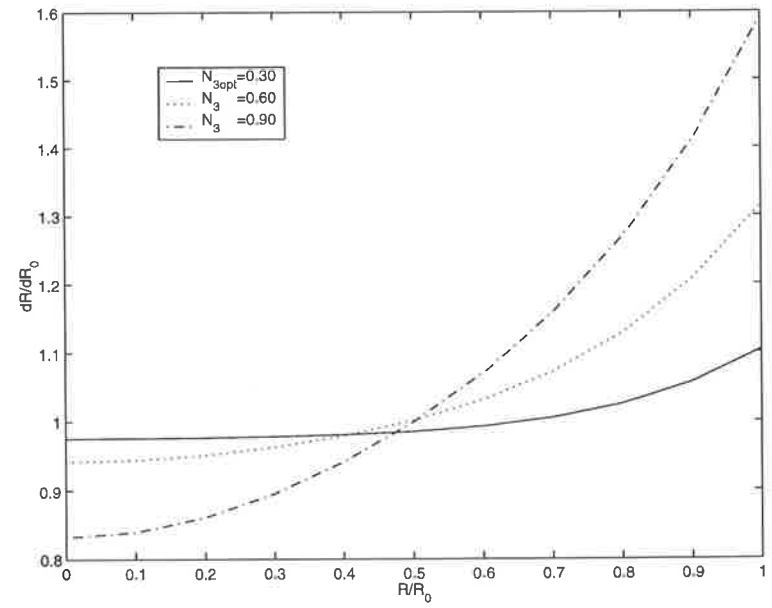

Figure 3.5: $\frac{\dot{R}}{\dot{R}_0}$ versus $\frac{R}{R_0}$ under AOPN-II with $N_1 = 4$, $c = 1$ and three different N_3 values.

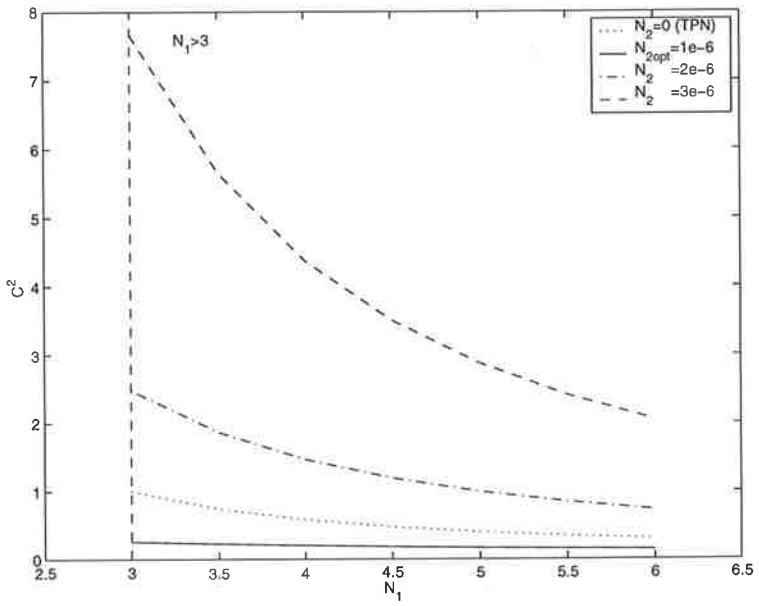

Figure 3.6: Capture area for AOPN-I with four different N_2 values when $c = 1$. Note that N_1 must be larger than 3, and that a small C^2 represents less favorable initial engagement conditions needed to achieve interception.

The capture areas achieved by TPN, AOPN-I, and AOPN-II are compared in Figure 3.7. The comparison confirms that AOPN-I covers the largest capture area among these three guidance laws, and the capture area attainable by TPN is the smallest. From Figure 3.7, it is suggested that the AOPN guidance laws perform better than TPN when C^2 is small. A small value of C^2 represents a small initial range rate, or a large initial LOS angular rate. In other words, the pursuer is under less favorable initial engagement conditions. Under these circumstances, the AOPN laws with optimal values have a larger capture area than those under TPN.

The upper bounds of N_2 and the optimal values of N_2 for AOPN-I with different target maneuver acceleration c, and those of N_3 are compared in Table 3.1, where subscript upb denotes the upper bound. From the table, we find that the upper bound of N_3 is much larger than that of N_2. The larger range of acceptable value of N_3 facilitates the realization of the AOPN-II guidance law.

To confirm the findings that AOPN improves system observability compared with TPN

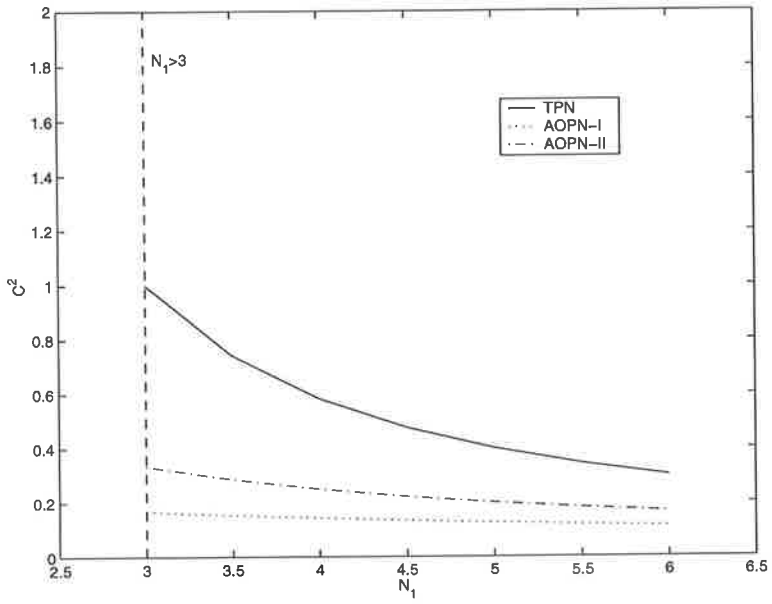

Figure 3.7: Largest attainable capture areas by TPN, AOPN-I, and AOPN-II

c	$N_{2opt}(10^{-6})$	$N_{2upb}(10^{-6})$	N_{3opt}	N_{3upb}
0	0.63	3.39	0.15	1.30
1	1.03	3.80	0.30	1.45
2	1.42	4.18	0.45	1.60

Table 3.1: Optimal values and upper bounds of N_2 and N_3 with different c values when $N_1 = 4$

as discussed in section 3.5, Monte Carlo simulations are carried out. The modified gain extended Kalman filter, due to its consistent performance [42, 43], is used to estimate the system state variables. Tests are conducted with the control law fed with true state variables so as to study effects of the control law on system observability. Meanwhile, the Kalman filter is incorporated to estimate state variables.

In order to demonstrate the ability of the AOPN guidance laws in enhancing system observability, comparison between those results obtained under AOPN with those under TPN is made in every simulation run. The performances of the AOPN-I, AOPN-II, and TPN are measured in terms of tracking error which is defined as the magnitude of the difference between the true vector and the estimated vector.

As $N_1 = 4$ is a typical value used in proportional navigation, it is used in all three guidance laws when conducting simulations. The second navigation constant N_2 in the AOPN-I law and N_3 in the AOPN-II law are set to their optimal values, i.e., $N_2 = 1 \times 10^{-6}$, and $N_3 = 0.15$. The sampling is taken every 0.02 second, and the noisy measurement is modeled by subjecting the actual LOS angle measurements to zero-mean additive Gaussian noise with the variance of 1 $m^2 rad^2$.

The estimation errors of the relative range, the relative velocity, and the target acceleration are plotted in Figure 3.8–Figure 3.10 for non-maneuvering target engagement, and in Figure 3.11–Figure 3.13 for maneuvering target engagement. All the results presented are the averages of 20 Monte Carlo runs.

For the non-maneuvering target, the estimates with TPN in Figure 3.8–Figure 3.10 demonstrate divergent behavior in the end game phase, as shown by the solid line. These results confirm that TPN does have difficulty in providing the guidance system with observable data near the end course when the range observability index defined in (2.65) is nearly zero. On the other hand, the trajectories generated by AOPN laws enable the Kalman filter to produce a much better estimation performance.

The maneuvering target is assumed to be the first-order lag model as [16], i.e.,

$$\dot{A}_T + \lambda A_T = 0 \tag{3.72}$$

with $\lambda = 0.1$ and the initial target acceleration $A_{T0} = 5g$. This target model gives a sim-

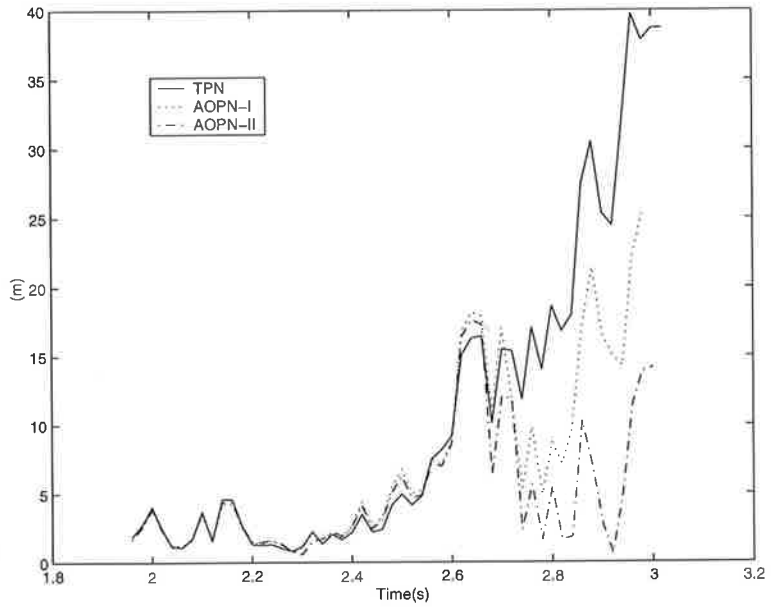

Figure 3.8: Position estimation error for non-maneuvering target engagement

ilar dynamic characteristic to the one modeled by (3.8) in simulations. From Figure 3.11–Figure 3.13, it appears that the filters with AOPN laws outperform their TPN counterpart near the end of pursuit. It should be pointed out that the tests are conducted in such a way that the filters are not within the control loop, hence the accuracy of the estimates generated by the filters does not affect the trajectory generated by the guidance law. The results in Figure 3.11–3.13 confirm our analytical finding that AOPN guidance has the effect of enhancing the observability, and thus offers an advantage in improving the filter performance.

In practical applications, the estimates must be used to implement the control laws. To investigate whether the interception can actually occur when the estimates from the modified gain extended Kalman filter are fed to the control law, the state estimates take the place of the actual state variables in realizing the control law. Figure 3.14 presents the trajectories of the maneuvering target and the pursuer using TPN, while Figure 3.15 and Figure 3.16 show the trajectories under AOPN-I and AOPN-II, respectively. When comparing with that of TPN, the pursuer under AOPN laws tends to be more oscillatory during the pursuit course, so that more information about the relative range and the range rate is generated for observation in the process.

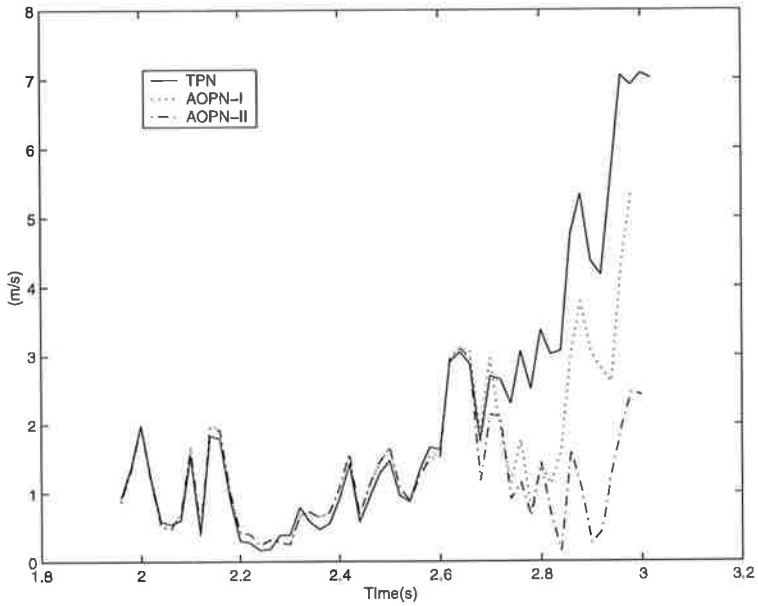

Figure 3.9: Velocity estimation error for non-maneuvering target engagement

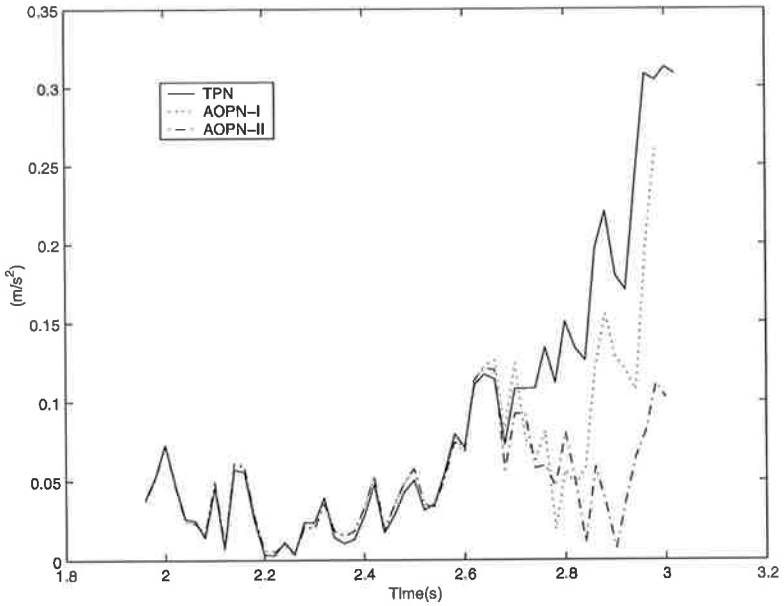

Figure 3.10: Target acceleration estimation error for non-maneuvering target engagement

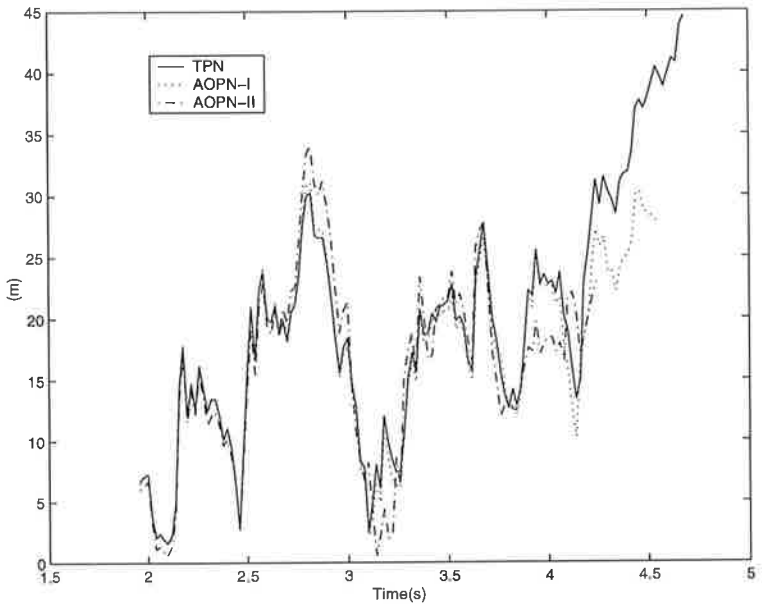

Figure 3.11: Position estimation error for maneuvering target engagement

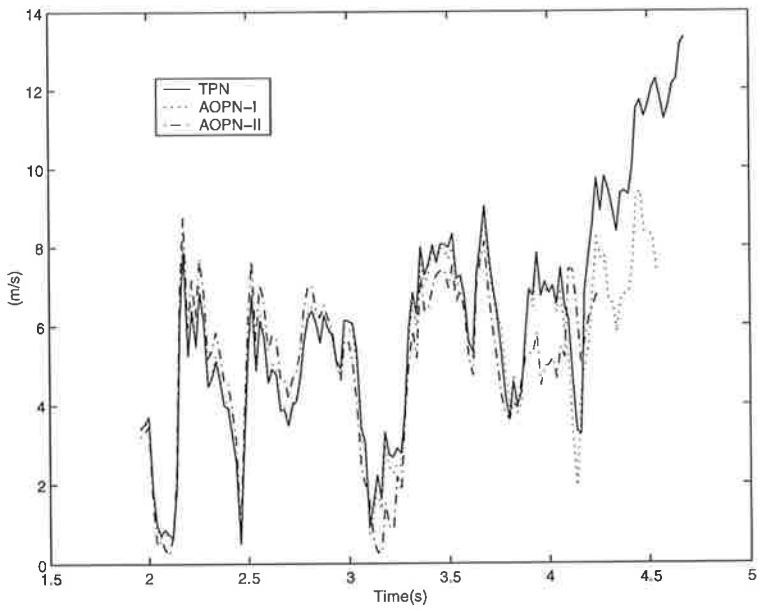

Figure 3.12: Velocity estimation error for maneuvering target engagement

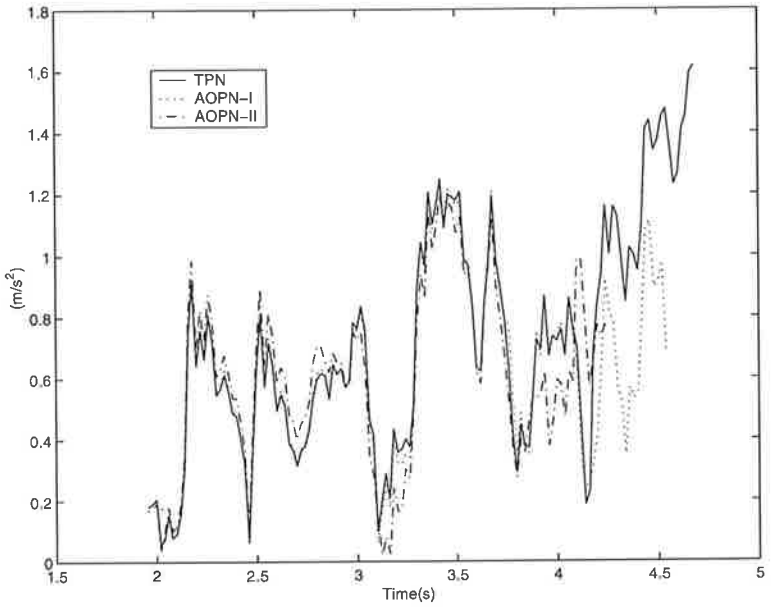

Figure 3.13: Target acceleration estimation error for maneuvering target engagement

The final miss distance, which is a measure of how far the target is from the pursuer at the end of an engagement, is measured. Under the scenarios of Figure 3.14, Figure 3.15, and Figure 3.16, the final average miss distance from 20 Monte Carlo simulation runs is $6.0m$ when TPN is used, $2.1m$ with AOPN-I, and $2.9m$ with AOPN-II. The result indicates that AOPN laws are better than TPN. Additional scenarios are simulated, and the results on the miss distance and the filter performance have been consistent.

3.8 Summary

A new additive observable proportional navigation law, AOPN-II, which is well-suited for systems with bearings-only measurements, has been developed through this study. Further investigation on AOPN-I based guidance systems has also been conducted. Based on the closed-form solutions to pursuer-target motion equations under AOPN guidance laws, guidelines on how to select navigation constants have been presented. The optimal value of N_2 for AOPN-I and that of N_3 for AOPN-II have been given in (3.51) and in (3.54)

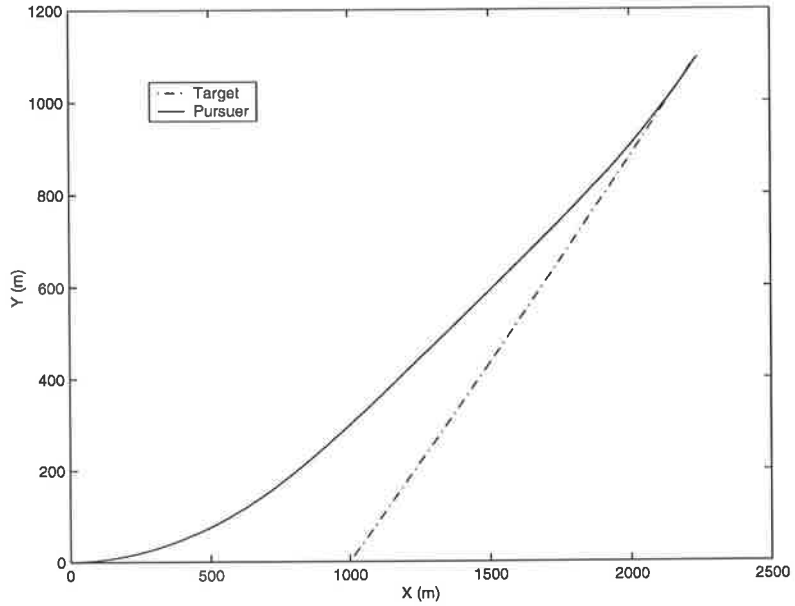

Figure 3.14: Pursuer and target trajectories using TPN with $N_1 = 4$ when subject to noise

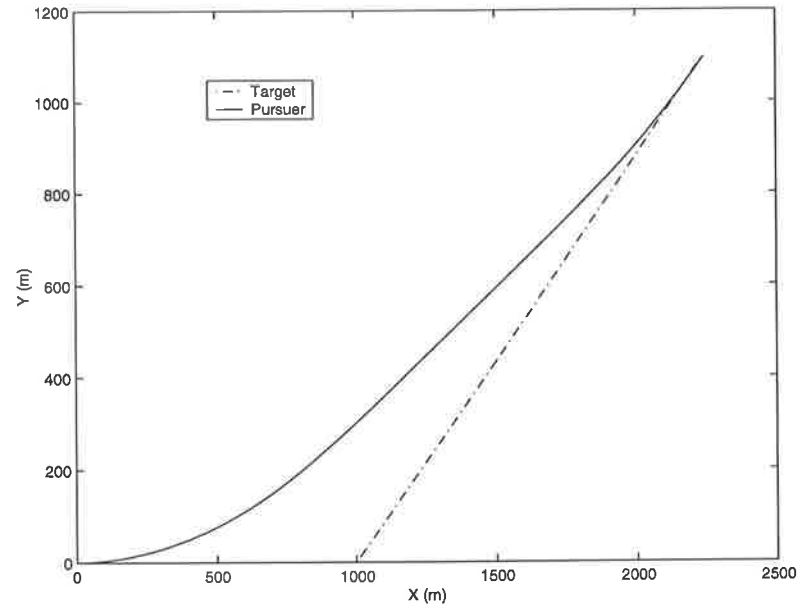

Figure 3.15: Pursuer and target trajectories under AOPN-I with $N_1 = 4$ and $N_2 = 1 \times 10^{-6}$ when subject to noise

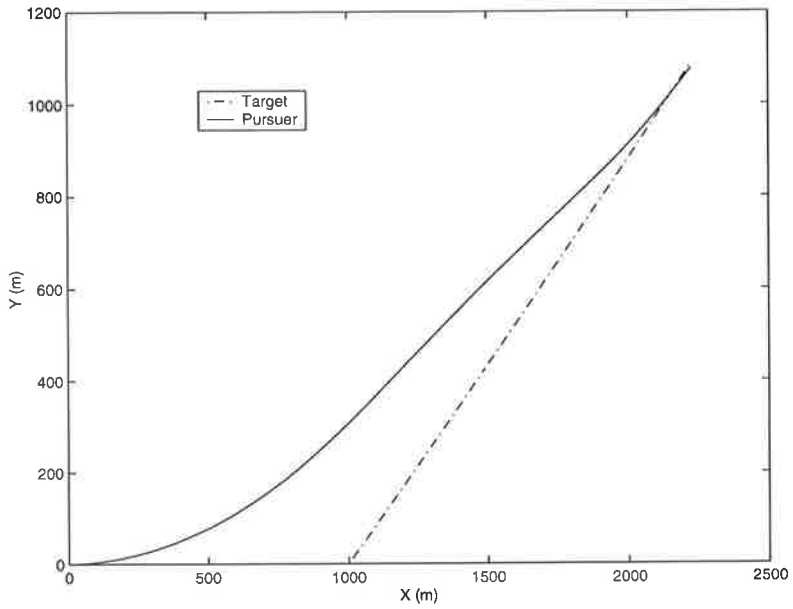

Figure 3.16: Pursuer and target trajectories using AOPN-II with $N_1 = 4$ and $N_3 = 0.15$ when subject to noise

respectively, in terms of the fastest closing speed and the largest capture area.

In analyzing system observability, both AOPN guidance laws have been shown to provide a better possibility for the system to be observable than TPN does, due to the additive information-enhanced term. This finding has also been confirmed by simulation studies.

Analytical comparison between TPN, AOPN-I, and AOPN-II shows that AOPN based guidance systems perform better than TPN based systems. AOPN guidance laws offer a larger capture area, a better possibility of observable systems, and less sensitivity to uncertainty in initial conditions. Between AOPN-I and AOPN-II, on one hand, the capture area achievable by AOPN-I with the optimal N_2 is larger than that by AOPN-II with the optimal N_3; on the other hand, the AOPN-II control law, without demanding the range information to realize, is simpler in form. As the upper bound of the effective second navigation constant of AOPN-II is larger, AOPN-II is therefore easier to implement in practical applications.

Chapter 4

Saturation Constraint Problems

The effects of saturation constraints on the performance of guidance systems under true proportional navigation, and additive observable proportional navigation are studied via rigorous analysis and extensive simulations. For each guidance law, saturation constraints are modeled when establishing pursuer-target motion equations. Conditions to achieve effective interception are derived for both unsaturated and saturated modes. Then, the impacts of saturation constrains on total control effort and observability are mathematically analyzed. Finally, the generality and accuracy of the derived conditions are confirmed by simulations.

4.1 Introduction

We have studied several important characteristics of guidance systems, such as interception performance, observability, and total control effort. All the analyses are carried out under the assumption that the pursuer is able to provide adequate acceleration without saturation constraints. In reality, an achievable pursuer acceleration is limited by angle-of-attack constraints at high altitudes, by the pursuer's structure at low altitudes in endoatmospheric interceptors, and by lateral engine thrust-to-weight ratio in exoatmospheric interceptors [25].

While the acceleration saturation of guidance systems is an interesting and important issue, it has not been fully addressed, except in some studies mainly via simulations [6], [22] and [23]. Simulation results [6] show that interception with zero miss distance can be achieved when acceleration saturation occurs only during the initial part of the pursuit; if the saturation persists throughout the entire engagement, it will result in a finite miss distance. The effects of acceleration saturation on miss distance are also considered for sinusoidal target models [22, 23]. Rigorous analytical study on the influence of acceleration saturation on system performance has not, however, been reported in the literature.

In this chapter, an analytical study of the impacts of acceleration saturation on system performance is presented. In section 4.2, a mathematical model is firstly established for a pursuer with acceleration constraints under TPN guidance to intercept a maneuvering target. Conditions for effective interception are derived for both non-saturation and saturation acceleration modes. These conditions are usable in computing the most favorable pursuer's launch conditions, and in predicting the occurrence of target interception. Analysis reveals that interception can be accomplished under saturation mode if the derived interception conditions are satisfied, but at the expense of greater total control effort than that when acceleration is not saturated. Numerical simulations are conducted to confirm that the interception conditions are sufficiently general to cater for a range of maneuvering target models.

In section 4.3, approaches used in analyzing TPN based systems are extended to additive observable proportional navigation II (AOPN-II) based systems. System equations are set up to describe a pursuer-target engagement with pursuer acceleration constraints under the AOPN-II guidance law. Based on the established system equations, interception conditions

are then derived for different operating modes. Finally, simulations verify the generality of these interception conditions to accommodate variation of maneuvering target models.

4.2 TPN Based Systems

4.2.1 System Equations and Problem Formulation

The governing equations describing the pursuer-target motion take the form [6, 12]

$$\ddot{R} - R\dot{\sigma}^2 = A_{TR} - A_{PR} \tag{4.1}$$

$$R\ddot{\sigma} + 2\dot{R}\dot{\sigma} = A_{T\sigma} - A_{P\sigma} \tag{4.2}$$

where R is the relative range with initial value R_0; $\dot{\sigma}$ is the LOS angular rate with initial value $\dot{\sigma}_0$; A_{TR} and $A_{T\sigma}$ are the target acceleration components along LOS and normal to LOS, respectively; A_{PR} and $A_{P\sigma}$ are the pursuer acceleration components along LOS and normal to LOS, respectively.

With TPN, the pursuer acceleration A_P is given as

$$A_{PR} = 0; \qquad A_{P\sigma} = -N_1\dot{R}\dot{\sigma} \tag{4.3}$$

where N_1 is a positive navigation constant.

To account for the finite acceleration capability of the pursuer due to its structure, angle-of-attack constraints, actuator, etc [25], the maximum acceleration that a pursuer can provide must be incorporated when analyzing the performance. Figure 4.1 shows the simplified block diagram of a TPN based guidance system. The actuator is taken as unity gain with no dynamics for simplicity. However, saturation constraints represented by a nonlinear function are included.

The pursuer acceleration under TPN with saturation constraints is expressed as

$$A_{PR} = 0; \qquad A_{P\sigma} = \begin{cases} -N_1\dot{R}\dot{\sigma} & \text{when } \mid N_1\dot{R}\dot{\sigma} \mid \leq A_{max} \\ -\text{sign}(\dot{R}\dot{\sigma}) \cdot A_{max} & \text{otherwise} \end{cases} \tag{4.4}$$

where A_{max} is the pursuer acceleration saturation constraint. We will discuss in section 4.2.2 how this nonlinearity affects the interception performance, the total control effort, and the observability.

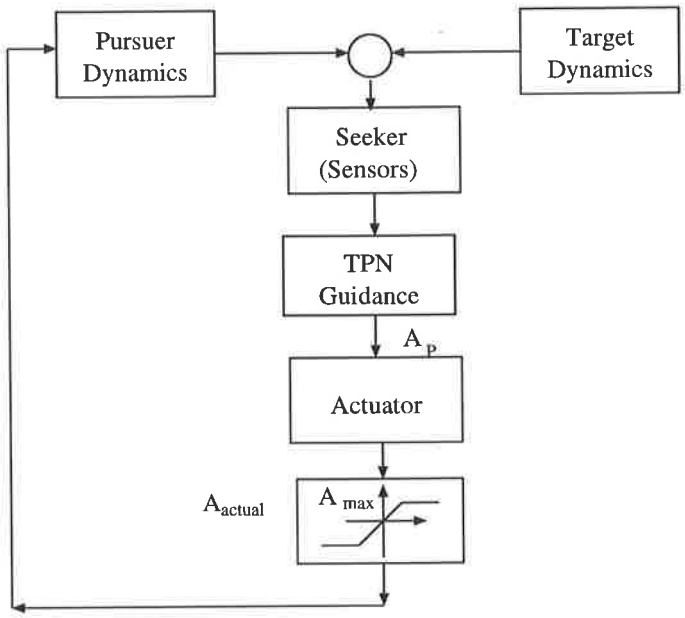

Figure 4.1: Block diagram of TPN based guidance system with acceleration saturation constraint A_{max}

In modeling pursuer target dynamics, the maneuvering target is assumed to have acceleration proportional to the range rate $\dot{R}$ and normal to LOS. The target maneuver acceleration takes the form, as [31],

$$A_{TR} = 0; \qquad A_{T\sigma} = -c\dot{\sigma}_0\dot{R} \tag{4.5}$$

where c is a non-negative constant of the target maneuver acceleration, and is directly proportional to the maneuverability of the target. The model (4.5) reduces to a non-maneuvering target case when $c = 0$.

From (4.1) to (4.5), the governing equations of the target-pursuit motion are obtained as

$$\ddot{R} - R\dot{\sigma}^2 = 0 \tag{4.6}$$

$$R\ddot{\sigma} + 2\dot{R}\dot{\sigma} = \begin{cases} N_1\dot{R}\dot{\sigma} - c\dot{\sigma}_0\dot{R} & \text{when } \mid N_1\dot{R}\dot{\sigma} \mid \leq A_{max} \\ \text{sign}(\dot{R}\dot{\sigma}) \cdot A_{max} - c\dot{\sigma}_0\dot{R} & \text{otherwise} \end{cases} \tag{4.7}$$

which represent a pursuer tracking a maneuvering target under TPN, with the pursuer acceleration subjcct to saturation constraint A_{max}.

The problem of the acceleration saturation constraint is studied by first deriving condi-

tions for the occurrence of target interception based on (4.6) and (4.7). Then, these conditions are used to find the pursuer's total control effort over the entire interval $[0, t_f]$, where t_f is the time when the interception occurs. Furthermore, the influence of saturation constraints on system observability is considered.

4.2.2 System Analysis

When pursuer acceleration is subject to saturation nonlinearity as given in Figure 4.1, the actual acceleration may operate in a normal, partial saturation, or saturation mode. The operations can be classified according to operating regions into four cases as shown in Figure 4.2a–4.2d. Target interception is analyzed for these cases.

Interception Conditions

Case I: Non-saturation with TPN

Consider Figure 4.2a when the pursuer operates in an unsaturated mode. That is, the pursuer under TPN guidance with commanded acceleration never exceeds the saturation constraint A_{max} throughout the entire engagement.

Theorem 4.1 *A necessary and sufficient condition for a non-saturated pursuer acceleration under TPN throughout the entire engagement, when the pursuer acceleration is subject to saturation constraint A_{max}, is*

$$\max\left(N_1, \frac{N_1 c}{N_1 - 2}\right) \leq b \tag{4.8}$$

where

$$b = \frac{A_{max}}{|\dot{R}_0 \dot{\sigma}_0|} \tag{4.9}$$

Proof. Because there is no acceleration component along the LOS under the TPN guidance strategy, the relative velocity vector remains closely aligned with LOS, and thus the range rate $\dot{R}$ is approximately a negative constant during the entire pursuit [6].

Since the magnitude of TPN guidance law is given as $|N_1 \dot{R} \dot{\sigma}|$, the variable $\dot{\sigma}$ determines whether the commanded acceleration exceeds the saturation constraints.

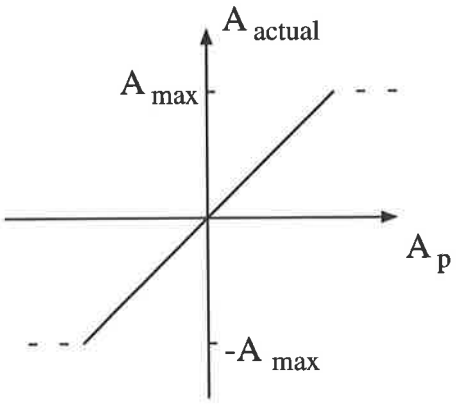

Figure 4.2a: Case I: Non-saturation mode

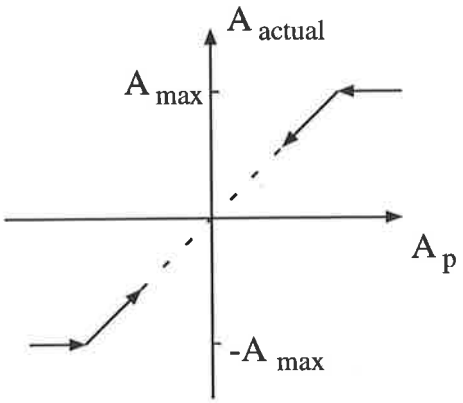

Figure 4.2b: Case II: Saturation followed by non-saturation mode

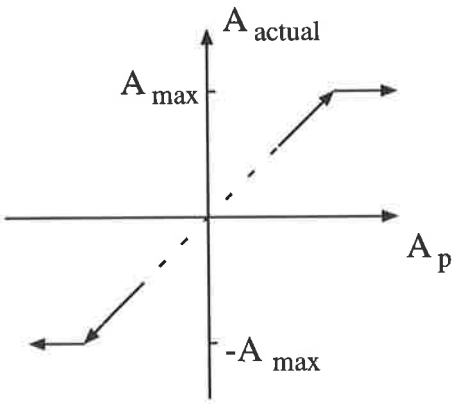

Figure 4.2c: Case III: Non-saturation followed by saturation mode

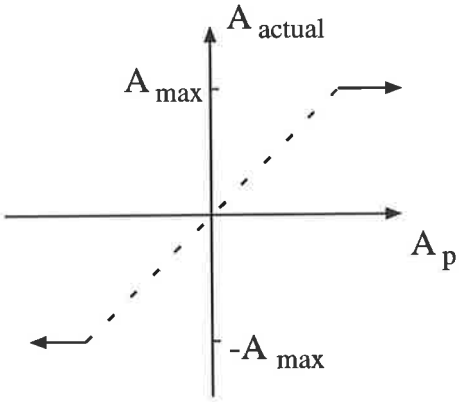

Figure 4.2d: Case IV: Saturation mode throughout

When TPN is to guide a pursuer to intercept a maneuvering target described in (4.5), the LOS angular rate is obtained as [31]

$$\dot{\sigma} = \dot{\sigma}_0 \left[\frac{N_1 - 2 - c}{N_1 - 2} \left(\frac{R}{R_0} \right)^{N_1 - 2} + \frac{c}{N_1 - 2} \right] \tag{4.10}$$

Differentiating (4.10) yields

$$\ddot{\sigma} = \dot{\sigma}_0 (N_1 - 2 - c) \left(\frac{R}{R_0} \right)^{N_1 - 3} \left(\frac{\dot{R}}{R_0} \right) \tag{4.11}$$

Because $\frac{R}{R_0} > 0$, $\frac{\dot{R}}{R_0} < 0$, $\dot{\sigma}_0$ is the system initial value, and $(N_1 - 2 - c)$ is the system constant, it is clear from (4.11) that the sign of $\ddot{\sigma}$ remains the same throughout the entire engagement, that is, $\dot{\sigma}$ monotonically increases, decreases, or remains the same. In others words, $\dot{\sigma}$ will not oscillate during the pursuit. It follows that the maximum value of $|\dot{\sigma}|$ occurs either at the beginning, or at the end of the engagement, i.e.,

$$\begin{aligned} \max |\dot{\sigma}| &= |\dot{\sigma}_0| \quad \text{or,} \\ \max |\dot{\sigma}| &= |\dot{\sigma}_f| = \frac{c}{N_1 - 2} |\dot{\sigma}_0| \end{aligned}$$

where $\dot{\sigma}_f$ is the LOS angular rate at the final interception, and is obtained by substituting $\frac{R}{R_0} = 0$ into (4.10). The maximum pursuer acceleration commanded by TPN is either at the beginning of the pursuit, i.e., $N_1 |\dot{R}_0 \dot{\sigma}_0|$, or at the end, i.e., $\frac{N_1 c}{N_1 - 2} |\dot{R}_f \dot{\sigma}_0|$, where $\dot{R}_f$ is the final range rate.

Note that with $\dot{R}$ approximately remaining as a negative constant, we have $\dot{R}_0 \approx \dot{R}_f$. Then, if

$$\max \left(N_1 |\dot{R}_0 \dot{\sigma}_0|, \quad \frac{N_1 c}{N_1 - 2} |\dot{R}_0 \dot{\sigma}_0| \right) \leq A_{max} = b |\dot{R}_0 \dot{\sigma}_0|,$$

the acceleration issued by TPN is not greater than the saturation constraints. It follows that if inequality (4.8) is satisfied, then saturation will not occur. Conversely, if saturation does not occur, then condition (4.8) should be satisfied. ■

Theorem 4.2 *For a pursuer with normal (i.e., unsaturated) acceleration throughout the entire engagement under TPN, the following conditions must be satisfied for effective interception of a maneuvering target,*

$$N_1 > 3 \tag{4.12}$$

$$C^2 > \frac{1}{N_1 - 1} + \frac{c^2 + 2c}{N_1 (N_1 - 1)} \tag{4.13}$$

where

$$C = \frac{\dot{R}_0}{R_0\dot{\sigma}_0} \tag{4.14}$$

is defined by the system initial conditions.

Proof. See the proof of Theorem 2.2. ∎

Remarks.

This theorem is identical to Theorem 2.2 in Chapter 2, except that we explicitly state here that the constraints obtained are specifically applicable to a pursuer operating in normal (i.e., unsaturated) mode, which is implicitly assumed in Chapter 2. Theorem 4.2 is included here for completeness.

Case II: A_{max} first, followed by TPN

This mode of operation is illustrated in Figure 4.2b where a maximum thrust is applied during the initial phase of the course due to insufficient available acceleration. The target-pursuit motion equations (4.6) and (4.7) under this scenario are

$$\ddot{R} - R\dot{\sigma}^2 = 0 \tag{4.15}$$

$$R\ddot{\sigma} + 2\dot{R}\dot{\sigma} = \text{sign}(\dot{R}\dot{\sigma}) \cdot A_{max} - c\dot{\sigma}_0\dot{R} \tag{4.16}$$

For a saturated mode to become unsaturated under TPN, $|N_1\dot{R}\dot{\sigma}|$ must decrease, so the commanded acceleration becomes an attainable value. Then, the motion equations are

$$\ddot{R} - R\dot{\sigma}^2 = 0 \tag{4.17}$$

$$R\ddot{\sigma} + 2\dot{R}\dot{\sigma} = N_1\dot{\sigma}\dot{R} - c\dot{\sigma}_0\dot{R} \tag{4.18}$$

The acceleration saturated at the beginning of the engagement implies that

$$N_1|\dot{R}_0\dot{\sigma}_0| > A_{max} = b|\dot{R}_0\dot{\sigma}_0|,$$

that is,

$$N_1 > b. \tag{4.19}$$

The interception conditions for this case are summarized as follows.

Theorem 4.3 *To effectively intercept a maneuvering target under TPN, the following conditions must be satisfied for a guidance system with initial pursuer acceleration saturation,*

$$b > c+2 \tag{4.20}$$

$$N_1 > 3 \tag{4.21}$$

$$C^2 > \frac{b^2k^2 + 2cbk^2 + c^2k^2N_1}{N_1^2(N_1-1)} \tag{4.22}$$

where b and C are given in (4.9) and (4.14), respectively, and

$$k = \sqrt{\frac{N_1(b-c-2)}{N_1(b-c)-2b}}. \tag{4.23}$$

Proof. To make (4.16) more tractable, we simplify the formulation by using the fact that the range rate $\dot{R}$ is approximately a negative constant during the course as there is no acceleration component along the LOS.

At the beginning, a maximum acceleration A_{max} is applied because of the saturation,

$$\begin{aligned} \text{sign}(\dot{R}\dot{\sigma})A_{max} &= \text{sign}(\dot{R}_0\dot{\sigma}_0)\cdot b\cdot|\dot{R}_0\dot{\sigma}_0| \\ &= -\text{sign}(\dot{\sigma}_0)|\dot{\sigma}_0|b(-\dot{R}_0) \\ &\approx b\dot{R}\dot{\sigma}_0 \end{aligned} \tag{4.24}$$

Substituting (4.24) into (4.16), and solving (4.15) and (4.16) yields the LOS angular rate

$$\dot{\sigma} = \dot{\sigma}_0\left[\frac{(c+2-b)}{2}\left(\frac{R}{R_0}\right)^{-2} + \frac{(b-c)}{2}\right] \tag{4.25}$$

From (4.25), an important fact emerges: *interception with zero miss distance is not attainable if acceleration saturation persists throughout the entire pursuit.* This is because $\dot{\sigma}$ approaches infinity when R approaches zero near the end of the engagement.

Differentiating (4.25) gives

$$\frac{\ddot{\sigma}}{\dot{\sigma}_0} = (b-c-2)\left(\frac{R}{R_0}\right)^{-3}\left(\frac{\dot{R}}{R_0}\right).$$

Since $\frac{R}{R_0} > 0$ and $\frac{\dot{R}}{R_0} < 0$, if $b > c+2$, then $\frac{\ddot{\sigma}}{\dot{\sigma}_0} < 0$. This means that if $\dot{\sigma}_0 > 0$, then $\ddot{\sigma} < 0$, i.e., $\dot{\sigma}$ decreases; or if $\dot{\sigma}_0 < 0$, then $\ddot{\sigma} > 0$, i.e., $\dot{\sigma}$ increases. Both cases give the same result, that is, $|\dot{\sigma}|$ decreases from the very beginning.

When $|\dot{\sigma}|$ reduces to a point at which $A_{max} = |N_1 \dot{R}\dot{\sigma}|$, then the saturated mode switches to an unsaturated mode. At the transition,

$$\dot{\sigma} = \frac{b}{N_1}\dot{\sigma}_0 \tag{4.26}$$

$$R = kR_0 \tag{4.27}$$

where k is given in (4.23), and $k \in (0,1) \subset \mathbf{R}$ under the interception condition (4.20) and the implied condition (4.19), i.e., when $N_1 > b > c+2$. (4.26) is derived because of $|N_1 \dot{R}\dot{\sigma}| = A_{max} \approx |\dot{\sigma}_0 b\dot{R}|$, and (4.27) is obtained by substituting (4.26) into the left-hand side of (4.25).

Note that after transition from a saturated mode to a normal (i.e., unsaturated) mode, we must have new system initial values for the unsaturated TPN based system. The new initial relative range, given in (4.27), is denoted as R_0^*. The new initial LOS angular rate, given in (4.26), is denoted as $\dot{\sigma}_0^*$. The pursuit motion is given in (4.17) and (4.18).

Solving (4.17) and (4.18) yields

$$\dot{\sigma} = \dot{\sigma}_0^* \left(\frac{R}{R_0^*}\right)^{N_1-2} + \frac{N_1 c \dot{\sigma}_0^*}{b(N_1-2)}\left[1 - \left(\frac{R}{R_0^*}\right)^{N_1-2}\right] \tag{4.28}$$

We can check the sign of $\frac{\ddot{\sigma}}{\dot{\sigma}_0^*}$ to determine the trend of $|\dot{\sigma}|$, as

$$\text{sign}\left(\frac{\ddot{\sigma}}{\dot{\sigma}_0^*}\right) = \text{sign}\left[(bN_1 - 2b - N_1 c)\left(\frac{R}{R_0^*}\right)^{N_1-3}\left(\frac{\dot{R}}{R_0^*}\right)\right] = -1 \tag{4.29}$$

The last equal sign is because of conditions (4.19) and (4.20). (4.29) shows that $|\dot{\sigma}|$ will decrease from $\dot{\sigma} = \dot{\sigma}_0^*$. It follows that the commanded acceleration reduces after TPN is applied, and thus will not exceed the saturation constraints again.

Following the approach in the proof of Theorem 2.2, when TPN guidance law is used to direct the pursuer, condition (4.21) should hold for an effective interception within the capture area which is given in inequality (4.22). ■

Remarks.

The interception condition (4.20) can be rewritten as

$$A_{max} > (c+2)|\dot{R}_0\dot{\sigma}_0| \tag{4.30}$$

by using the definition of b given in (4.9).

From the engagement geometry, we can obtain

$$\dot{\sigma}_0 = \frac{V_T \sin(\phi_0 - \sigma_0) - V_P \sin(\theta_0 - \sigma_0)}{R_0} \tag{4.31}$$

$$\dot{R}_0 = V_T \cos(\phi_0 - \sigma_0) - V_P \cos(\theta_0 - \sigma_0). \tag{4.32}$$

Condition (4.30), which gives the lower bound of the pursuer saturation constraints to ensure interception, can be equivalently written as

$$\begin{aligned} A_{max} > \frac{c+2}{R_0} | & [V_T \sin(\phi_0 - \sigma_0) - V_P \sin(\theta_0 - \sigma_0)] \\ & \cdot [V_T \cos(\phi_0 - \sigma_0) - V_P \cos(\theta_0 - \sigma_0)] | \end{aligned} \tag{4.33}$$

Inequality (4.33) shows that the minimal acceleration, which the pursuer should provide to intercept a maneuvering target, is proportional to the target maneuverability. It reveals that the larger the target maneuver constant c, the greater the pursuer acceleration capability required for effective interception.

Note further that the minimal pursuer acceleration required is inversely proportional to the initial range between the pursuer and the target. It can be explained as the longer the initial distance, the more time to adjust the pursuer, and the less strict requirement on the saturation constraints. The result can be used to derive a more favorable launch condition for target interception.

Case III: TPN first, followed by A_{max}

In this case, a normal (unsaturated) mode commanded by TPN is maintained until $\dot{\sigma}$ increases to such a value that the pursuer acceleration becomes saturated, as shown in Figure 4.2c. For this mode, interception with zero miss distance is not achievable.

Theorem 4.4 *The conditions for a TPN based pursuer to operate in an initial unsaturated mode followed by a saturated mode are*

$$b < \frac{N_1 c}{N_1 - 2} \tag{4.34}$$

$$N_1 < \min(c+2, b). \tag{4.35}$$

In such a pursuer-target engagement, the pursuer cannot intercept a target modeled by (4.5).

Proof. If $N_1 < b$, i.e., $N_1|\dot{R}_0\dot{\sigma}_0| < b|\dot{R}_0\dot{\sigma}_0| = A_{max}$, TPN is attainable during the first portion of the pursuit. The LOS angular rate under the TPN guidance law is given as in (4.10). If $c+2 > N_1$, we then have from (4.11) that $\frac{\ddot{\sigma}}{\dot{\sigma}_0} > 0$, which shows $|\dot{\sigma}|$ will monotonically increase. Condition (4.34) implies that

$$A_{max} < N_1 \frac{c}{N_1 - 2}|\dot{R}\dot{\sigma}_0| = N_1|\dot{R}\dot{\sigma}_f| \tag{4.36}$$

Inequality (4.36) suggests that before an interception can occur, acceleration becomes saturated. This is because as $|\dot{\sigma}|$ has increased to such a value that $N_1|\dot{R}\dot{\sigma}| = A_{max} < N_1|\dot{R}\dot{\sigma}_f|$, the acceleration commanded by TPN is no longer attainable, and hence A_{max} is used.

When A_{max} is applied, the LOS angular rate is derived as

$$\dot{\sigma} = \dot{\sigma}^* \left\{ \left(\frac{R}{R^*}\right)^{-2} + \frac{N_1(b-c)}{2b}\left[1 - \left(\frac{R}{R^*}\right)^{-2}\right] \right\} \tag{4.37}$$

where R^* and $\dot{\sigma}^*$ denote the range and the LOS angular rate at the transition, respectively. With condition (4.34), we have $\frac{\ddot{\sigma}}{\dot{\sigma}^*} > 0$. This result indicates that $|\dot{\sigma}|$ increases monotonically after the transition, and will lead to an acceleration saturation for the rest of the pursuit. Consequently, the pursuer cannot hit the target because $|\dot{\sigma}|$ will approach infinity at the closing moment of the engagement when $R \to 0$. ∎

Case IV: A_{max} throughout

The occurrence for saturation throughout the entire engagement can be expressed as

$$b < \min(N_1, c+2). \tag{4.38}$$

Since $b < N_1$ implies that pursuer acceleration is saturated at the beginning, while $b < c+2$ implies that commanded acceleration must increase, hence saturation is maintained throughout the engagement. As we have pointed out in the proof of Theorem 4.3, zero miss distance is not achievable for this case.

Total Control Effort

The effects of saturation constraints on total control effort are studied. Only Case I and Case II, i.e., non-saturation with TPN and A_{max} followed by TPN, are considered here. Case III and Case IV are discarded because there is no finite time for an interception to occur.

The total control effort is determined by cumulative velocity increment, which is defined as [39]

$$\Delta V = \int_0^{t_f} |A_P| dt \tag{4.39}$$

where t_f is the final time when interception occurs, and A_P is the pursuer acceleration.

For a non-saturated TPN command (i.e., Case I), the total control effort is given as [40]

$$\Delta V = \frac{R_0 N_1 (1+c)}{N_1 - 1} |\dot{\sigma}_0| \tag{4.40}$$

For Case II in which A_{max} is followed by TPN, it is proved that even when the pursuer acceleration is not sufficient at the beginning, an interception is still achievable provided conditions (4.20)–(4.22) are satisfied. It appears likely that the interception achieved by this saturated mode is at the expense of greater total control effort than that necessary for an unsaturated mode with TPN. It can now be shown that this is indeed the case.

The total control effort for Case II consists of two parts, the first part is that when A_{max} is used because of the saturation, and the second part is when TPN can be applied. That is,

$$\Delta V = \int_0^{\tau} |A_{max}| dt + \int_{\tau}^{t_f} |N_1 \dot{R} \dot{\sigma}| dt \tag{4.41}$$

where τ denotes the time at the transition. By using the approximation of A_{max} given in (4.24), the cumulative velocity increment can be rewritten as the integral with respect to $\frac{R}{R_0}$, i.e.,

$$\Delta V = R_0 \left[\int_k^1 |b\dot{\sigma}_0| d\left(\frac{R}{R_0}\right) + \int_0^k |N_1 \dot{\sigma}| d\left(\frac{R}{R_0}\right) \right] \tag{4.42}$$

where k is the ratio $\frac{R}{R_0}$ at the transition and is given in (4.23). Further mathematical manipulation obtains the analytical solution as

$$\Delta V = |\dot{\sigma}_0| R_0 \left[(1-k)b + \frac{b + cN_1}{N_1 - 1} k \right] \tag{4.43}$$

which admits the following interpretation. (i) When $b = N_1$, i.e., $k = 1$, from (4.42), we can see that this corresponds to one scenario of Case I, and the control effort computed by (4.43) agrees with that by (4.40). (ii) When $b = c+2$, then $k = 0$, it represents one scenario of Case IV. (iii) When $N_1 > b > c + 2$, i.e., $1 > k > 0$, it corresponds to Case II.

Partial differentiating (4.43) with respect to b leads to

$$\frac{\partial\left(\frac{\Delta V}{|\dot{\sigma}_0|R_0}\right)}{\partial b} = 1 - \frac{k}{N_1 - 1}\left(N_1 - 2 + \frac{N_1 - c - 2}{b - c - 2}\right) < 0 \tag{4.44}$$

Note that k is also the function of b, and conditions (4.19)–(4.22) must be satisfied. Inequality (4.44) shows that (i) for Case II, i.e., $N_1 > b > c + 2$, the total control effort monotonically reduces with the increase of saturation constraints A_{max}, which is represented by b, and (ii) the total control effort reaches its minimum at $b = N_1$; this implies, *cf* (4.8), one scenario of Case I. Thus the propellant required in Case II is greater than that necessary in Case I.

Observability with Saturation Constraints

As observability is the central theme of this thesis, the question on whether and how saturation constraints influence the system observability will be naturally raised. We analyze the observability of the guidance systems subject to acceleration saturation constraints in four operating modes.

The observability issue in Case I, when the systems is under a normal non-saturated TPN control throughout, has been discussed in section 2.6.3.

For Case II in which A_{max} is followed by TPN, the range observability index defined in (2.65) is

$$I_A(t_0, t_f) = \int_{t_0}^{\tau}(t - s)(A_{max} - A_T)ds + \int_{\tau}^{t_f}(t - s)(N_1\dot{R}\dot{\sigma} - A_T)ds \tag{4.45}$$

where τ denotes the time at transition. Note that t_0 represents the time when observability is of particular interest. When analyzing the observability near the end game, which is critical to achieve the interception, the range observability index (4.45) reduces to

$$I_A(t_0, t_f) = \int_{t_0}^{t_f}(t - s)(N_1\dot{R}\dot{\sigma} - A_T)ds, \tag{4.46}$$

which is the same as the index for a non-saturation with TPN, i.e., Case I. Evidently, the results obtained on system observability toward the end of the engagement under a normal TPN command are applicable to Case II, even though saturation occurs initially.

For Case III and Case IV in which A_{max} takes effect in the final stage of an engagement, the index is

$$I_A(t_0, t_f) = \int_{t_0}^{t_f} (t - s)(A_{max} - A_T)ds, \tag{4.47}$$

Since A_{max} is a constant, the index obtained in (4.47) is not equal to zero when the system is engaging a non-maneuvering target, i.e., when $A_T = 0$. It follows that when acceleration is operating in the Case III and Case VI regions, an observable system in pursuit of a non-maneuvering target is still feasible. This result differs from that of Case I. However, the overriding condition that an interception cannot occur in Case III and Case IV diminishes the potential observability advantage.

In summary, for those cases in which an interception is achievable, the saturation constraints do not affect the system's observability significantly. This is simply because TPN eventually takes its place as the guidance law.

4.2.3 Simulation Results

To confirm the results derived in section 4.2.2 and to check the generality of the interception conditions, simulation studies with different scenarios are conducted.

All the simulations use the following data,

Velocity of the pursuer,	$V_P = 600m/s$;
Velocity of the target,	$V_T = 300m/s$;
Initial heading angle of the pursuer,	$\theta_0 = 0°$;
Initial heading angle of the target,	$\phi_0 = 30°$;
Initial LOS angle,	$\sigma_0 = 0°$,

which are the same as those used in section 3.7 except the initial relative range R_0. The initial range R_0 is fixed to $1000m$ in most simulations in this section, expect that R_0 is variable in producing Figure 4.5. The initial conditions $\dot{R}_0$ and $\dot{\sigma}_0$ are computed from (4.31) and

(4.32). In realizing the guidance law (4.4), $N_1 = 4$, a typical value of the TPN navigation constant, is used throughout the simulation.

In order to verify the derived interception conditions for different cases, the trajectories of a maneuvering target and a pursuer with acceleration constraints under TPN are plotted in Figure 4.3. The target model is given in (4.5) with the maneuver constant $c = 1$. Three different acceleration constraints selected are $21g$, $16g$ and $13g$.

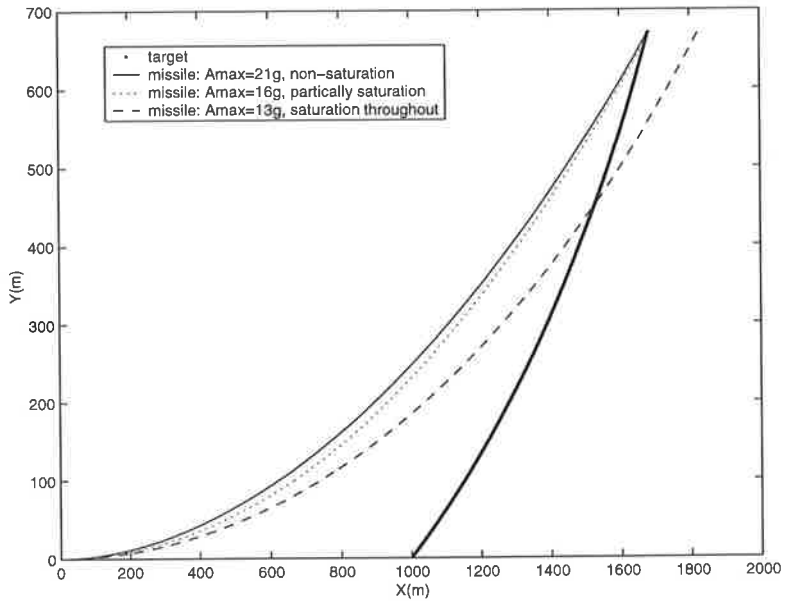

Figure 4.3: Trajectories of a maneuvering target and a pursuer under TPN with acceleration saturation constraints

When $A_{max} = 21g$, we have, based on inequality (4.8), a scenario representing an unsaturated TPN mode for the entire engagement. As the given system initial values and the navigation constant N_1 satisfy the Case I interception conditions (4.12) and (4.13), an interception can occur. This is confirmed by the trajectory of the pursuer in solid line in Figure 4.3. When $A_{max} = 13g$, a Case IV scenario occurs, according to inequality (4.38). It is observed from Figure 4.3 that the pursuer with $A_{max} = 13g$ is unable to turn sufficiently fast to accomplish the interception task, which confirms the remark in section 4.2.2 that an interception is not achievable for Casc VI. Interception conditions (4.20)–(4.22) allow us to predict that only when the saturation constraint A_{max} is larger than $15.6g$ for this scenario

then can the pursuer successfully hit the target. This predication is confirmed by the ability of the pursuer with $A_{max} = 16g$ to capture the target, in spite of the saturation at the first stage of pursuit. We thus see that the derived interception conditions are practically useful for predicting the occurrence of target interception.

The effects of acceleration saturation constraints on the pursuer system performance are now investigated.

Figure 4.4 shows how the pursuer acceleration saturation constraints A_{max} are linked to the maximum maneuver constant c of the target: A_{max} attainable is proportional to c. Note that the larger the target maneuver constant, the more maneuverable the target. It appears from Figure 4.4 that the smaller the pursuer saturation constraints, the less maneuverable the target with which the interception is achievable.

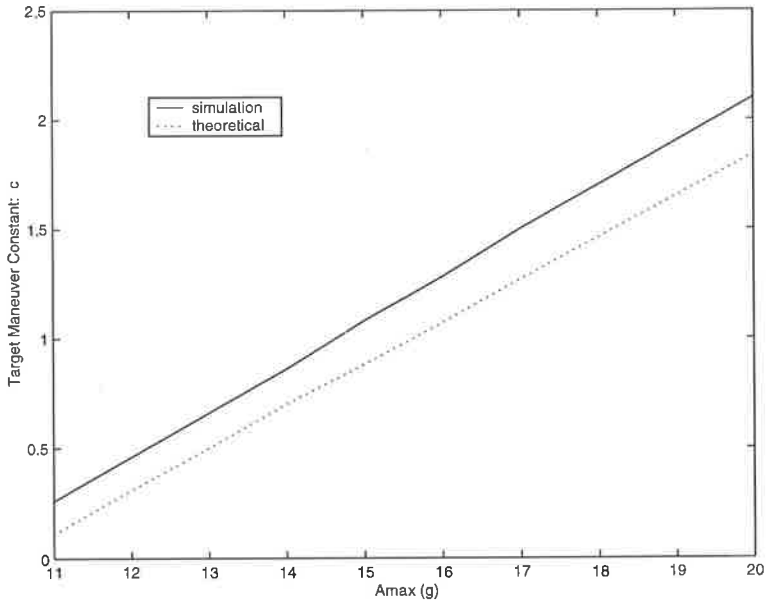

Figure 4.4: Pursuer acceleration constraint A_{max} versus target maneuver constant c under TPN

Figure 4.5 demonstrates that the initial range R_0 is inversely proportional to A_{max}. That is, the smaller initial range R_0, the larger A_{max} needed to hit the target. Note that a small R_0 represents a less favorable initial condition because of the lack of sufficient time to maneuver. This confirms the discussion in section 4.2.2.

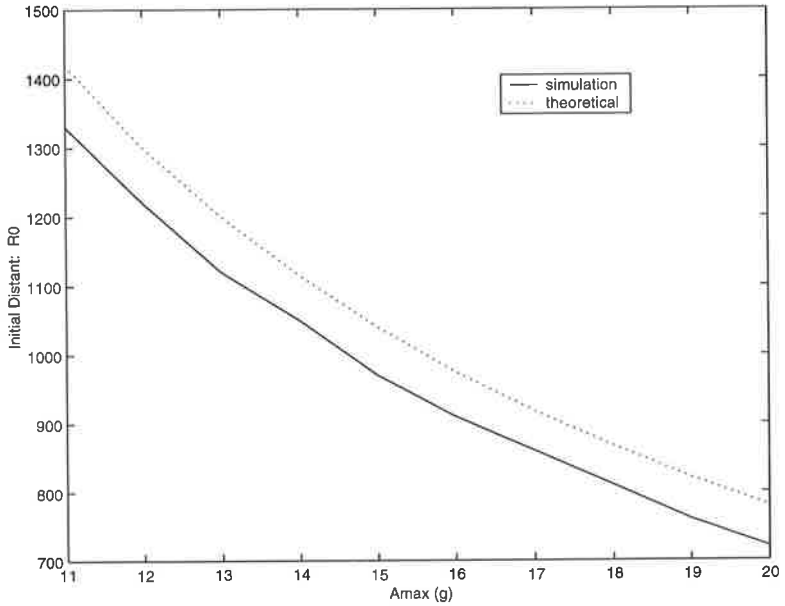

Figure 4.5: Pursuer acceleration constraint A_{max} versus initial relative range R_0 under TPN

Both solid lines in Figure 4.4 and Figure 4.5 are obtained from simulations, while the dotted lines are computed analytically from (4.33). They show that the simulation results, where A_{max} is actually used instead of the model $A_{max} \approx |b\dot{R}\dot{\sigma}_0|$, are identical to their theoretical counterparts. Therefore, the model $A_{max} \approx |b\dot{R}\dot{\sigma}_0|$ established in (4.24) is adequate for investigating the saturation effects.

Total control efforts are given in Figure 4.6 under different acceleration saturation constraints, for both simulation and theoretical computation obtained from (4.43). When A_{max} is adequate for interception to occur, the total control effort decreases with the A_{max} increases. It reaches its minimum when the pursuer acceleration capability is sufficient for an unsaturated TPN to be maintained throughout the entire game, i.e., Case I. This is because more propellant is needed for correcting the pursuit error due to the saturation. Figure 4.6 confirms that interception for an unsaturated mode can be achieved by less total control effort than that for a saturated mode, as discussed in section 4.2.2. Simulation and theoretical results shown in Figure 4.6 validate the model $A_{max} \approx |b\dot{R}\dot{\sigma}_0|$ once again.

All the interception conditions are derived based on the target model in (4.5), which

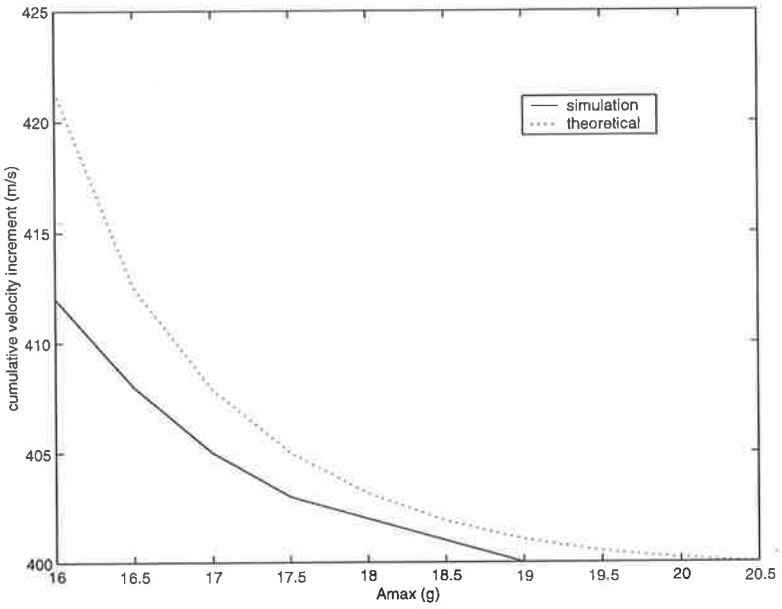

Figure 4.6: Total control efforts of pursuers with different acceleration saturation constraints under TPN

represents a near constant target acceleration with respect to the pursuer. To evaluate how general are the interception conditions when the target model varies, we use six target models in the simulation. They are: near constant acceleration target [31], (i.e., the model used in our analytical study), constant acceleration target [23], modified smart target [44], TPN based target [45], first order lag target [16], and sinusoidal target [23].

Table 4.1 gives the mathematical models and simulation results on the proximity between the pursuer and the target. In column two of Table 4.1, λ_T denotes the constant of the target models. All target constants are determined by assuming targets to have the same initial acceleration as the near constant acceleration target with $c = 1$. That is, the initial target acceleration A_{T0} equals $5.2g$, which is derived from $|A_{T0}| = c\dot{R}_0\dot{\sigma}_0$. This allows the same interception conditions to be used for all target models. In the simulation study, the pursuer is assumed to have $A_{max} = 17g$, which gives a Case II scenario. Based on the Case II interception conditions (4.20)–(4.22), the pursuer is capable of intercepting the near constant acceleration target with $c = 1$.

All the final miss distances shown in Table 4.1 for different target models are well within

Target type with respect to pursuer	Model	Miss distance
near constant acceleration	$A_{TR} = 0;\ A_{T\sigma} = c\dot{\sigma}_0\dot{R}$	$1.2m$
constant acceleration	$A_{TR} = 0;\ A_{T\sigma} = \lambda_T$	$2.5m$
modified smart	$A_{TR} = 0;\ A_{T\sigma} = \lambda_T/(\dot{R}\dot{\sigma})$	$1.5m$
TPN based	$A_{TR} = 0;\ A_{T\sigma} = \lambda_T\dot{R}\dot{\sigma}$	$1.5m$
first order lag	$A_{TR} = A_{T\sigma} = \lambda_T \exp(-0.1t)$	$3.6m$
sinusoidal	$A_{TR} = A_{T\sigma} = \lambda_T \cos\dot{\sigma}t$	$4.0m$

Table 4.1: Miss distance for different target models with initial acceleration $A_{T0} = 5.2g$ when the saturation constraint $A_{max} = 17g$ under TPN

$5m$, which is sufficient to cause damage to the target in practice. The results indicate that the interception conditions (4.20)–(4.22) are sufficiently general to cater for variations in target models.

4.3 AOPN Based Systems

4.3.1 System Equations

The pursuer acceleration A_P with AOPN-II given in (3.7) is expressed as

$$A_{PR} = 0; \qquad A_{P\sigma} = -N_1\dot{R}\dot{\sigma} - N_3\dot{R} \tag{4.48}$$

where A_{PR} and $A_{P\sigma}$ are components of the pursuer's acceleration along the LOS and normal to LOS, respectively; N_1 and N_3 are navigation constants.

The pursuer acceleration under AOPN-II with saturation constraints is given as

$$A_{PR} = 0; \qquad A_{P\sigma} = \begin{cases} -N_1\dot{R}\dot{\sigma} - N_3\dot{R} & \text{when } \mid N_1\dot{R}\dot{\sigma} + N_3\dot{R} \mid \leq A_{max} \\ -\text{sign}(\dot{R}\dot{\sigma}) \cdot A_{max} & \text{otherwise} \end{cases} \tag{4.49}$$

where A_{max} is the pursuer acceleration saturation limit.

Substituting the pursuer acceleration in (4.49) and the target acceleration model in (4.5) into the general equations of the target-pursuit motion given in (4.1) and (4.2), the governing equations become

$$\ddot{R} - R\dot{\sigma}^2 = 0 \tag{4.50}$$

$$R\ddot{\sigma} + 2\dot{R}\dot{\sigma} = \begin{cases} N_1\dot{R}\dot{\sigma} + N_3\dot{R} - c\dot{\sigma}_0\dot{R} & \text{when } \mid N_1\dot{R}\dot{\sigma} + N_3\dot{R} \mid \leq A_{max} \\ \text{sign}(\dot{R}\dot{\sigma}) \cdot A_{max} - c\dot{\sigma}_0\dot{R} & \text{otherwise} \end{cases} \tag{4.51}$$

which represent a maneuvering target engagement under AOPN-II with the pursuer acceleration subject to saturation constraint A_{max}.

We will analyze how the saturation nonlinearity affects the interception performance by deriving conditions for the occurrence of target interception based on (4.50) and (4.51).

4.3.2 System Analysis

Similar to the analysis of TPN based systems, there are four different cases to consider since the actual pursuer acceleration commanded by AOPN-II may operate in a normal, partial saturation, or saturation mode. Target interception conditions for these cases are analyzed.

Case I: Non-saturation with AOPN

Theorem 4.5 *A necessary and sufficient condition for a AOPN-II based pursuer to operate in a normal (i.e., unsaturated) mode throughout the entire engagement, when the pursuer acceleration is subject to saturation constraint A_{max}, is*

$$\max\left(\left|N_1 + \frac{N_3}{\dot{\sigma}_0}\right|, \left|\frac{N_1 c\dot{\sigma}_0 - 2N_3}{\dot{\sigma}_0(N_1 - 2)}\right|\right) \leq b \tag{4.52}$$

where

$$b = \frac{A_{max}}{|\dot{R}_0\dot{\sigma}_0|} \tag{4.53}$$

Proof. The derivation is identical to that for TPN based systems in the proof of Theorem 4.1, and thus is omitted here. ■

Remarks.

When $N_3 = 0$, condition (4.52) reduces to (4.8), which is a necessary and sufficient condition for TPN based systems. The difference between (4.52) and (4.8) is caused by the additive term of the AOPN-II guidance law to enhance system observability.

Theorem 4.6 *For an effective interception of a maneuvering target, a pursuer with normal (i.e., unsaturated) acceleration throughout the entire engagement under AOPN-II must satisfy the following conditions*

$$N_1 > 3 \tag{4.54}$$

$$(1+c+d) > \frac{N_3}{\dot{\sigma}_0} > (1+c-d) \tag{4.55}$$

$$C^2 > \frac{1}{N_1} \tag{4.56}$$

where

$$C = \frac{\dot{R}_0}{R_0 \dot{\sigma}_0}, \tag{4.57}$$

and

$$d = \sqrt{(N_1 - 1)(N_1 C^2 - 1)}. \tag{4.58}$$

Proof. See the proof of Theorem 3.4. ∎

Remarks.

Theorem 4.6 is the same as Theorem 3.4, except the explicit statement of operating in unsaturated regions in Theorem 4.6.

Case II: A_{max} first, followed by AOPN-II

In this case, a thrust at its maximum limit is applied in the initial phase of the pursuit due to insufficient available acceleration. The target-pursuit motion equations (4.50) and (4.51) under such an operation are

$$\ddot{R} - R\dot{\sigma}^2 = 0 \tag{4.59}$$

$$R\ddot{\sigma} + 2\dot{R}\dot{\sigma} = \text{sign}(\dot{R}\dot{\sigma}) \cdot A_{max} - c\dot{\sigma}_0 \dot{R} \tag{4.60}$$

For a saturated mode to become unsaturated, the magnitude of the acceleration commanded by AOPN-II must reduce sufficiently. Then, the motion equations become

$$\ddot{R} - R\dot{\sigma}^2 = 0 \tag{4.61}$$

$$R\ddot{\sigma} + 2\dot{R}\dot{\sigma} = N_1\dot{\sigma}\dot{R} + N_3\dot{R} - c\dot{\sigma}_0\dot{R} \tag{4.62}$$

The acceleration saturated at the beginning of the engagement implies that

$$|N_1\dot{R}_0\dot{\sigma}_0 + N_3\dot{R}_0| > A_{max} = b|\dot{R}_0\dot{\sigma}_0|,$$

that is,

$$\left|N_1 + \frac{N_3}{\dot{\sigma}_0}\right| > b. \tag{4.63}$$

The interception conditions for Case II are summarized as follows.

Theorem 4.7 *The conditions for a pursuer with initial acceleration saturation to be able to intercept a maneuvering target under AOPN-II are*

$$b > c+2 \tag{4.64}$$

$$N_1 > 3 \tag{4.65}$$

$$(1+c+d) > \tfrac{N_3}{\dot{\sigma}_0} > (1+c-d) \tag{4.66}$$

$$C^2 > \frac{1}{N_1} \tag{4.67}$$

$$b > \left|\frac{N_1 c\dot{\sigma}_0 - 2N_3}{\dot{\sigma}_0(N_1-2)}\right| \tag{4.68}$$

where b, C, and d are defined in (4.53), (4.57), and (4.58), respectively.

Proof. Following the approach used in section 4.2.2, the approximation $A_{max} \approx b\dot{R}\dot{\sigma}_0$ is adopted to make (4.60) more tractable. The LOS angular rate, when A_{max} is applied at the beginning, is obtained as

$$\dot{\sigma} = \dot{\sigma}_0\left[\frac{(c+2-b)}{2}\left(\frac{R}{R_0}\right)^{-2} + \frac{(b-c)}{2}\right] \tag{4.69}$$

Note that (4.69) is same as (4.25). This is because TPN and AOPN-II based systems have the same system equations when the commanded acceleration is saturated at the beginning.

Differentiating (4.69) gives

$$\frac{\ddot{\sigma}}{\dot{\sigma}_0} = (b - c - 2)\left(\frac{R}{R_0}\right)^{-3}\left(\frac{\dot{R}}{R_0}\right).$$

Since $\frac{R}{R_0} > 0$ and $\frac{\dot{R}}{R_0} < 0$, if $b > c + 2$, then $\frac{\ddot{\sigma}}{\dot{\sigma}_0} < 0$. This means that $|\dot{\sigma}|$ decreases from the start of the engagement.

When $|\dot{\sigma}|$ reduces to a point at which $A_{max} = |N_1 \dot{R}\dot{\sigma} + N_3 \dot{R}|$, the mode switches from saturated to unsaturated. Such transition will incur new system initial values which must be used in the subsequent unsaturated AOPN-II based system. The new initial relative range is denoted as R_0^*, and the new initial LOS angular rate as $\dot{\sigma}_0^*$. At the transition,

$$\dot{\sigma}_0^* = l\dot{\sigma}_0 \tag{4.70}$$

where $l < 1$ is used to account for the fact that $|\dot{\sigma}|$ reduces from the beginning when A_{max} is used.

When the acceleration commanded by AOPN-II is inside the non-saturation range, solving (4.61) and (4.62) yields

$$\dot{\sigma} = \dot{\sigma}_0^*\left(\frac{R}{R_0^*}\right)^{N_1-2} + \frac{c\dot{\sigma}_0 - N_3}{(N_1 - 2)}\left[1 - \left(\frac{R}{R_0^*}\right)^{N_1-2}\right] \tag{4.71}$$

To determine the trend of $|\dot{\sigma}|$, we check the sign of $\frac{\ddot{\sigma}}{\dot{\sigma}_0^*}$

$$\text{sign}\left(\frac{\ddot{\sigma}}{\dot{\sigma}_0^*}\right) = \text{sign}\left\{[(N_1 - 2)\dot{\sigma}_0^* + N_3 - c\dot{\sigma}_0]\left(\frac{R}{R_0^*}\right)^{N_1-3}\left(\frac{\dot{R}}{R_0^*}\right)\right\} \tag{4.72}$$

Because $\frac{R}{R_0^*} > 0$, $\frac{\dot{R}}{R_0^*} < 0$, and $[(N_1 - 2)\dot{\sigma}_0^* + N_3 - c\dot{\sigma}_0]$ is determined by the system's initial values and constants, the sign of $\ddot{\sigma}$ remains the same for the rest of the engagement. It follows that maximum value of $|\dot{\sigma}|$ occurs either at the transition, or at the end of the pursuit. That is,

$$\begin{aligned} \max|\dot{\sigma}| &= |\dot{\sigma}_0^*| \quad \text{or,} \\ \max|\dot{\sigma}| &= |\dot{\sigma}_f| = \left|\frac{c\dot{\sigma}_0 - N_3}{(N_1 - 2)}\right| \end{aligned}$$

If the condition in (4.68) is satisfied, it then ensures that the pursuer acceleration is not saturated at the end of the engagement. It follows that the acceleration by AOPN-II remains unsaturated after the transition.

Following the approach used in the proof of Theorem 3.4, when AOPN-II guidance law is used to direct the pursuer, the two conditions (4.65) and (4.66) should hold for an effective interception within the capture area which is defined by the new system initial values. We now derive condition (4.67).

According to (4.56), when AOPN-II is applied after the transition, the system's new initial values should satisfy

$$\left(\frac{\dot{R}_0^*}{R_0^*\dot{\sigma}_0^*}\right)^2 > \frac{1}{N_1}. \tag{4.73}$$

where $\dot{R}_0^*$ denotes the range rate at the transition. Because $\dot{R}$ remains approximately a negative constant, we have: (i) $\dot{R}_0^* \approx \dot{R}_0$, and (ii) $0 < R_0^* < R_0$ because $\dot{R} < 0$. The latter suggests that R must decrease. From these two relationships and (4.70), we have

$$\left(\frac{\dot{R}_0^*}{R_0^*\dot{\sigma}_0^*}\right)^2 > \left(\frac{\dot{R}_0}{R_0 \cdot l\dot{\sigma}_0}\right)^2 > \left(\frac{\dot{R}_0}{R_0\dot{\sigma}_0}\right)^2 \tag{4.74}$$

If the system initial values $\dot{R}_0$, R_0, and $\dot{\sigma}_0$ satisfy (4.67), then from (4.74), inequality (4.73) is valid. Therefore, (4.67) is a sufficient condition for (4.73) in regard to the capture area for Case II. ■

Remarks.

Whatever guidance strategy is used, A_{max} will be used as long as the commanded acceleration exceeds the available acceleration. As TPN based systems and AOPN-II based systems have the same dynamics when A_{max} is applied during the first stage of pursuit, the interception condition (4.64) and its equivalent form (4.33), which define the lower bound of the pursuer acceleration capability, are equally applicable to both TPN and AOPN-II systems. For ease of reference, the condition (4.33) is repeated below.

$$\begin{aligned} A_{max} > \; & \frac{c+2}{R_0}|[V_T \sin(\phi_0 - \sigma_0) - V_P \sin(\theta_0 - \sigma_0)] \\ & \cdot[V_T \cos(\phi_0 - \sigma_0) - V_P \cos(\theta_0 - \sigma_0)]|. \end{aligned} \tag{4.75}$$

Further investigation shows that no matter which guidance law is used after initial acceleration saturation, condition (4.75) is necessary to ensure interception. Therefore, condition (4.75) is a general condition for interception when the initial pursuer acceleration is reaching its saturation limit. According to (4.75), we obtain that the minimal acceleration to

intercept a maneuvering target is proportional to the target maneuverability, and inversely proportional to the initial range between the pursuer and the target.

Case III: AOPN-II first, followed by A_{max}

In Case III, a normal acceleration commanded by AOPN-II is applied until the pursuer acceleration increases to such a value that it exceeds the saturation constraints, and then A_{max} is used.

We analyze only a set of scenarios in Case III, namely, those scenarios with $N_1 + \frac{N_3}{\dot{\sigma}_0} > 0$ because they are mathematically tractable. For this set of scenarios, the interception with zero miss distance is not achievable.

Theorem 4.8 *When the pursuer-target engagement satisfies*

$$b < \frac{N_1 c\dot{\sigma}_0 - 2N_3}{\dot{\sigma}_0(N_1 - 2)} \tag{4.76}$$

$$0 < N_1 + \frac{N_3}{\dot{\sigma}_0} < \min(c+2, b) \tag{4.77}$$

which represent a normal AOPN-II mode first followed thereafter by A_{max}, the pursuer cannot intercept a target modeled by (4.5).

Proof. If $0 < N_1 + \frac{N_3}{\dot{\sigma}_0} < b$, i.e., $|N_1\dot{R}_0\dot{\sigma}_0 + N_3\dot{R}_0| < b|\dot{R}_0\dot{\sigma}_0| = A_{max}$, AOPN-II is attainable at the beginning. The LOS angular rate is obtained as in (3.28)

$$\dot{\sigma} = \dot{\sigma}_0 \left\{ \left[1 - \frac{c\dot{\sigma}_0 - N_3}{\dot{\sigma}_0(N_1 - 2)} \right] \left(\frac{R}{R_0} \right)^{N_1 - 2} + \frac{c\dot{\sigma}_0 - N_3}{\dot{\sigma}_0(N_1 - 2)} \right\} \tag{4.78}$$

and the LOS angular acceleration is given by differentiating (4.78) as

$$\ddot{\sigma} = \dot{\sigma}_0 \left(N_1 - 2 - c + \frac{N_3}{\dot{\sigma}_0} \right) \left(\frac{R}{R_0} \right)^{N_1 - 3} \left(\frac{\dot{R}}{R_0} \right). \tag{4.79}$$

If $N_1 + \frac{N_3}{\dot{\sigma}_0} < c + 2$, from (4.79), we have $\frac{\ddot{\sigma}}{\dot{\sigma}_0} > 0$; this shows that $|\dot{\sigma}|$ will monotonically increase, and implies that $\dot{\sigma}$ will not change its sign. Therefore, we obtain $\frac{\dot{\sigma}}{\dot{\sigma}_0} \geq 1$. From (4.76), we have

$$A_{max} \approx b|\dot{R}_f\dot{\sigma}_0| < |\dot{R}_f\dot{\sigma}_0| \frac{N_1 c\dot{\sigma}_0 - 2N_3}{\dot{\sigma}_0(N_1 - 2)} = |\dot{R}_f\dot{\sigma}_0| \left(N_1 \frac{\dot{\sigma}_f}{\dot{\sigma}_0} + \frac{N_3}{\dot{\sigma}_0} \right) \tag{4.80}$$

As

$$\left(N_1\frac{\dot{\sigma}_f}{\dot{\sigma}_0}+\frac{N_3}{\dot{\sigma}_0}\right) > N_1+\frac{N_3}{\dot{\sigma}_0} > 0,$$

inequality (4.80) can be rearranged as

$$A_{max} < |N_1\dot{R}_f\dot{\sigma}_f + N_3\dot{R}_f| \tag{4.81}$$

Inequality (4.81) implies that before an interception can occur, the acceleration becomes saturated. This is because $|\dot{\sigma}|$ has increased to such a value that $|N_1\dot{R}\dot{\sigma}+N_3\dot{R}| = A_{max} < |N_1\dot{R}_f\dot{\sigma}_f + N_3\dot{R}_f|$, the acceleration commanded by AOPN-II is no longer within the attainable limit, and hence A_{max} is used.

At the transition, from $|N_1\dot{R}\dot{\sigma}+N_3\dot{R}| = \left(N_1\frac{\dot{\sigma}}{\dot{\sigma}_0}+\frac{N_3}{\dot{\sigma}_0}\right)|\dot{R}_0\dot{\sigma}_0| = A_{max}$, the LOS angular rate is derived as

$$\dot{\sigma} = \frac{b\dot{\sigma}_0 - N_3}{N_1} \tag{4.82}$$

When A_{max} is applied, the LOS angular rate is obtained as

$$\dot{\sigma} = \left[\frac{2\dot{\sigma}^* + (c-b)\dot{\sigma}_0}{2}\right]\left(\frac{R}{R^*}\right)^{-2} + \frac{(c-b)\dot{\sigma}_0}{2} \tag{4.83}$$

where R^* denotes the range at the transition, and $\dot{\sigma}^*$ denotes the LOS angular rate at the transition. The value of $\dot{\sigma}^*$ is given in (4.82).

The trend of $|\dot{\sigma}|$ is examinable from the sign of $\frac{\ddot{\sigma}}{\dot{\sigma}^*}$.

$$\begin{aligned}\text{sign}\left(\frac{\ddot{\sigma}}{\dot{\sigma}^*}\right) &= -\text{sign}\left\{\left[2+(c-b)\frac{\dot{\sigma}_0}{\dot{\sigma}^*}\right]\left(\frac{R}{R_0}\right)^{-3}\left(\frac{\dot{R}}{R_0}\right)\right\} \\ &= \text{sign}\left[2+(c-b)\frac{N_1}{b-\frac{N_3}{\dot{\sigma}_0}}\right]\end{aligned} \tag{4.84}$$

Condition (4.76) yields $(c-b)N_1 + 2b - \frac{N_3}{\dot{\sigma}_0} > 0$, while (4.77) gives $\frac{N_3}{\dot{\sigma}_0} < b$; hence, from (4.84), we have $\text{sign}\left(\frac{\ddot{\sigma}}{\dot{\sigma}^*}\right) = 1$. This result indicates that $|\dot{\sigma}|$ increases monotonically after the transition, and will give rise to an acceleration saturation for the rest of the course. As a result, the pursuer cannot hit the target due to the fact $|\dot{\sigma}|$ will approach infinity when $R \to 0$. ■

Case IV: A_{max} throughout

The condition for the pursuer acceleration to be saturated throughout the entire engagement is

$$b < \min\left(\left|N_1 + \frac{N_3}{\dot{\sigma}_0}\right|, c+2\right). \tag{4.85}$$

$b < \left|N_1 + \frac{N_3}{\dot{\sigma}_0}\right|$ suggests that the pursuer acceleration is saturated during the first portion of the pursuit, and $b < c+2$ implies that the commanded acceleration must increase. Therefore, the saturation is maintained throughout the engagement, and zero miss distance is not achievable for this case.

4.3.3 Simulation and Discussion

All the simulations use the same initial values as those in section 4.2.3. In realizing the AOPN-II guidance law (4.49), $N_1 = 4$ and $N_3 = 0.1$ are used throughout the simulation, unless otherwise stated.

To verify the derived interception conditions for different cases, the trajectories of a maneuvering target modeled by (4.5) with $c = 1$ and a pursuer with acceleration constraints under AOPN-II are displayed in Figure 4.7. Three different acceleration constraints selected are $21g$, $16g$, and $13g$.

Interception conditions (4.64)–(4.68) allow us to predict that only when A_{max} is larger than $15.6g$ can the pursuer hit the target. With $A_{max} = 16g$, although the commanded acceleration by AOPN-II is not attainable at the first stage of pursuit, an interception is still achievable, i.e., a scenario of Case II. With $A_{max} > 25g$, according to condition (4.52), it corresponds to a scenario of Case I, i.e., non-saturation with AOPN-II. Figure 4.7 confirms that an interception can occur for this scenario of Case I, since interception conditions (4.54)–(4.56) are satisfied. A pursuer with $A_{max} = 13g$, a scenario of Case IV based on (4.85), is unable to turn sufficiently fast to capture the target, due to inadequate available acceleration throughout the entire engagement.

To illustrate a scenario of Case III, the trajectory of a pursuer with $A_{max} = 16g$ and navigation constant $N_3 = -0.3$ is also plotted in Figure 4.7. The simulation result verifies

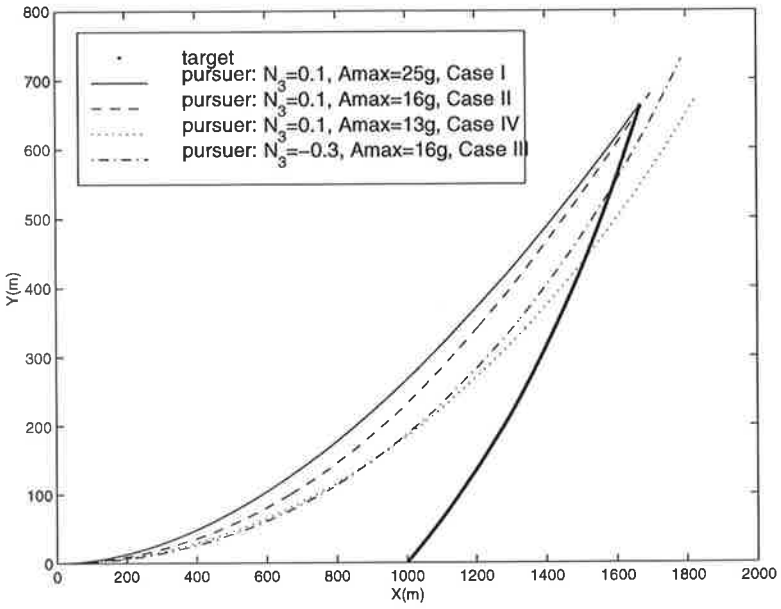

Figure 4.7: Trajectories of a maneuvering target and a pursuer under AOPN-II with acceleration saturation constraints

the analytical finding that the interception is not attainable if the pursuer-target engagement satisfies conditions (4.76)–(4.77), as discussed in Theorem 4.8. We observe that in this Case III scenario, the pursuer is subject to the same acceleration constraint $A_{max} = 16g$ as that in the previous Case II scenario, but with different N_3. That is, $N_3 = -0.3$ in Case III and $N_3 = 0.1$ in Case II are used. Comparing the pursuer's trajectories in these two cases, we further observe that with a given acceleration saturation constraint, a scenario of Case III under AOPN-II can be converted into a scenario of Case II by adjusting N_3, and hence accomplishing the pursuit mission. Simulation studies show that the derived interception conditions are practically useful in predicting the occurrence of target interception.

Based on the results from simulations, total control efforts under different acceleration saturation constraints are depicted in Figure 4.8. Interpretation of Figure 4.8 admits the following: (i) for those cases in which A_{max} is adequate for an interception to occur, total control effort monotonically reduces with the increase of saturation constraints; and (ii) total control effort reaches its minimum when the pursuer acceleration capability is sufficient for an unsaturated AOPN-II to be maintained throughout the entire engagement, i.e., Case I. We

can see from Figure 4.8 that an interception achieved in a partial saturation mode consumes more control effort than in a non-saturation mode, because more propellant is needed for removing the error caused by saturation.

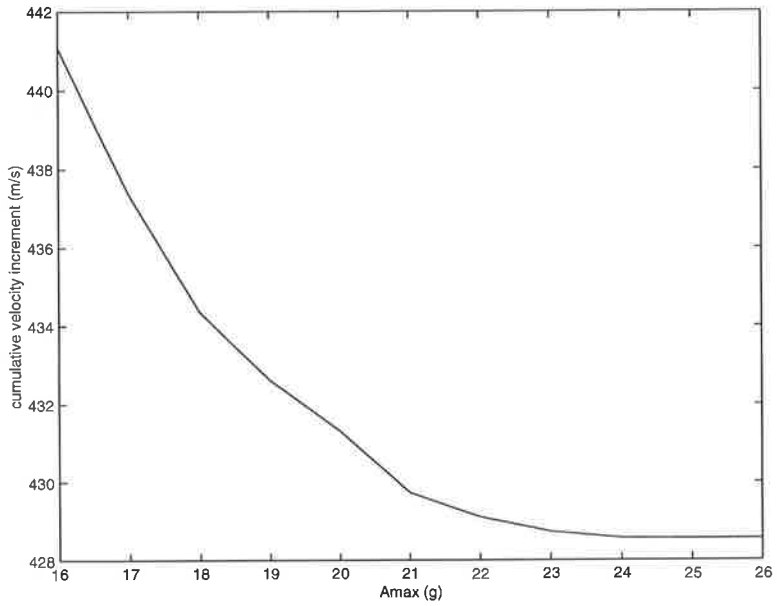

Figure 4.8: Total control efforts of pursuers with different acceleration saturation constraints under AOPN-II

The interception conditions for different operating modes under AOPN-II are derived based on the target model in (4.5), which gives a near constant target acceleration. To investigate how general these interception conditions are with variation in target models, the six target models used in the performance evaluation of the TPN based systems in section 4.2.3 are employed here. Table 4.2 gives their mathematical models and simulation results on the miss distance between the missile and the target.

In this part of simulation study, $A_{max} = 16g$ is used. This gives a Case II scenario. The simulation results confirm that even with initial saturation, the missile is still capable of intercepting the near constant acceleration target with $c = 1$. In order to allow the same interception conditions to be used for all target models, the target constant, denoted as λ_T in Table 4.2, is determined by assuming all target models to have the same initial value as the chosen near constant acceleration target. That is, $A_{T0} = 5.2g$ is used for all models. This

numerical value is derived from $|A_{T0}| = c\dot{R}_0\dot{\sigma}_0$.

From the results in Table 4.2, we observe that all the miss distances are well within $5m$, which in practice is regarded as sufficiently close to cause damage to the target. The results serve to confirm the generality of interception conditions (4.64)–(4.67) in catering for considerable different target models.

Target type with respect to missile	**Model**	**Miss distance**
near constant acceleration	$A_{TR} = 0;\ A_{T\sigma} = c\dot{\sigma}_0\dot{R}$	$1.3m$
constant acceleration [23]	$A_{TR} = 0;\ A_{T\sigma} = \lambda_T$	$2.8m$
modified smart [44]	$A_{TR} = 0;\ A_{T\sigma} = \lambda_T/(\dot{R}\dot{\sigma})$	$1.5m$
TPN based [45]	$A_{TR} = 0;\ A_{T\sigma} = \lambda_T\dot{R}\dot{\sigma}$	$2.0m$
first order lag [16]	$A_{TR} = A_{T\sigma} = \lambda_T \exp(-0.1t)$	$3.6m$
sinusoidal [23]	$A_{TR} = A_{T\sigma} = \lambda_T \cos\dot{\sigma}t$	$1.6m$

Table 4.2: Miss distance for target models with initial acceleration $A_{T0} = 5.2g$ when $A_{max} = 16g$ under AOPN-II

4.4 Concluding Remarks

The effects of acceleration saturation constraints on system performance have been investigated. Analysis of TPN based and AOPN-II based guidance systems with acceleration saturation constraints demonstrates that saturation constraints do degrade the system's interception performance and cause more total control efforts to be consumed.

Four different operating modes have been considered when deriving the interception conditions. These conditions are useful to predicate the occurrence of target interception. In particular, conditions (4.20)–(4.22) for TPN and conditions (4.64)–(4.68) for AOPN-II are significant. Analysis indicates that even thought the commanded acceleration cannot always be provided, if condition (4.20)–(4.22) are met for TPN based systems, an interception with zero miss distance can be accomplished. Similarly, for an initially saturated AOPN-II com-

mand, conditions (4.64)–(4.68) must be satisfied in order to achieve a zero miss distance interception. Otherwise, a finite possible large miss distance will result, due to inadequate pursuer's acceleration capability.

Condition (4.33), which is equally applicable to both TPN based systems and AOPN-II based systems, defines the minimal acceleration capability a pursuer should provide with respect to its system initial conditions. In practical terms, it allows one to compute a favorable launch condition for target interception.

Both analytical study and simulation have proved that more total control efforts are needed to achieve an interception with a saturated TPN command than that with a normal TPN command. Similar results are registered in AOPN-II commanded systems.

To complete the work on observability analysis, the impacts of saturation constraints on the observability of TPN based systems have been studied. For those cases in which target interception can occur, the saturation constraints impose no influence at all on system observability near the end of pursuit.

Finally, simulations demonstrate that the derived interception conditions are sufficiently general to cater for significant variations in target models.

Chapter 5

Conclusion

5.1 Summary

Motivated by poor observability problems suffered by bearings-only measurement systems under conventional proportional navigation guidance strategy, this research is primarily concerned with the performance improvement and observability enhancement of proportional navigation based guidance systems.

To achieve the *Aim One* of this research, that is to explore the characteristics of classical proportional navigation guidance laws, a study of true proportional navigation (TPN), the foundation for more advanced guidance techniques, was chosen. Analysis of TPN based systems has been performed by deriving closed-form solution, developing necessary conditions for interception, determining total control effort, and examining system observability. It has been shown that the target maneuver affects interception unfavorably in terms of slowing down the closing speed, tightening the interception conditions, and utilizing more control energy.

Necessary and sufficient observability conditions have been established in Theorem 2.4 for non-maneuvering target cases and in Theorem 2.5 for maneuvering targets, and thus *Aim Two* of this research is fulfilled. The generality of these derived conditions has been substantiated by identifying most previous results as covered by these conditions. Extensions of the conditions obtained in (2.60) and (2.64) are particularly useful in observability analysis

with guidance laws in closed loop. With the range observability index defined in (2.65), application of the extensions to TPN based systems has revealed that the lack of range observability problem suffered by TPN based systems is due to the very strategy of nullifying the LOS angular rate in TPN.

In working toward achieving *Aim Three*, a new form of additive observable proportional navigation, AOPN-II, has been proposed in Chapter 3, to improve observability as well as to ensure effective interception. Another version of AOPN guidance law, AOPN-I, has also been investigated in Chapter 3. This study has demonstrated that both AOPN laws with their optimal navigation constants perform far better than TPN does in terms of covering a larger capture area. Theorem 3.3 and Theorem 3.4 provide bounds on navigation constants of AOPN laws to ensure interception, and can serve as design aids. Both analytical and simulation studies have confirmed that system observability under AOPN laws is enhanced when compared with the TPN counterpart. Therefore, AOPN guidance laws are well-suited for angle-only measurement systems.

To achieve *Aim Four*, investigation into the influence of saturation constraints on system performance has been conducted and the findings are presented in Chapter 4. Analysis has shown that despite initial saturation, an interception is still achievable if more stringent constraints on systems initial launch conditions are satisfied. However, the mission of intercepting a target is accomplished at the expense of using more control effort. Constraint (4.33), which defines the minimum acceleration capability to ensure interception, is particular useful in computing favorable launch conditions. Simulation runs with different maneuver models have confirmed the validity of the derived conditions in predicting the interception of targets.

5.2 Future Work

Despite the progress made in guidance and control systems during the past decades, there will always be demand for performance enhancement in guidance systems, due to the continual advances in aircraft and related technologies. Considerable progress in enhancing

performance and observability of bearings-only measurement systems have been reported in this thesis. An extension of this research project in a more specific way could center on the area of target acceleration modeling. When deriving the solutions to system motion equations engaging a maneuvering target, the target acceleration model is taken as (2.6), because it is mathematically solvable. While the model does provide insights into how target maneuver influences system performance, it becomes intractable in state equation form set up in Cartesian coordinate. There is clearly a need to derive a general target model that is realistic in practice, tractable in analysis, and suitable for many purposes. Recently a new target model, regarded as realistic, has been presented [44]. Difficulty exists however in solving the motion equations incorporating this target model, and thus increasing the complexity of further system investigation. Despite this major drawback, the new model still constitutes a good starting point. Indeed, modeling the acceleration of a highly maneuverable target has always been an active research area. Different specific-purpose target acceleration models have been proposed, including target models for guidance design [28, 16], and for target state estimation [29, 47]. To date, a sufficiently general target model is still an open research topic. The gains from incorporating a good target model in the design of control laws are numerous, including enhancement of robustness of guidance systems in terms of their ability in coping with unpredictable target dynamics.

Bibliography

[1] C.F. Lin. *Advanced Control Systems Design*. PTR Prentice Hall, Englewood Cliffs, New Jersey, 1994.

[2] J.R. Cloutier, J.H. Evers, and J.J. Feeley. Assessment of air-to-air missile guidance and control technology. *IEEE Control Systems Magazine*, pages 27–34, October 1989.

[3] C.F. Lin. *Modern Navigation, Guidance, and Control Processing*. Prentice Hall, Englewood Cliffs, New Jersey, 1991.

[4] W. Grossman. Bearings-only tracking: a hybrid coordinate system approach. *Journal of Guidance, Control and Dynamics*, 17(3):451–457, May-June 1994.

[5] B. Friedland. *Advanced Control System Design*. PTR Prentice Hall, Englewood Cliffs, New Jersey, 1996.

[6] S.A. Murtaugh and H.E. Criel. Fundamentals of proportional navigation. *IEEE Spectrum*, 3:75–85, December 1966.

[7] C.D. Yang, H.B. Hsiao, and F.B. Yeh. Generalized guidance law for homing missiles. *IEEE Transactions on Aerospace and Electronic Systems*, AES-25(2):197–211, March 1989.

[8] J.L. Speyer, D.G. Hull, and C.Y. Tseng. Estimation enhancement by trajectory modulation for homing missiles. *Journal of Guidance, Control and Dynamics*, 7(2):167–174, 1984.

[9] S.C. Nardone and V.J. Aidala. Observability criteria for bearings-only target motion analysis. *IEEE Transactions on Aerospace and Electronic Systems*, ASE-17(2):162–166, March 1981.

[10] S.E. Hammel and V.J. Aidala. Observability requirements for three-dimensional tracking via angle measurements. *IEEE Transactions on Aerospace and Electronic Systems*, ASE-21(2):200–207, March 1985.

[11] E. Fogel and M. Gavish. Nth-order dynamics target observability from angle measurements. *IEEE Transactions on Aerospace and Electronic Systems*, ASE-24(4):305–308, May 1988.

[12] S.A.R. Hepner and H.P. Geering. Observability analysis for target maneuver estimation via bearing-only and bearing-rate-only measurements. *Journal of Guidance, Control and Dynamics*, 13(6):977–983, Nov-Dec 1990.

[13] T.L. Song and T.Y. Um. Practical guidance for homing missiles with bearings-only measurements. *IEEE Transactions on Aerospace and Electronic Systems*, 32(1):434–442, January 1996.

[14] A.N. Payne. Observability problem for bearings-only tracking. *International Journal of Control*, 49(3):761–768, 1989.

[15] T.L. Song. Observability of target tracking with bearing-only measurements. *IEEE Transactions on Aerospace and Electronic Systems*, ASE-32(4):1468–1472, October 1996.

[16] D.G. Hull, J.L. Speyer, and D.B. Burris. Linear-quadratic guidance law for dual control of homing missiles. *Journal of Guidance, Control and Dynamics*, 13(1):137–144, Jan-Feb 1990.

[17] R.J. Casler Jr. Dual-control guidance strategy for homing interceptors taking angle-only measurements. *Journal of Guidance, Control and Dynamics*, 1(1):63–70, Jan-Feb 1978.

[18] D.G. Hull and J.L. Speyer. Maximum-information guidance for homing missiles. *Journal of Guidance, Control and Dynamics*, 8(4):494–497, July-August 1985.

[19] G.E. Hassoun and C.C. Lim. Advanced guidance control system design for homing missiles with bearings-only measurement. In *IEEE International Conference on Industrial Technology*, pages 250–254, Guangzhou, China, December 1994.

[20] B.L. van der Waerden. *Mathematical Statistics*. George Allen and Unwin Ltd. London Springer-Verlag, 1969.

[21] G.E. Hassoun. *A Study of Observability-Enhanced Guidance System*. PhD thesis, The University of Adelaide, October 1995.

[22] P. Zarchan. Proportional navigation and weaving targets. *Journal of Guidance, Control and Dynamics*, 18(5):969–974, Sept-Oct 1995.

[23] E.J. Ohlmeyer. Root-mean-square miss distance of proportional navigation missile against sinusoidal target. *Journal of Guidance, Control and Dynamics*, 19(3):563–568, May-June 1996.

[24] H.L. Pastrick, S.M. Seltzer, and M.E. Warren. Guidance laws for short-range tactical missiles. *Journal of Guidance and Control*, 4(2):98–108, March-April 1981.

[25] P. Zarchan. *Tactical and Strategic Missile Guidance*. American Institute of Aeronautics and Astronautics, second edition, 1994.

[26] U.S. Shukla and P.R. Mahapatra. The proportional navigation dilemma - pure or true. *IEEE Transactions on Aerospace and Electronic Systems*, ASE-25(1):73–79, January 1989.

[27] M. Guelman. A qualitative study of proportional navigation. *IEEE Transactions on Aerospace and Electronic Systems*, AES-7(4):637–643, July 1971.

[28] F.W. Nesline and P. Zarchan. A new look at classical versus modern homing guidance. *Journal of Guidance and Control*, 4(1):75–85, Jan-Feb 1981.

[29] J.L. Speyer and K.D. Kim. Passive homing missile guidance law based on new target maneuver model. *Journal of Guidance, Control and Dynamics*, 18(5):803–812, Sept-Oct 1990.

[30] D. Ghose. True proportional navigation with maneuvering target. *IEEE Transactions on Aerospace and Electronic Systems*, AES-30(1):229–237, January 1994.

[31] P.J. Yuan and J.S. Chern. Solutions of true proportional navigation for maneuvering and nonmaneuvering targets. *Journal of Guidance, Control and Dynamics*, 15(1):267–271, Jan-Feb 1992.

[32] M. Guelman. The close-form solution of true proportional navigation. *IEEE Transactions on Aerospace and Electronic Systems*, AES-12(4):472–482, July 1976.

[33] C.D. Yang and F.B. Yeh. Closed-form solution for a class of guidance laws. *Journal of Guidance, Control and Dynamics*, 10(4):412–415, July-August 1987.

[34] P.R. Mahapatra and U.S. Shukla. Accurate solution of proportional navigation for maneuvering target. *IEEE Transactions on Aerospace and Electronic Systems*, AES-25(1):81–88, January 1989.

[35] C.D. Yang and Yang C.C. Analytical solution of three-dimensional realistic true proportional navigation. *Journal of Guidance, Control and Dynamics*, 19(3):569–577, May-June 1996.

[36] S.C. Nardone and M.L. Graham. A closed-form solution to bearings-only target motion analysis. *IEEE Journal of Oceanic Engineering*, 22(1):168–178, January 1997.

[37] T. Takehira, N.X. Vinh, and P.T. Kabamba. Analytical solution of missile terminal guidance. *Journal of Guidance, Control and Dynamics*, 21(2):342–348, March-April 1998.

[38] D. Ghose. On the generalization of true proportional navigation. *IEEE Transactions on Aerospace and Electronic Systems*, AES-30(2):545–555, April 1994.

[39] U.S. Shukla and P.R. Mahapatra. Optimization of biased proportional navigation. *IEEE Transactions on Aerospace and Electronic Systems*, ASE-25(1):73–79, January 1989.

[40] P.J. Yuan and J.S. Chern. Analytic study of biased proportional navigation. *Journal of Guidance, Control and Dynamics*, 15(1):185–190, Jan-Feb 1992.

[41] R.A. Decarlo. *Linear System – A State Variable Approach with Numerical Implementation*. Prentice-Hall International, INC, 1989.

[42] T.L. Song and J.L. Speyer. A stochastic analysis of a modified gain extended Kalman filter with applications to estimation with bearings only measurements. *IEEE Transactions on Aerospace and Electronic Systems*, AC-30(10):940–949, October 1985.

[43] P.J. Galkowski and M.A. Islam. An alternative derivation of the modified gain function of Song and Speyer. *IEEE Transactions on Automatic Control*, 36(11):1323–1326, November 1986.

[44] S. K. Rao. Comments on "true proportional navigation with maneuvering target". *IEEE Transactions on Aerospace and Electronic Systems*, 33(AES-1):273–274, January 1997.

[45] C.D. Yang and C.C. Yang. A unified approach to proportional navigation. *IEEE Transactions on Aerospace and Electronic Systems*, AES-33(2):557–567, April 1997.

[46] C.D. Yang and H.Y. Chen. Nonlinear H_∞ robust guidance law for homing missiles. *Journal of Guidance, Control and Dynamics*, 21(6):882–890, Nov-Dec 1998.

[47] R.A. Singer. Estimating optimal tracking filter performance for manned maneuvering targets. *IEEE Transactions on Aerospace and Electronic Systems*, AES-6(4):473–482, July 1970.